Personalization and Adaptation in Physical Human-Robot Interaction

by **Sugeeth Gopinathan**

Ph.D. Thesis

Faculty of Technology, Bielefeld University
October 2018

Printed on permanent paper as per ISO 9706

Declaration

I declare that this thesis was composed by myself and that the work contained therein is my own, except where explicitly stated otherwise in the text.

(*Sugeeth Gopinathan*)

Acknowledgement

Over the past three and half years I have received constant support and encouragement from a great number of wonderful individuals to whom I am greatly indebted.

First and foremost, I would like to thank my supervisor and mentor Prof. Jochen J. Steil for his constant support through out this thesis. Without his constant push and motivation this thesis would not have materialized, his timely advice and suggestions helped me overcome each stumbling block that was thrown ahead of me with relative ease.

I would like to thank Anke Kloock, Heike Leifhelm, Ruth Moradbakhti and Ilona Engles for taking care of the administrative aspects of my PhD. Special thanks to Harald Kirk Meyer, Stefan Hössler, Erik Reimer, Stefan Krüger, Michael Götting who provided quick and professional technical support.

The field of robotics is an interdisciplinary domain where team work and collaboration bear more fruits than individual work. I had the great opportunity to work at two great research institutes, CoR-Lab and iRP where I was able to work with a couple of great fellow researchers whose collaboration and suggestions had been invaluable for my work. I would like to thank Sonja Ötting, Pouya Mohammedi, Arne Muxfeldt and Heiko Donat for the works we did together. I would like to extend my special thanks to Daniel Kubbus, Milad Malekzadeh, Zeeshan Sheriff and Christian Emmerich for their helpful advice and fruitful discussion which helped me boost this thesis.

The past years had been intense but fruitful, I was fortuitous enough to have a group of cheerful and friendly colleagues who made this intense time a relaxing and joyful memory to remember. I am glad to have met Micheal Wojtynek, Dennis Wigand and Sonja Ötting with whom I share a lot of memories in both my professional and personal sphere.

Last but far from least, I thank my family and friends for their emotional support and especially my wife Reshmi for having stood by my side through all ups and downs.

Abstract

Recent advancements in physical human-robot interaction (pHRI) makes it possible for compliant robots to assist the human counterpart while closely working together. An ideal control mode designed for pHRI should be easy to handle, intuitive to use, ergonomic and adaptive to human habits and preferences. The major stumbling block in achieving this is that each user has varying physical capabilities and characteristics. This variance in the user behavior and other features is often high and rather unpredictable, which hinders the development of such systems. To tackle this problem, the idea of personalized adaptive stiffness control for pHRI is introduced in this thesis. Extensive user-studies are conducted in scope of this thesis and various control modes for pHRI are proposed and evaluated using appropriate user-studies. Both naive and expert users were considered in the user-studies and inferences from each study were used to improve the control mode to be better suited for pHRI.

The thesis follows a meticulous research plan, an initial user-study confirms the importance of pHRI and kinesthetic guidance in industrial tasks. Subsequently, the user interactive force based adaptation is proposed and a second user-study is conducted where it is compared with standard control modes for pHRI. Importance of task specific parameters and the need for combining the task and human factors emerged from the results of the second user-study. In the next phase manipulability based approaches which combine both task and human parameters are proposed and validated by conducting a third user-study. In the final phase a fourth user-study is conducted where the proposed control modes are compared against more complex methods that have been proposed in the literature.

The importance of human physical factors and needs for human centered systems for pHRI is validated in this thesis. The results show that including these human factors not only improve the performance but also improves the interaction quality and reduces the complexity of the pHRI.

Contents

List of Figures

List of Tables

Chapter 1

Introduction

"An essential face of Industry 4.0 is autonomous production methods powered by robots that can complete tasks intelligently, with the focus on safety, flexibility, versatility, and collaborative. Without the need to isolate its working area, its integration into human workspaces becomes more economical and productive, and opens up many possible applications in industries" [1]

1.1 Motivation: Industrial Robots as Assistance Systems

During the past few decades the field of robotics has grown in leaps and bounds. Now the term robotics epitomizes the field of automation and is at the top of technological advancement. While there is no doubt that more improvements could be made, the current state of the art in robotics has definitely boosted the industrial growth. While the prominence of robot manipulators and robotics in general is growing steadily in industry, its influence in civilian domain is also undeniable [2]. In dawn of *Industry 4.0*, industrial manufacturing is heralded towards smart and flexible systems, which are intelligent as well as cost efficient. Small and Medium-sized enterprises (SMEs), which are the major benefactors of Industry 4.0 [3], require highly flexible processes that can be changed without additional overheads for enabling cost efficient mass production [4, 5].

The novel vision of *Industry 4.0* is realized through the implementation of *cyber-physical systems* (CPS). This enables the basic entities of industry such as machines, storage systems and other utilities to share information as well as act and control each other autonomously [6]. This empowers smart robotic factories that can concurrently facilitate both flexibility and high productivity. For this aim to be accomplished, robots will take up most of the workload, while the human co-worker will be designated with the task of supervision or collaboration on tasks which the robots cannot learn [7]. The collaboration of a human and a robot brings forth the major advantage that the hierarchical level where a *supervisor instructs a subordinate* is replaced by human-machine interactions with simultaneous information exchange and task resolution. These systems requires a dual design approach which needs improved technical developments as well as integration of human aspects in human-machines systems [8].

Physical Human-Robot Interaction (pHRI) which is a subset of advanced cyber phys-

ical systems can contribute towards cost efficient high productive and ergonomic work places [9]. With the developments in collaborative robotics and safe physical Human-Robot collaboration, it is now possible for humans and robots to share workspaces, as opposed to classical industrial cages for robots, fully isolated from human counterparts [10]. As for the controllers, impedance [11], admittance [12], and hybrid [13] controllers which are specifically designed for compliant platforms makes it possible to take into consideration interaction forces between robots and their surroundings. Interaction with humans has an extra critical requirement and that is the human's safety to be guaranteed. This problem can be viewed from two complementary perspectives, namely detecting human presence and reacting to that [14]. Cutting edge compliant robot platforms like Kuka iiwa, ABB Yumi, Franka Emika come with all the above mentioned features necessary for safe pHRI.

Effective pHRI requires the robotic system to be easy to handle, intuitive, and adaptive to human habits and preferences. It is imperative that the interaction is smooth, intuitive and ergonomically well designed. Robotic assistance systems are becoming increasingly relevant in Small and Medium scale Industries, where flexible robotic systems assists the human worker by collaborating with them, increasingly often through actual physical interaction between human and robot. Lightweight robots are replacing the traditional industrial robots in such tasks due to their obvious advantages: they are less dangerous, and the added compliance allows the users to work in close proximity and thus collaborate with the robot. This collaboration is a major step forward in achieving flexibility in industrial tasks, because the implicit technical knowledge that the human workers possess about the task can be incorporated directly by collaboration, without added effort of modeling or programming. Here, humans act more like a resource for the robot, providing information and working like other system modules. With this approach the task execution by robot is more likely to find a good solution since the human knowledge is automatically imparted to them by the system where the human is the center [15].

Although it is clear that pHRI will improve flexibility and productivity by taking advantage of the human's cognitive and perceptual skills, it is unclear how this interaction may be made more ergonomic and pleasant for the user. For this aim, a few novel platforms are commercially available, that allow the adaptation of the robot controller to make the human-robot interaction smoother. The on-line adaptation of impedance characteristics is possible, and such manipulators behave like a spring damper system that reacts to external forces [16]. However, substantial variation in human interaction forces coupled with unpredictable human behavior makes it difficult to design a suitable pHRI system. Another factor, which will substantially affect pHRI, is the task itself. Unique task characteristics, such as geometry, difficulty level, and requirement of precision, have a sizable effect on how a human worker interacts with the robot during task completion. Each task is unique and each individual approaches a task with a unique strategy, which might be substantially different among users. This variance in interaction is strongly connected to their physical limitations as well as to their personal preferences. Hence, not only user interaction forces but also the physical characteristics of the users such as differences in height, body proportions, left or right handedness, the distance the user keeps with the robot, or varying cognitive skills can introduce substantial variance. This demands personalization of the robots to be capable of accommodating user-specific

dynamics.

1.2 Problem Statement

The task characteristics and human physical parameters play an important role in pHRI, as these results in variance in user behavior. This variance is highly significant and should be investigated further as it affects the overall interaction quality and efficiency. In the relevant works like [17–19], these aspects are focused on while many others ignore these factors and focus entirely on adapting robot controllers to the user interaction forces.

For improving the pHRI and robotic assistance systems, extensive research has been done in the past decade. The major contributions are discussed in Section 2.2. Most of the works incorporate novel methods, algorithms such as machine learning and fuzzy systems into the control side of the robot to improve the interaction between human and robot. Variable admittance and impedance schemes, where the robot parameters are varied to coincide with the instantaneous interaction and the human intent, are proposed and discussed. Despite recent efforts and inclusion of advanced methods like machine learning, these works lack certain aspects which could make the interaction intuitive. At the same time, it is not clear if complex methods could actually be beneficial for the whole work flow. Therefore the following problems are addressed in this thesis.

The importance of the human factors in pHRI and identification of these factors. While most of the existing literature focuses on improving the control modes and their stability, not much effort has been given for considering human factors. One of the main goals of this thesis is to establish the importance of human factors in pHRI and to identify the important parameters whose inclusion could instinctively improve the interaction.

Dependency of interaction on task specific parameters. Human workers tend to approach each task in a distinct manner due to which each task is unique and a control scheme designed for a particular task may not be reusable for another task. Current literature rarely takes into consideration the importance of task parameters in pHRI. In this thesis, the importance of task parameters is studied experimentally and its influence on the control method design for pHRI is discussed.

Simplicity vs Complexity in control mode design for pHRI. Most of the current literature incorporates advanced learning methods as in [16], or fuzzy logic [20], to vary the impedance parameters of the robot. But it is not clear if such methods excessively increase the complexity of interaction and affect intuitiveness. Also, complex methods need exhaustive training phases which are time-consuming which reduces their deployment in industrial tasks. This aspect is discussed in detail in the thesis and experimentally verified.

Evaluation of control methods and verifying their effectiveness. The most important step in designing control methods for pHRI is to verify if the designed method is suitable for pHRI and easy to use, for naive users, in a real industry scenario. Unfortunately this crucial aspect is ignored by most of the literature and their effectiveness is never tested with naive users. In addition, the implicit assumption that such adaptations are beneficial for task performance or user satisfaction has not yet been validated on any reasonable tasks. In this thesis, each proposed control mode is extensively studied on user studies involving naive and expert users.

Effective adaptation scheme considering both human and task factors. The various important facets of pHRI which are discussed above are experimentally studied in the framework of this thesis. From the results observed from the experiments, determining and including highly variable human characteristics as well as task parameters and analyzing their effects on the smoothness and efficiency of the pHRI, can all be concluded to be highly imperative and therefore worthy of attention. Despite these clear indications, apparently no commercially available and practically used control scheme embodies such adaptivity or personalization and experimental experience is shallow.

1.3 Contribution and Goal of Thesis

While this thesis shares the basic hypothesis that adaptivity of stiffness and/or damping may be important to account for user variability, it is crucial that this hypothesis must be validated as most likely task-dependencies play an important role. Additionally, the sources of user variance are plenty including differences in height, body proportions, force profile, left or right handedness, the distance the user keeps with the robot, or varying cognitive skills.

The problems that are discussed above indicate that these factors needs to be looked at. Table 2.1 and Table 2.2.3 shows the recent related works and their properties. It is clear from the table that most of the works propose certain methods but do not care about validating if they are suited for pHRI. The evaluation is mostly done with very few users and most of them are not naive users, rather they are already well versed with how the system works. At the same time, the tasks are seldom tested on real industrial scenarios or complex tasks. In most related works the control modes are tested with straight line motions which are too simple. It is a known fact that people adapt fast to such motions after a few trials. Another observed disadvantage is that many such methods need exhaustive training phases, which needs lot of time and training data. Such systems might not be suited for industrial cases where the task might change over time.

This thesis aims at observing pHRI and learning more about it through actual human robot interaction experiments involving naive users performing tasks which are similar to commonly used tasks in industry. The lessons learned from each experiments will be used to improve the aspects of pHRI control methods which are substantial for improving the interaction quality. Such an incremental approach ensures that what is missing and relevant is carefully determined and subsequently it is added to control side so as to ensure that users benefit from the pHRI. The relationship between tasks and the interaction quality is another topic of interest and will be looked into closely by analyzing the experiment results. The main goal of this thesis is to propose a control scheme for pHRI which takes into account both the human factors and the task parameters and incorporates them in a meaningful manner to improve the pHRI quality.

A series of user-studies is conducted in the scope of this thesis. Table 1.1 shows the list of user studies conducted in the context of this thesis and their properties. The first user-study proves the importance of pHRI in industrial tasks as opposed to the current standard methods of human intervention. The second user-study evaluates a force based variable stiffness scheme and compares it with standard interaction methods.

User Study	Purpose of the Study	Users	Complex Task	Task
1	Comparison of HRI Interfaces	31	✓	Industrial Assembly
2	Validation of Personalized Force based Adaptation	49	✓	Contour-following, Drawing Task
3	Validation and comparison of Manipulability based Adaptation schemes	40	✓	Contour-following, Pick and Place
4	Validation and Comparison of Directional Adaptation scheme	50	✓	Contour-following

Table 1.1: The list of user-studies conducted in the context of this thesis and their properties.

The stiffness adaptation was chosen as it was more intuitive for the users and directly affects the interaction quality. The results from this experiment proved the importance of task specific details in pHRI. From the inferences drawn from this study, different control modes based on manipulability of human arm are proposed. These control modes take into consideration both task and human factors. In the third user study these control modes are compared to find out which one works better. In the final user study the proposed methods are compared against two complex methods which are similar to the standard techniques used in the current literature. The results of these experiments prove that, even though methods proposed in this thesis are not complex, they still edge the sophisticated methods as they have better performance and less setting up time. The final outcome of this thesis is a basis for intuitive ways to combine both task and human factors concurrently to improve the pHRI, at the same time it proved the importance of human factors in pHRI.

1.4 Outline

This thesis is structured as follows. Chapter 2 discusses the various control methods for pHRI and the recent related works which aim at achieving a better pHRI. A brief background about the thesis and the evaluation measures used in the rest of the thesis are also explained in this chapter. In Chapter 3, results of a user-study conducted to prove the importance of pHRI and kinesthetic guidance is explained. This chapter compares various other interacting mediums to physical interaction and the results emphasize the intuitiveness of pHRI, while compared to other methods. In Chapter 4, the idea of personalization of control modes for pHRI is introduced. A control method based on personalized force limits and a subsequent interaction force based stiffness adaptation is proposed in this chapter. A user study is conducted to evaluate effectiveness of this control mode and the results of the conducted user-study and the inferences are explained in this chapter. In Chapter 5, the task specificity and the influence of the task in pHRI is discussed in detail, the results from the previous user-study and its task specific facets are analyzed. The concept of manipulability and the force transmission ratio are introduced

in this chapter. Chapter 6 combines both the user specificity and task specificity and different control modes to combine these two significant facets of pHRI are discussed. Three control modes for pHRI which are based on manipulability of human arm are proposed here. A user-study is conducted to verify their effectiveness and to see which mode performs better. Furthermore, the results form the study are explained in this section. In Chapter 7, the results of the final user-study are reported. In this study different control modes proposed in this thesis are compared with stiffness adaptations based on complex methods like machine learning and optimization. Finally, Chapter 8 summarizes and concludes on the results and the inferences obtained in this thesis.

Chapter 2

Background and Related Work

In this chapter the basic control methods suited for pHRI are discussed and a literature review on the related work which comes under the scope of this thesis is elaborated. It is clear from the comparison of the related work that most of the methods are too complicated for the use in real industrial scenarios and the exhaustive training makes them incompatible with the demands of SMEs. Most of the methods needs to be re-trained while the task is changed or need explicit task information.

2.1 Control methods for pHRI

As mentioned earlier the advancement in hardware and the control approaches made it possible for humans and robots to work in tandem and collaborate with each other. Widely used control methods for pHRI are Impedance and Admittance control. As illustrated in Fig. 2.1, A physical system that accepts motion as input and gives out force output is regarded as an impedance. On the other hand, a system that accepts force as input and gives out motion output is regarded as an admittance [13].

2.1.1 Impedance Control

Impedance control is widely used to establish a dynamic relationship between the robot and environment [21]. In this approach unlike the classical control where the force or position is controlled independently, the dynamic parameters of the robot such as stiffness, damping and inertia are regulated to modify the robot behavior [20]. In Impedance control the robot controller behaves like a mechanical impedance, it receives a reference position as input and yield force output. The robot manipulator on the other hand behaves as an admittance, see Fig. 2.2

As explained in [13], consider a single DOF system with mass, m and the displacement produced be x. If there is a control force of F and an external force of F_{ext} is acting on the system, then:

$$m\ddot{x} = F + F_{ext} \tag{2.1}$$

For Impedance and Admittance control, the main control objective is to establish a relation between the external force and the displacement, i.e. the deviation from the

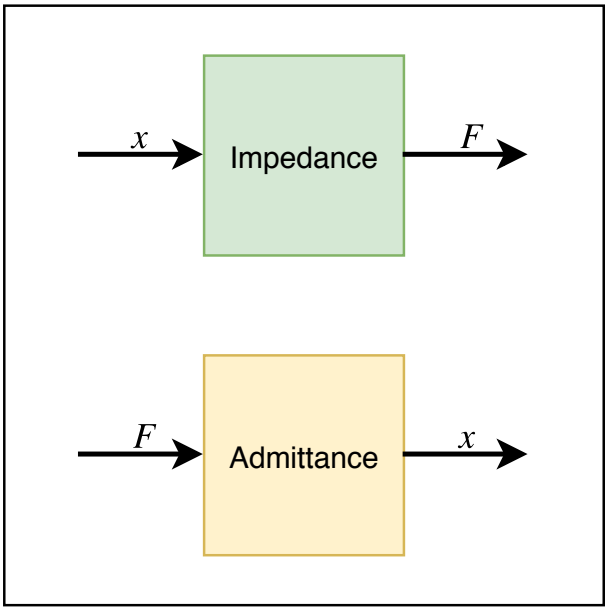

Figure 2.1: Figure illustrating impedance and admittance behavior.

equilibrium trajectory x_0. If $e = (x - x_0)$ is the deviation, then:

$$M_d\ddot{e} + D_d\dot{e} + K_d e = F_{ext} \tag{2.2}$$

Where M_d, D_d, K_d represents the desired inertia, damping and stiffness respectively. From Eqn. 2.1 and Eqn. 2.1, the impedance control law can be derived as:

$$F = \left(\frac{m}{M_d} - 1\right) F_{ext} + m\ddot{x}_0 - \frac{m}{M_d}\left(D_d\dot{e} + K_d e\right) \tag{2.3}$$

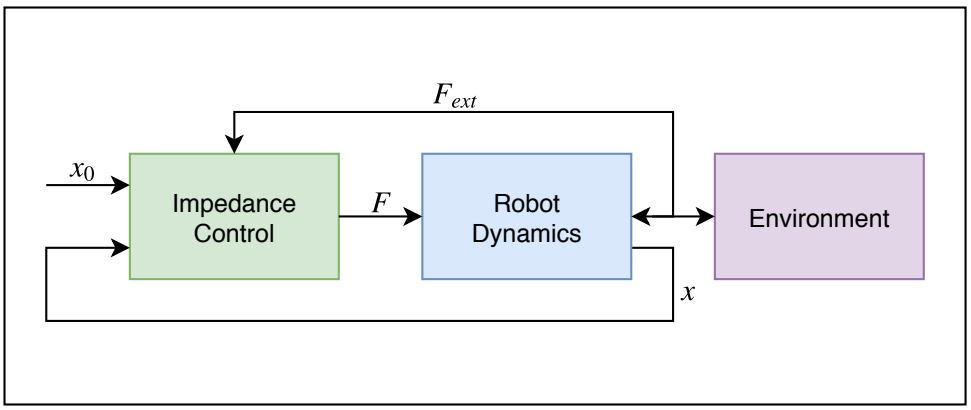

Figure 2.2: Figure illustrating impedance control scheme.

Impedance Control provides very good performance when the environment is stiff but results in poor accuracy when the environment is soft [13].

2.1.2 Admittance Control

In pHRI, interaction between the robot and environment is minimum and it is the human counterpart who will be constantly interacting with the robot. In such cases a mapping can be made between the humans interaction force and robot motion by means of admittance control. In this way the human counterpart will be able to move the robot by applying force at the robot end-effector [22]. The admittance control can be considered as an inverse of impedance control. As mentioned in [13], in admittance control the manipulator is position controlled and behaves as a mechanical impedance. Hence the controller is designed to be a mechanical admittance, see Fig. 2.3.

The position controller could be implemented using a PD regulation controller of the form:

$$F = k_p (x_d - x) - k_d \dot{x} \tag{2.4}$$

here, k_p and k_d are the positive gains and the desired position is denoted by x_d.
Using Eqn. 2.2 and Eqn. 2.4 the complete system dynamics can be written as:

$$m\ddot{x} + k_d \dot{x} + k_p (x - x_d) = F_{ext} \tag{2.5}$$

$$M_d (\ddot{x}_d - \ddot{x}_0) + D_d (\dot{x}_d - \dot{x}_0) + K_d (x_d - x_0) = F_{ext} \tag{2.6}$$

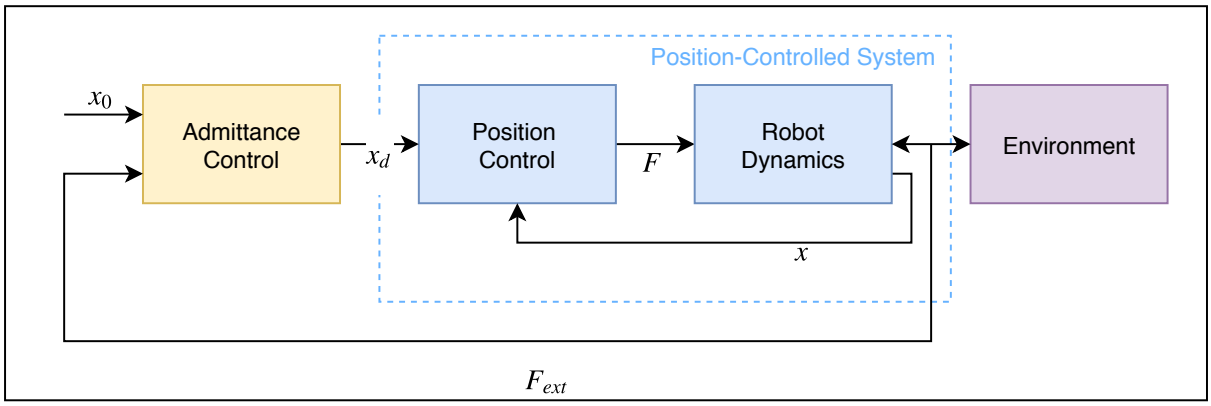

Figure 2.3: Figure illustrating admittance control scheme.

Admittance Control provides very good performance for soft environments but results in contact instability for stiff environments [13].

2.1.3 Variable Impedance Schemes

The concept of variable impedance control was introduced by [23], where the impedance parameter of the robot was adapted with respect the interaction velocity. Recent efforts in the field of physical Human-Robot Interaction have been done in the direction of adapting the robot's stiffness or damping to match the human intentions. [24] states that in Human-Robot Interaction, the quality of performance is not only a criterion of accuracy and repeatability, but also has a strong dependency on how the robots adapt

their behaviors dynamically with respect to the task and human intentions. There were a handful of recent works which tried to predict this human intent and adapt the robot's behavior based on such predictions, but human and task specific parameters are rarely considered in such approaches. In Section 2.2, the related work in this field which is significant from within the scope of this thesis is discussed. Table 2.2.3 list significant methods based on varying impedance parameters and the approach used.

2.2 Related Works: Literature Review

2.2.1 Admittance Control based approaches

Recent related works for improving pHRI based on Admittance control scheme are elaborated in this section.

Fuzzy model based approaches:

Variable admittance control is used for human-robot cooperation tasks in [20], the proposed method utilizes a fuzzy inference system that takes into consideration the desired velocity and the force applied by the user. The damping of the robot manipulator is adjusted on-line according to the prediction of the fuzzy inference system. A fuzzy model reference learning controller is used for adapting the fuzzy inference system towards the minimum jerk trajectory model. The system was evaluated with 12 users including 10 naive users, the task considered in the evaluation consisted of 10 predefined Point to Point (PTP) motions. The system needed a training phase which involved users moving the robot effector in a simple straight line for multiple times.

A variable admittance controller that regulates the virtual damping for rotational axis is discussed in [25], this is done as an extension of [20]. Using partial state representation of the system, the controller is trained to regulate the virtual damping appropriately by minimizing the trajectory deviation of the cooperative rotational motion from the minimum jerk model. An on-line tool compensation technique is used for compensating the tool weight in this system. The system is validated with seven users on a relatively simple task. The users rotated the robot to and fro around two fixed axes multiple times. Each user had to participate in two sets of 30 interactions each. As discussed in the previous section, the training process is time consuming and might not be recommended in cases where the task can change on the fly. In addition the system was never tested in challenging scenarios which are common in pHRI.

Machine Learning based approaches:

A hybrid variable admittance model was proposed in [26], a fuzzy reinforcement learning method is employed in this work. The proposed scheme provides virtual damping in response to the human intentions. The scheme consists of three modules namely admittance model, human intent estimator and damping modulator. The admittance model facilitates the compliant behavior of the manipulator in joint space. The human intent estimator estimates the user's intention and provides the damping values to the damping modulator. The system is evaluated with eight users including naive users with a task

involving simple motion of the end-effector to a target position in a single direction. This method needs exhaustive training as well. The experiment results showed that the time invested for training in this method was not sufficient: *Theoretically, the reinforcement learning algorithm can converge to an optimal solution thorough sufficient training, which may require more time to achieve* [26]. It is highly unlikely that this method could find its application in real world tasks as it might be too complex.

A reinforcement learning based admittance control of human-robot co-manipulation tasks is proposed in [27]. The objective of the reinforcement learning algorithm in this method is to minimize the jerk along point-to-point movement. The controller is designed to learn the damping parameter, without taking into consideration the task characteristics. A fuzzy Q-Learning algorithm was used for training the reinforcement learning agent. This agent regulates the virtual damping towards minimization of the jerk of the movement. The system was tested with seven users and the task involved motion along straight lines. Each user was required to record two consecutive sets of 50 interactions each. The training is tedious and the final task evaluated is too simple to verify the effectiveness of the proposed control methods.

An adaptive scheme which takes into account human intent, task models and the variance in robot dynamics while interacting with the robot is taken into account in [28]. In this work a two loop system is used, the outer loop incorporates the adaptive inverse control technique and tunes the admittance model to suit the human intent. The inner-loop neuro-adaptive controller linearizes the robot dynamics. This method does not need an off-line tuning and can compensate for the varying human interaction with the robot system. The system is later evaluated with two users having three trials doing a simple PTP motion. The extension of [28] was presented in [29], in this work the non-linear inner loop is replaced by a two layer neural network with 44 inputs. The system was later evaluated with three users doing a simple point-to-point task.

Heuristics based approaches:

The user's arm muscle co-contraction is taken into account in [30], inorder to adjust the damping of the robot in real time using surface EMG electrodes placed on the arm muscles. The damping is adjusted with respect to the calculated muscle co-activation. The underlaying assumption is that if the user's grip is firm the co-activation will increase and subsequently, for improving the accuracy the damping is also increased. Here the co-activation level of the arm muscles is used as a switch between predefined damping values. For evaluating the system 20 subjects including naive users were considered. The task involved a wire-loop game and the users were instructed to move the electrode attached to the end-effector without having collision with the central wire. Each user repeated the tasks 10 times.

A novel methodology for on-line adaptation of the admittance parameters of a robot for pHRI is proposed in [31]. A heuristic is proposed in this work, which is used to detect the deviation of the robot's behavior from the intended behavior. Later the intended robot behavior is restored by adapting the admittance parameters without increasing the pHRI effort for the user. This is a highly theoretical approach and has not been evaluated in a real pHRI scenario, despite the claims that it reduces the user effort.

A variable admittance scheme based on inference of human intentions using desired

Table 2.1: List of significant related works and how they are evaluated

Related Work	Year	Evaluation	No of users	Industrial task	Naive users	Exhaustive training	Task
[20]	2014	✓	12	×	✓	✓	Straight line motions
[27]	2015	✓	7	×	×	✓	Straight line motions
[25]	2015	✓	7	×	×	✓	Rotation along fixed axis
[30]	2016	✓	20	✓	✓	✓	Wire-loop game
[33]	2007	✓	6	×	×	✓	Cooperative Drawing task
[26]	2017	✓	8	×	✓	✓	Single arc motion
[34]	2014	×	0	×	×	✓	Only tested in simulation
[19]	2018	✓	1	×	×	✓	Joint manipulation of heavy object
[31]	2017	×	0	×	×	×	-
[35]	2002	✓	1	✓	×	×	Peg-in-hole, Carry over task
[32]	2012	✓	6	✓	×	×	Drawing task, Impulse
[28]	2015	✓	2	×	×	×	Simple PTP motion
[29]	2017	✓	6	✓	×	×	Simple PTP motion

velocity and acceleration is proposed in [32]. A heuristic is used in this method to infer if the user is accelerating, decelerating or stopping the motion. According to the deduced human intent the damping parameter of the robot is varied. The system is later evaluated with six users, in two different tasks. An admittance based scheme was proposed in [17], a method for gaining knowledge as well as acquiring semantic labels for interaction experience on joint manipulation without supervision, aiming at improving the robot's joint-manipulation skills is proposed in this work.

2.2.2 Impedance Control based approaches:

Recent related works for improving pHRI based on Impedance control scheme are elaborated in this section.

A novel velocity based variable impedance control for human-robot cooperation was

proposed in [33]. The intention of the human user is predicted from the user interaction force profile and the impedance parameters are calculated accordingly. The time derivative of the force is used to infer the intentions of the human operator. The work also justifies the usage of velocity control over conventional position control as a low level controller for human-robot interaction. The system is evaluated using six users who conducted a cooperative drawing task.

An on-line trajectory based impedance control was proposed in [34]. In this work, an event controlled on-line trajectory generator associated to a classical structure of impedance control is used to generate an optimal trajectory for the user. The underlaying assumptions used is that the force applied by the user is the only physically exchanged signal between the robot and the users. It is assumed that this interaction force has all the necessary information about the user intention. Therefore based on the interaction force a robot trajectory is calculated on-line and updated in every control cycle. This work is proposed as an alternative for variable admittance control. No evaluation being done with real users, instead a human model is designed and tested in simulation with a two link planar robot. It is highly doubtful whether this might work well with real human users, since the underlaying assumptions about the human intention prediction seems flawed. In addition contrary to the claims it was never tested with real users.

The method presented in [35] was one of the earliest works related to pHRI. In this work a novel variable impedance control scheme had been proposed with a virtual stiffness term. A heuristic was used to determine the type of task the user is intending to execute, i.e. if the velocity is low then the task is a peg in hole task, else it is a carry over task. The stiffness is varied accordingly based on that task. The proposed approach is evaluated using one operator for a peg in hole task and a carry over task.

2.2.3 Other approaches:

A novel approach for human-robot collaboration control was proposed in [19], this approach alerts the user and minimizes the static joint torque overloading of a human partner while executing shared tasks with a robot. The center of pressure variation between the pre-calculated human model and the current status is calculated on-line and is later used for on-line estimation of the joint torque variation in the whole body poses. Later the robot motion is optimized to reduce the overloading in the human joints by taking into consideration the calculated task constraints. This method comes outside the scope of the tasks discussed in this thesis, but it carefully takes into consideration the users physical constraints and limitations and adapts the robot to aid the user in a meaningful manner. The initial model of the user's center of pressure is obtained from 50 user poses subjected to constraints and later an evaluation is done with one expert user.

An admittance based system using Gaussian mixture model to learn cooperative robot skills in the context of human-robot object transportation was proposed in [18]. This method allows the robot to automatically encode the human demonstrations and its relation to the task parameters, thus improving the robots joint manipulation capabilities. A novel method for identifying the joint stiffness of human arm was proposed in [36], a model based estimation technique to estimate seven-dimensional joint stiffness of human arm is presented in this work. A robotic interface for human-robot-skill transfer, where the robot act as the tutor and the human acts as the pupil was presented in [37]. In this

novel approach, the skill captured from the human tutor is passed on to another human pupil with help of this interface.

Table 2.2: List of significant related works and the methods they employed for enabling pHRI.

Related Work	Method used	Input interaction parameter	Varied robot parameters	Control mode
[27]	Reinforcement Learning + Fuzzy Model	Cartesian Velocity	Damping	Admittance Control
[25]	Fuzzy Model	Joint Velocity	Damping	Admittance Control
[20]	Fuzzy Model+ Heuristics	Cartesian Velocity	Damping	Admittance Control
[30]	Heuristics	Muscle Co-Activation	Damping	Admittance Control
[33]	Heuristics	Interaction Force	Damping	Impedance Control
[26]	Reinforcement Learning + Fuzzy Model	Interaction Force	Damping	Admittance Control
[34]	On-line Trajectory based Impedance Control	Interaction Force	Impedance gains	Impedance Control
[28]	Neural Network	Force + Velocity	Damping	Admittance Control
[31]	Heuristics	Interaction Force	Damping	Admittance Control
[32]	Heuristics	Cartesian Acceleration	Damping	Admittance Control
[38]	Neural Network	Interaction Force	Impedance gains	Impedance Control
[28]	Neural Network	Force + Velocity	Damping	Admittance Control
[16]	Reinforcement Learning	Velocity	Damping	Impedance Control
[39]	Heuristics	Interaction Force	Stiffness	Admittance Control

2.3 Evaluation measures

In this thesis the results of four user-studies are evaluated, the evaluation is done both qualitatively and quantitatively. The measures used for evaluation of the user studies are briefly described in this section.

2.3.1 Subjective measures

Perceived ease of use is the degree to which a user believes that using a system will be free of effort [40]. *Reliability* refers to the degree to which a user believes that the system's operations are reliable [41]. The *perceived control* is the degree to which a user believes to have control over using the system [42]. *Enjoyment* is the extent to which the activity of using a specific system is perceived to be enjoyable, aside from any performance consequences resulting from system [43]. *User satisfaction* represents the degree of favorableness the user shows with respect to the system [41]. Table A.1 shows one example item for each criterion.

2.3.2 Objective measures

Time of Completion

Time of completion of a task is the time required by the user to accomplish the given task. In the scope of the experiments in this thesis, it is the time required by the user to move the end-effector from the starting point to the target point. It is a good benchmark for the comparison of the performance of a system under different constraints.

Procrustes Analysis

Procrustes analysis is a rigid shape analysis that uses isomorphic scaling, translation, and rotation to find the best fit between two or more landmarked shapes [44]. The goodness-of-fit criterion used in this analysis is the sum of squared errors and this returns the minimized value of this dissimilarity(d). The similarity measure is calculated as $s = (1 - d)$.

Smoothness

Smoothness is generally used to determine the controllability of a system [45]. Hence, a trajectory with maximum smoothness will result in maximum movement efficiency [46]. Also a smooth interaction ensures a reduced interaction effort from the user side, hence improving the human-robot interface ([47]).

Number of Peaks: In this case, smoothness measures is obtained by counting the number of peaks. The peaks are identified as the number of maxima in a given trajectory, see Eqn.2.7. This quantifies the smoothness to a measurable quantity [48]. The total number of peaks in each dimension X,Y and Z is calculated from the recorded data.

$$NP \triangleq \#\left\{ \left(\frac{dX}{dt}\right)_{maxima} \right\}$$
$$\left(\frac{dX}{dt}\right)_{maxima} \triangleq \left\{ \left(\frac{dX}{dt}\right) : \left(\frac{d^2X}{dt^2}\right) = 0 \; and \left(\frac{d^3X}{dt^3}\right) < 0 \right\} \tag{2.7}$$

Jerk: Smoothness of a trajectory can be represented as a function of jerk, see Eqn.(2.8), which is the time derivative of acceleration [21]. The jerk cost is a scalar which could be used for judging the smoothness of the trajectory [49]. The jerk cost of the individual axis are calculated for each trajectory and the sum is then represented as the total jerk cost for each user generated trajectory.

$$\dddot{X}_i = \left(\frac{d^3X_i}{dt^3}\right) \; , j = \sum_{i=1}^{i=n} \left\| \dddot{X}_i \right\|_2 \; , X_i = \begin{pmatrix} x_i \\ y_i \\ z_i \end{pmatrix} \tag{2.8}$$

Arc Length

The total length traversed while moving along the given trajectory. It is related to the accuracy in task completion. Larger arc length means more deviation the user had from the intended path. The arc length can be calculated as Eqn.(2.9).

$$S = \sum_{i=1}^{i=n} \sqrt{\Delta x_i^2 + \Delta y_i^2 + \Delta z_i^2} \tag{2.9}$$

Total Effort

The total effort $[N]$ represents the amount of energy needed for the whole task execution. This criterion gives an insight on the efficiency of task execution under different interaction modes.

$$E = \sum_{i=1}^{i=n} \|F_i\|_2 \, , \; F = \begin{pmatrix} f_x \\ f_y \\ f_z \end{pmatrix} \tag{2.10}$$

Average Speed

The average speed $\left[\frac{mm}{s}\right]$ gives an idea about how fast the workpiece of interest is moved during the task execution. Higher speed means the task is being solved in less time.

2.3.3 Repeated Measures ANOVA

In this thesis various criteria mentioned above are evaluated statistically to find the significant difference in performance in different control modes. The mean values of each criterion are compared using the Repeated Measures Analysis of Variance (ANOVA). The results of the repeated measures ANOVA are reported accompanied by the full test statistics (e.g. repeated measures ANOVA on the dataset of Procrustes showed a significant difference between the controllers: $F(3) = 7.19$, $p < 0.001$, $\eta^2 = 0.14$). The

most important value here is the p-value. If the p-value is smaller than 0.05, the difference between means is significant at the 95 % level.

Chapter 3

Importance of pHRI in Industrial tasks

In chapter 2, pHRI was discussed in detail and the control schemes required for making pHRI possible were mentioned. The recent development in this field was discussed in detail as well. These mentioned control methods facilitate pHRI, but do not promise an efficient interaction and also the advantages these methods bring are neither clear nor investigated properly.

In this chapter, we discuss the significance of pHRI and its advantages in current industrial scenario. A user-study was conducted to compare different interaction methods for Human-Robot Interaction. The results of a user-study are discussed in the following sections, the study validates and proves that kinesthetic guidance through direct interaction with this robot is much better than classical methods used to program or interact with the robot. The results mentioned in this chapter are the result of a collaborative work which is published in [50]. The author of this thesis contributed to the study design, data analysis and to the programming and design of the Adaptive Kinesthetic Guidance mode.

3.1 Significance of pHRI

The prominence of robots in industry is growing steadily as anticipated, both traditional robots and newer advanced compliant platforms are widely used in industry. The use cases range from traditional fields like simple pick and place to newer concepts like shared workspaces [51, 52]. This is especially valid for SMEs where flexibility and short production cycle time is inevitable, here combining task-specific knowledge with efficiency of robotic systems can increase the productivity drastically [53].

In principle, the tasks can be automated to perform with increased speed and high quality [54–56], but this approach will not work that well then new situations arise in the task which are normally rectified by the factory workers with their innate task-specific knowledge and experience. As an example, in case of automatic assembly task, deviations from the model representation like, e.g. component tolerances or placement errors could lead to task failure. In such cases, compliance control [57] or recovery strategy where safe states defined on basis of additional task-specific knowledge are used to solve the

problems [58]. When automatic assembly is not feasible, a human worker can intervene and solve the existing error [59].

There exists multiple methods by which the human worker can interact with the robot to solve the assembly error situation. In the Programming by Demonstration paradigm (PbD) [60], the robot itself acts an input device for facilitating Kinesthetic Guidance (KG) and it is an intuitive approach which can be successfully used by subjects which are not familiar to robot programming [61], [62]. 3D mouse (space mouse), a 3D haptic input device and a gamepad were used as the interaction medium in [63], for finding the best input device for controlling continuum robots. Another study [64] used a keyboard, a joystick and a camera for robot control. Teleoperation using a virtual keyboard and flystick done by [65] and [66] respectively. Most of the industrial robots are controlled using a manual control pendant (MCP), this could be used for an interaction as well [67]. These solutions however lack practicality and in an industrial context these might not be viable in most cases. The cognitive load on the users can be much more than anticipated while using an external feedback device and these methods are often non intuitive.

The best solution in such cases is to facilitate the usage of pHRI, this allows the user to solve the problems or execute the assembly. Introduction of pHRI in such cases eliminates the necessity of an extra interface which might overload the cognitive requirements from the user. In order to prove this hypothesis an user-study was conducted in an industrial scenario, where a user interacts with a compliant robot in-order to solve a typical assembly problem. Though this scenario does not cover the whole pHRI cases, it shows the importance of pHRI and the advantages it brings forth. In the conducted user-study, commonly used input devices such as keyboard and space mouse are used and alongside with two other methods by which the user interacts with the robot directly.

3.2 Experiment Setup and User Study

The compliant platform used in this experiment was KUKA Light Weight Robot (LWR IV+). The robot is attached to the ceiling thereby it disturbs the participants as little as possible. The assembly scenario evaluated consists of a shaft with two mutually displaced keys on it and a conrod with a notch attached to robot's end-effector, See Fig. 3.1 and Fig. 3.4a. The shaft is placed on top of a force-torque (FT) sensor and the measured forces are visualized on a monitor. The participants in this study was instructed to to mate both workpieces in the mating direction shown in Fig. 3.4a, so that the conrod is placed at the lower end of the shaft.

In order to improve the intuitiveness of the interaction and to assist the participants, the experimental setup also consists of and augmented interface to facilitate manipulation of the robot's end-effector, See Fig. 3.1. The augmented interface visualizes the force vector, its components and the robot's motion is visualized. Due to the fact that the FT sensor is placed below the shaft only acting contact forces can be visualized. Working with this, the user can compensate any unintentional forces and motions just by observing the force vector performing corresponding inputs.

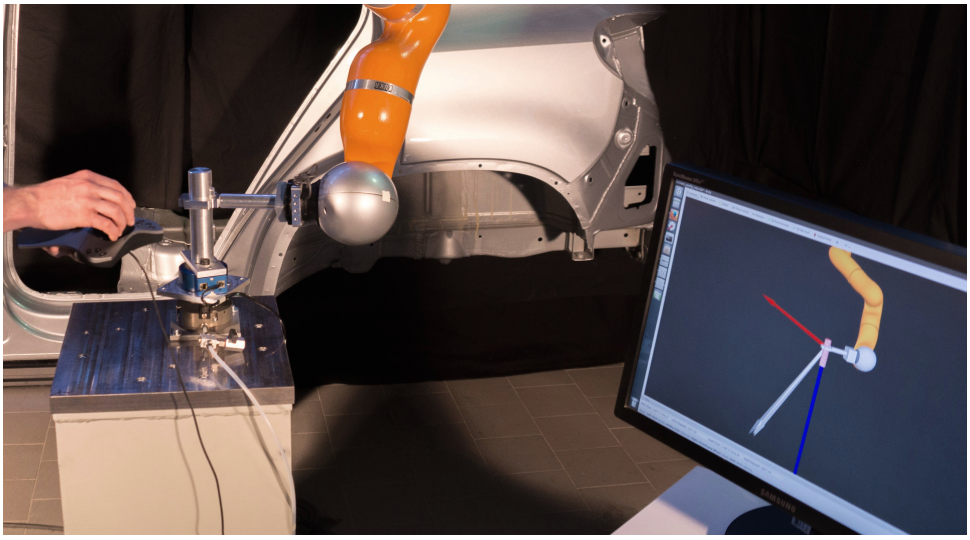

Figure 3.1: Experimental setup of the user study. The robot is attached to the ceiling and the user can be seen operating a space mouse.

3.2.1 Interaction Methods

In order to compare the significance of pHRI over other generic interaction methods, commonly used interfaces like keyboard and space mouse are selected for the user study. These two input devices are considered as interaction methods because they can be used without additional cost for deploying new hardware. In the pHRI paradigm two methods are compared, first one being a Kinesthetic Guidance (KG) which and second one being an adaptive KG.

3.2.2 Keyboard

A generic keyboard is used as an interface to interact with the robot to facilitate intuitive control. User can achieve this by the aid of visualized forces on a computer screen, see Fig. 3.1. Specific keys on the keyboard were designated to update the robot position and orientation in individual axis. If a key is pressed during a control cycle, constant displacements c_{dis} are added to the current pose incrementally. It is calculated by multiplying a displacement value d_v with the control cycle time t_{cycle}. Here, d_v was set to $0.5\frac{m}{s}$ based on previous experiments.

3.2.3 Space Mouse

Space mouse is another commonly used device for HRI where the user control one DOF at a time by exerting force / displacement in the desired direction of motion [63, 66]. The simple interaction scheme of the space mouse makes it intuitive for untrained and naive users. When the user interacts with the space mouse, the interaction amplitude $amp \in [0, 1]$ is measured, treated as a velocity (translation: $\left[\frac{m}{s}\right]$, rotation: $\left[\frac{rad}{s}\right]$), and scaled. This scaled value is later multiplied with the maximum velocity to obtain the commanded end-effector displacement.

3.2.4 Kinesthetic Guidance

Kinesthetic Guidance (*KG*) is one of the most popular approaches of pHRI following the Programming by Demonstration paradigm [61]. In this case, the human operator is required to physically guide a robot to perform the desirable skill or the task under consideration [60]. *KG* is considered a highly intuitive interaction method for both expert and naive users. *KG* allows tapping into task knowledge of the human worker without a need for accurate modeling of task constraints.

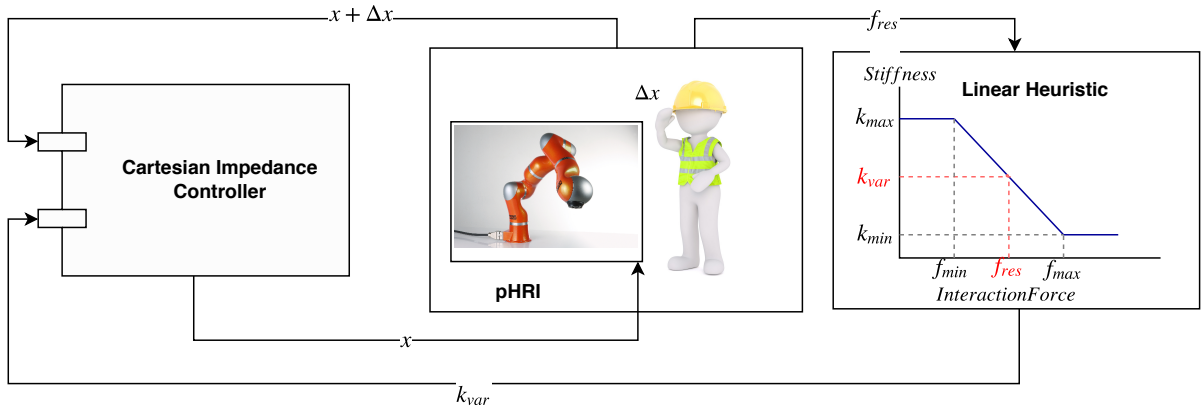

Figure 3.2: Each control cycle a stiffness adaptation is performed and the updated stiffness k_{var} is used by the impedance controller of the robot. The contact force of the HRI is used w.r.t. to the force limits f_{min} and f_{max} and to the stiffness limits k_{min} and k_{max} during the adaptation process.

Two *KG* methods were compared in the conducted user study. In the first method which is a normal *KG*, the robot is operated in a pseudo gravity compensation mode, here the robot can be guided physically by the users easily and the robot itself will compensate for its own weight. This is achieved by using the Cartesian Impedance mode of the KUKA LWR.

In the second mode, the adaptation of robot's cartesian stiffness to the forces which are applied by the user is used and therefore it is called *Adaptive KG*, See Fig. 3.2. *Adaptive KG* is based on the assumption that when the desired Cartesian force in a certain direction is higher, then the stiffness value in that direction it should be decreased and vice-versa. The resultant user interaction force f_{res} is measured and mapped linearly to stiffness domain. The limits of the stiffness heuristic are set based on preliminary experiments, the interaction force limits are $f_{min} = 5N$, $f_{max} = 30N$ and the stiffness limits are $k_{min} = 100\frac{N}{m}$, $k_{max} = 1000\frac{N}{m}$.

3.2.5 Study Design

The user study was conducted with 31 participants, 22 were male and 9 were female. The participants were from different backgrounds, both technical and non-technical. The user study titled **M-2017-02** was conducted with approaval of the ethics committee of the Technische Universität Braunschweig.

The user study employed a within-subjects design to compare the different interaction methods mentioned. The study was designed in such a way that each participant

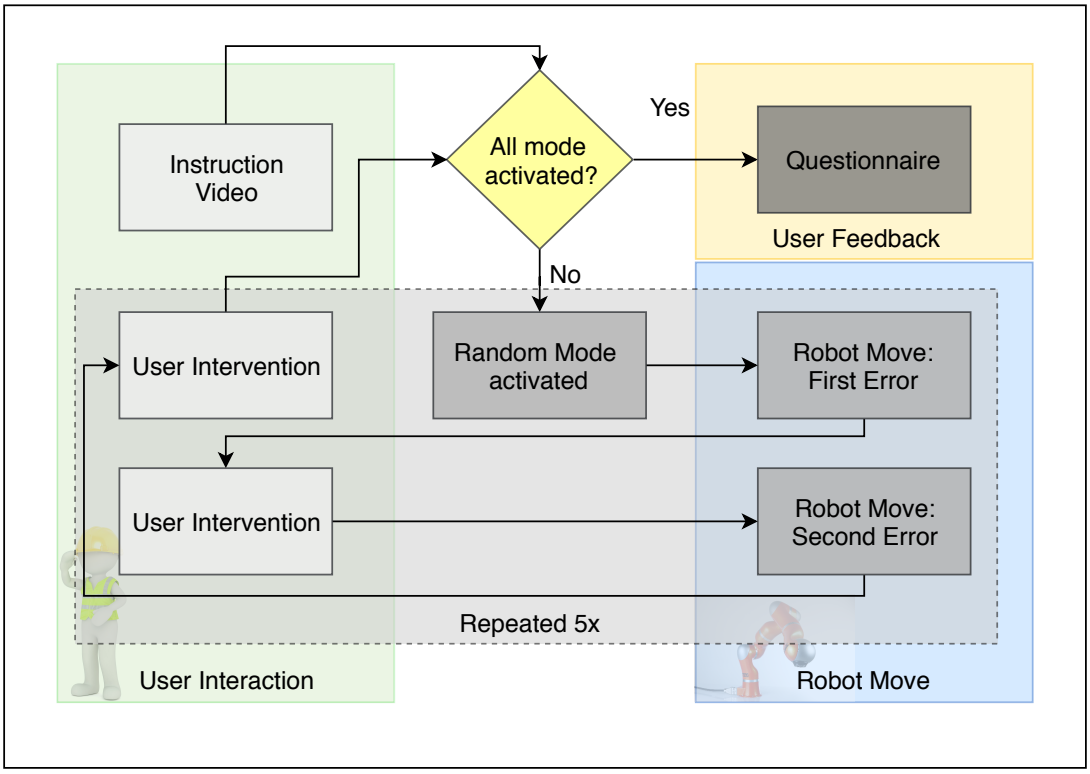

Figure 3.3: Experimental Flow of the user study.

experienced all four interaction methods during the task execution. The users solved two assembly problems with each interaction methods being used five times. The assembly problems which are on focus of this experiment is described in 3.2.6. The tasks were done one after the other, *top* assembly problem being the first task and *bottom* assembly problem is done after successfully finishing the first task. The sequence in which the interaction methods are activated was randomized for eliminating sequencing effects like learning and tiring.

A descriptive instruction video was shown to the participants at the beginning of the study to prevent biasing. Instructions about the tasks, the input devices used for each interaction method, the experiment protocol were explained in the video. The Cartesian impedance of the KUKA LWR is used for interacting with the robot. The user interaction data is recored and used for later analysis. During all trials the participants were free to walk around the setup. In this manner it was possible for each participant to choose always that field of view which was optimal for the used interaction method and the considered assembly problem. Directly after completing all experiments, the participants were required to fill in a questionnaire, where each participant ranked the interaction methods and gave general feedback.

3.2.6 Task Description

Top Assembly problem: The first task is to solve an assembly problem named *top* assembly problem. This occurs when the conrod, shown in Fig. 3.4a, is moved along the upper key of the shaft. In cases where the conrod is tilted against the against the normal mating

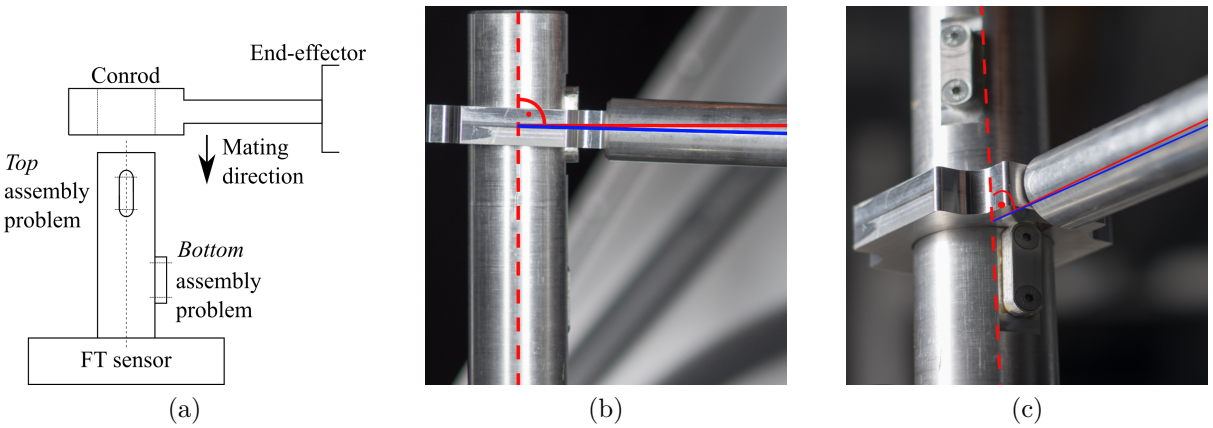

Figure 3.4: The overall approach. (a) Sketch of the experimental setup. (b) *Top* assembly problem. (c) *Bottom* assembly problem.

plane which is orthogonal to the longitudinal axis of the shaft, the assembly gets stuck and intervention is needed from user side. Fig. 3.4b, shows the top assembly problem, the dashed red line represents the longitudinal axis of the shaft, the blue line is the conrod's axis if there is an assembly problem. The red one shows how it should look like for being able to do the mating.

Bottom Assembly problem: The second task is to solve a similar assembly problem as mentioned above. This task named as *bottom* assembly problem occurs when there is a rotational incorrect alignment of the conrod with respect to the second key in the shaft. Fig. 3.4c shows this problem. The dashed red line represents the longitudinal axis of the shaft, the red line shows how the conrod's axis should be oriented and the blue line exemplary shows the orientation of the conrod during an assembly problem.

3.3 Evaluation

The evaluation is based on the data of Tab. 3.3 which has been generated by calculating the performance criteria mentioned in Section 2.3. TSM and FSM stands for Trajectory Smoothness and Force Smoothness respectively and denoted the results of the jerk analysis. The performance for each considered criterion are elaborated in the following sections.

3.3.1 Performance Criteria

Jerk analysis for the force profile showed that for *top* assembly problem and *bottom* assembly problem, *Adaptive KG* and *KG* had a better performance. Jerk analysis of the pose profiles yielded similar results with both *KG* methods performing better than other compared methods.

Considering the arc lengths, for the *top* assembly problem, $M_{KG} = 40.72$ is lower than other modes. For the *bottom* assembly problem, $M_{KA} = 24.17$ and $M_{KG} = 22.87$ are better than other two modes. Considering time of completion, for *top* assembly problem $M_{KA} = 4.14$ is the best and $M_S = 67.62$ is the worst. Results are similar for

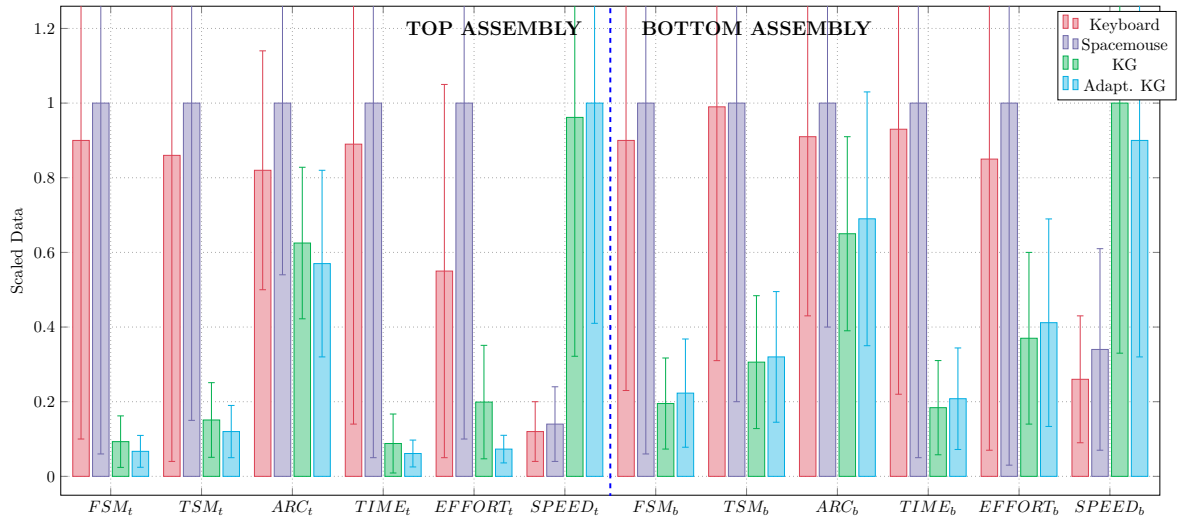

Figure 3.5: The figure illustrates the performance of each interaction method in the considered criteria, the scaled data is used for easier visualization and comparison.

Variables			FSM $\left[\frac{N}{s^3}\right]$	TSM $\left[\frac{mm}{s^3}\right]$	Arc $[mm]$	Time $[s]$	Effort $[N']$	Speed $\left[\frac{mm}{s}\right]$
Top	*K.*	M	12847	45.61	53.62	60.38	54.99	1.04
		SD	11326	34.19	21.07	50.72	49.74	0.78
	S.M	M	14197	52.85	65.00	67.62	100	1.27
		SD	13374	45.05	30.22	64.44	90.94	0.93
	KG	M	1330	7.99	40.72	5.96	19.98	8.46
		SD	979	5.42	13.40	5.37	15.23	5.70
	A.KG	M	960	6.39	37.34	4.14	7.30	8.80
		SD	618	3.78	16.34	2.57	3.73	5.21
Bot.	*K.*	M	7007	27.74	31.74	34.42	75.33	0.87
		SD	5206	18.97	16.75	26.32	69.59	0.58
	S.M	M	7718	27.78	34.82	36.68	88.88	1.15
		SD	7289	22.25	20.61	34.92	100	0.92
	KG	M	1506	8.51	22.87	6.78	33.64	3.23
		SD	947	4.97	9.20	4.63	20.48	2.25
	A.KG	M	1725	9.02	24.17	7.64	36.59	2.96
		SD	1118	4.87	11.92	5.01	24.70	1.94

Table 3.1: Mean and Standard Deviations of Performance criteria for each control mode and both assembly problems.

bottom assembly problem as well. In the criterion of mean effort, both *KG* methods performed better. The mean cartesian speeds during the *top* assembly task for each interaction mode are $M_{KA} = 8.80$, $M_{KG} = 8.46$, $M_K = 1.04$, $M_S = 1.27$ respectively and during the *bottom* assembly task are $M_{KA} = 2.96$, $M_{KG} = 3.23$, $M_K = 0.87$, $M_S = 1.15$ respectively.

User Satisfaction User satisfaction represents the degree of favorableness the user shows concerning the system [41]. This criterion was measured from the rating given by the users from the questionnaire which each participant filled in after the experiment. The rating was on a scale from 1 to 4 where 1 means the best, and 4 means the worst. The users rated their overall experience about the control modes, and there was no distinction made between the top and bottom assembly problems.

The results of the user satisfaction rating for the both assembly problems are as following, $M_{KA} = 1.48$ and $SD_{KA} = 0.88$, $M_{KG} = 1.77$ and $SD_{KG} = 0.95$, $M_K = 3.23$ and $SD_K = 0.84$, $M_S = 2.97$ and $SD_S = 1.96$.

Measure of Intuitiveness In the scope of this experiment, learning effect can be defined as observed if the users improve their performance while performing the task multiple times. Intuitiveness could be expressed as a function of a learning effect, so it can be argued that in an intuitive scenario, the performance of a user would already be much better [50]. This measure helps in understanding more about the intuitiveness of each control mode. Fig. 3.6 shows the learning curves of all considered interaction modes while performing the *top* assembly problem. A high slope of the learning curve reflects the user's inability to adapt to a particular mode, and it could be inferred that the mode is counter-intuitive. Similarly, learning curves with low slope points at that mode being intuitive. In such cases, the user's intuition will lead them automatically to the best solution.

3.3.2 Discussion

The results elaborated in the previous sections points at the fact that both *KG* modes are smoother and more suited for pHRI than the other compared interfaces. Both *keyboard* and *space mouse* resulted in large values of jerks in force profiles which are significantly higher than the *KG* methods. While analyzing the jerks in generated trajectory, the *KG* methods are far better than their counterparts. In this case, the *Adaptive KG* has the lowest jerk in the *top* assembly problem and both *KG* methods have comparable results in the *bottom* assembly problem.

Both *KG* methods resulted in shorter arc length allowing the users to solve the assembly task faster in an optimal manner without much deviation from the intended trajectory. While comparing both *KG* methods, *Adaptive KG* has smaller arc length in both *top* and *bottom* assembly problem. Similarly, while analyzing the time of completion, the*KG* methods are significantly faster than the other methods for both tasks. In this case, performance of both *space mouse* and *keyboard* are comparable.

The results show that the effort in task completion needed by the *KG* methods is much lesser than the *space mouse* and *keyboard*. Similarly, the Cartesian speed of both *KG* methods is similar and higher compared to the other two modes. An inference can

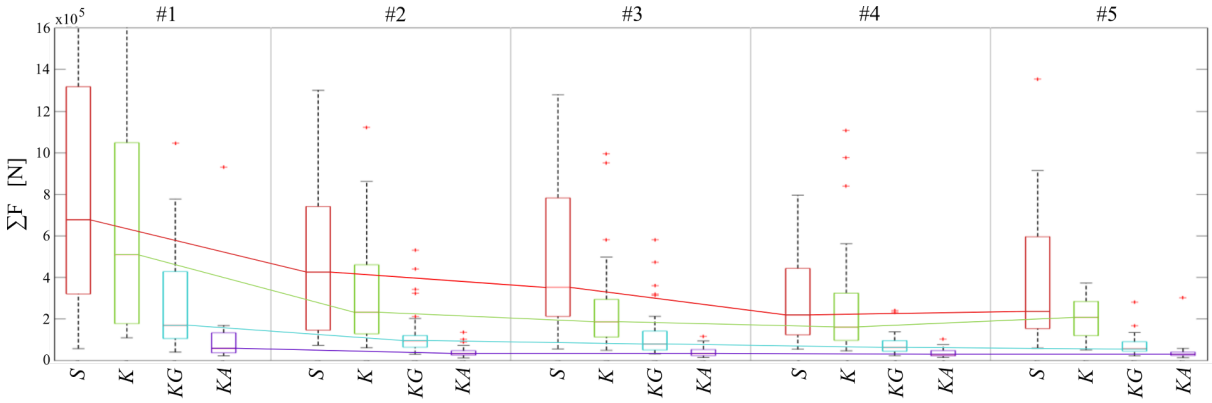

Figure 3.6: Learning curves for the *top* assembly problem based on the summed force of all participants for each trial. The curves shows the learning effects of the participants and the differences between the individual methods (Keybord, Space mouse, Kinesthetic Guidance, Adaptive Kinesthetic Guidance).

be drawn that the user's knowledge of how to solve a task intuitively while interacting kinesthetically is the main reason for the superior performance of *KG* modes.

While analyzing the measure of intuitiveness and user satisfaction, *KG* methods are superior. The user satisfaction with *keyboard* is the worst and with the *Adaptive KG* is the best. The learning curves from Fig. 3.6 suggest that both *KG* modes are intuitive compared to the other input methods. While comparing both *KG* methods, in the *top* assembly problem *Adaptive KG* outperforms the normal *KG* and in the *bottom* assembly problem both are comparable.

Fig. 3.7 illustrates the performance of the considered interaction modes based on their statistical significance. The *KG* methods always have a clear advantage over the other method as illustrated in the charts. The performance of *keyboard* and *space mouse* remains similar for both assembly problems, with *keyboard* having a slightly better performance to *space mouse*. The *Adaptive KG* is suited for the *top* assembly problem. While for the *bottom* assembly problem, stiffness adaptation might not be necessary since there is no statistical difference in the performances except in case of user satisfaction. One possible reason might be that the *bottom* assembly problem is easier to solve and therefore no stiffness adaption is essential.

3.4 Conclusion

It could be concluded from this user study that Kinesthetic Guidance is the best-suited method for Human Robot-Interaction in the considered industrial assembly scenario. *KG* methods had good performance as well as user satisfaction, and this could be attributed to the fact that the users get direct tactile feedback while interacting Kinesthetically, this makes the interaction more comfortable and more intuitive for the users. Analysis of learning curves shows that *KG* methods are the most intuitive way of interacting with the robots. Even a small amount of trials resulted in satisfactory interaction and superior performance. Also, the performance of the adaptive controller is higher during the top assembly, and further improvement of this control method would be a reliable strategy

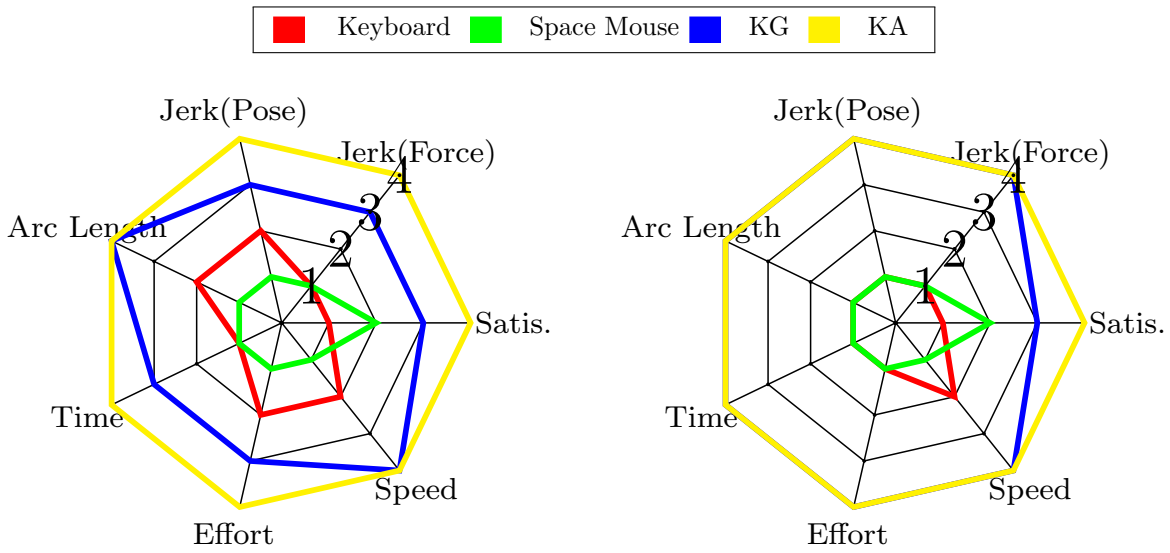

(a) Qualitative

(b) Quantitative

Figure 3.7: Radar chart showings the ranking of the control modes for each performance criterion depending on their statistical significance, 4 is best rank and 1 is the worst.

for improved pHRI. This result shows the significance of pHRI in industrial scenarios and how it could be used to simplify tasks, which could otherwise be cumbersome and time-consuming.

Chapter 4

Personalized Adaptation: User Force based approach

In chapter 3, pHRI was compared with standard interfaces and methods for Human Robot Interaction, it was clear from the results discussed that pHRI offers much more advantages compared to standard input devices. The results hinted at the intuitiveness, easiness and reduced overall effort while using pHRI. Among the two pHRI methods considered, adaptive Interaction based upon user forces offered more assistance for the Human-Robot Interaction in difficult scenario.

In this chapter, it is discussed how to improve the pHRI by taking into consideration the users parameters, e.g: Force limits of the user. A control method which is based on personal force parameters of the user is proposed and validated. The proposed control method is compared to standard industrial approaches through an experiment where 49 users participated. The results of the experiment and the noticeable findings from this experiment are elaborated in this chapter. The chapter is based on the work published in [68].

4.1 Need for Personalization in pHRI

As discussed in the previous chapters, including the human's cognitive and perceptual skills can improve the pHRI [69], allowing knowledge transfer from human entity to the robot. The variance in human factors are quite high and can hinder the development of pHRI systems which works well for every user. This motivates to research adaptive stiffness control to mitigate the effects of such uncertainty in the physical user behavior. Most of the current research in this direction are rather complicated adaptation schemes that have been demonstrated in laboratory prototypes on typically very simple tasks like following a straight line [20], as illustrated in Tab. 2.1. They have neither been evaluated, nor tested with naive target users. Nor has the implicit assumption that such adaptation is beneficial for task performance and or user satisfaction been validated on any reasonably complex task.

The results from the last Chapter 3, clearly show the benefits of adaptive stiffness control modes. It was shown that the efficiency, performance and intuitiveness can be improved by adapting the robot to parameters to the human factors. However the variance in the user behavior is often high and rather unpredictable. User variability occurs

in many respects, for instance in height, body proportions, force profile, left or right handedness, the distance the user keeps with the robot, varying cognitive skills, etc. Most of the related work proposes certain control schemes or learning methods, which focuses on optimization of one or more performance parameters. Even with the most complex and efficient learner the results might be different for different users, as each user is unique with highly variable and unpredictable characteristics as discussed.

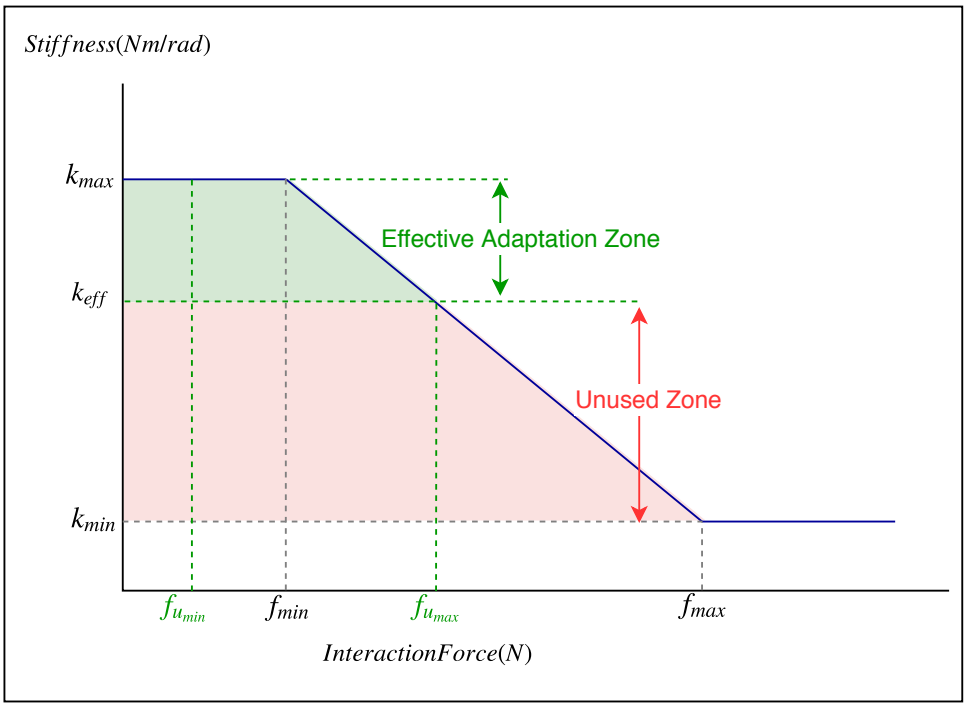

Figure 4.1: Figure illustrating the importance of personalization in pHRI. When the user physical capabilities are below the average limits.

Although the force based control scheme mentioned in previous chapter performed better than other control methods in the difficult task, this kind of adaptation is not optimal as the personal characteristics of each user is not respected. Fig. 4.1 and Fig. 4.2 illustrates the problems that could occur if the variance among humans are not taken into consideration. If the force limits for the adaptation (f_{min}, f_{max}) of the controller is set to an average value and if the users interaction forces are much below this average the controller may not adapt well to the user interaction forces, this is shown in Fig. 4.1. In such case the maximum and minimum force the user is capable of producing is $(f_{u_{min}}, f_{u_{max}})$, therefore the effective adaptation zone is restricted between the region k_{max} and k_{eff}. This is a region, represented as green area in the illustration is a region of high stiffness and hence a weak user will experience a stiff robot and this will affect the overall interaction. They will find it hard to move the robot well and the performance will drop over time. The red region in the illustration represents the unused low stiffness range which would have made the interaction easier for this particular set of users.

The second case of improper stiffness adaptation is illustrated in Fig. 4.2. In this case the user is stronger than the average human, and the use force limits $(f_{u_{min}}, f_{u_{max}})$ are much higher than the calibrated limits (f_{min}, f_{max}) of the controller. Hence in this

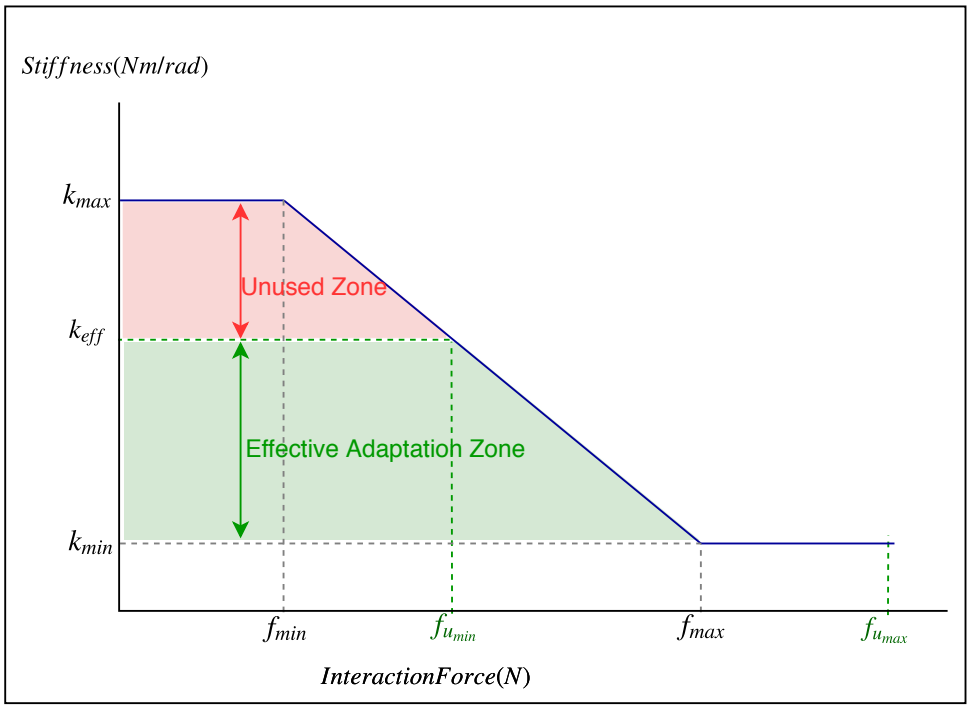

Figure 4.2: Figure illustrating the importance of personalization in pHRI. When the user physical capabilities are above the average limits.

case the effective adaptation zone is limited between k_{eff} and k_{min}, represented as green region in the illustration. This is a region of low stiffness and the users will interact only with low stiffness range of the robot. In such cases, the probability of them making error will increase. The red unused zone would have been a better operating zone for this set of users.

It is clear from the above mentioned example that the controllers needs to be calibrated to each user individually in-order to maximize the interaction quality. Taking these factors into consideration a novel personalized control and adaptation strategy was designed. This is explained in Section 4.2, It was taken into consideration that the proposed control mode is feasible in practical terms by avoiding tedious and complex training. In this way, it can be readily applied to real world scenarios and evaluated with naive users.

4.2 Personalized Adaptive Stiffness Control

Motivated by the facets discussed in Section 4.1, a controller scheme is proposed which takes into consideration the user's personalized limits. It was devised that from the prior interaction of a particular user with the robotic system, it is possible to calibrate their force range (f_{min} and f_{max}). This force range when given as the limits of the linear heuristic for the stiffness adaptation results in better performance. In such case the whole stiffness range could be used effectively. Meticulous calibration of the user limits combined with fast and effective heuristic shall increase the performance and comfort of the user. The following section describes the implementation details of the Personalized

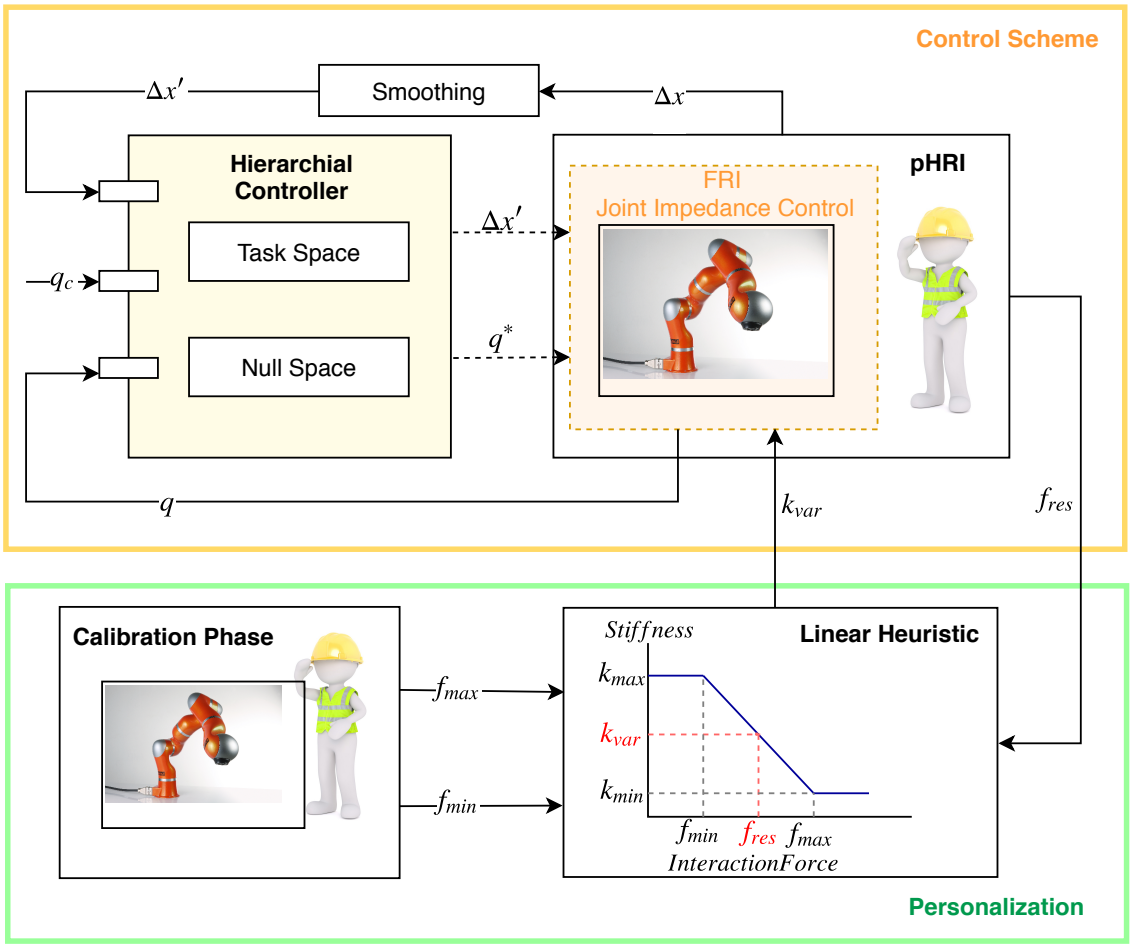

Figure 4.3: Block diagram showing the the Personalized Adaptive Stiffness mode implementation and the control architecture.

Adaptive Stiffness control mode.

Compliant Robot Platform

A redundant 7-DOF KUKA Light Weight Robot (LWR IV) [70] equipped with a BarrettHand (BH8) [71] is used to develop and test the above mentioned control schemes. The LWR IV is a redundant robot with seven joints. This redundancy allows the end-effector to reach one point in task space by multiple joint configurations. Based on torque sensing in each joint, the LWR IV is an active compliant robot and has an impedance based control scheme [72]. The BarretHand deployed in this experiment consists of three fingers equipped with fingertip torque sensors and has tactile sensing at the palm. A fixed tool is mounted on the end-effector of the robot to facilitate the experimental tasks.

Interaction Control Scheme

The user interaction at the end effector of the compliant robotic arm will produce a Cartesian displacement Δx relative to the currently controlled equilibrium point x for

the end-effector. Hence, the new desired Cartesian equilibrium can be represented as:

$$x^* = x + \Delta x. \tag{4.1}$$

The CBF controller proposed in [73] is used to convert the target displacement Δx into joint space through standard velocity kinematics with hierarchical redundancy resolution. The CBF controller which in turn is based on hierarchical framework proposed in [74] generates nullspace motion to maintain a preferred redundancy resolution configuration q_c, while achieving as primary task the Cartesian target displacement as:

$$\begin{aligned} \Delta q &= J^{\dagger}(q)\Delta x^{'} + (I - J^{\dagger}J)\Delta q_c \\ \Delta q_c &= q - q_c, \quad \Delta x^{'} = (1-\alpha)\Delta x \\ q^* &= q + \Delta q \end{aligned} \tag{4.2}$$

$J^{\dagger}$ represents the Moore-Penrose-Pseudoinverse of the task Jacobian. The smoothing factor α, can have values between 0.1 and 0.5 to smooth the displacements and prevent drift. Such an implementation allows the user to interact seamlessly with the robot while physically guiding the end-effector. This controlled mode was introduced in [73] as "Assisted Gravity Compensation", allows for mimicking Gravity compensation from the points of view of the user while concurrently controlling for a preferred redundancy resolution. Fig. 4.3 shows the complete control architecture. During the interaction the LWR's native *joint impedance mode* is used. The control modes are implemented within *Compliant Control Architecture* [75] and the program flow and state machines for the experiment are implemented using the Domain-Specific Language described in [76]. As illustrated in the Fig. 4.3, the adaptive scheme have two parts. The first part being the control scheme responsible to the robot control and the second part being the personalization part where there user parameters are calibrated. Another advantage of this implementation is that the users get assistance since the redundancy resolution is being suitably selected for the given task. This concept was introduced in [73], this makes the kinesthetic teaching and interaction with the robot much easier for the user.

In the *Personalized Adaptive Stiffness mode*, a simple heuristic is used to adapt the stiffness of the robot on-line dependent upon the applied interaction force with a simple linear law. This model was selected for its simplicity and the mapping of the user's interaction forces to stiffness is straight forward and fast, hence it could be used for on-line adaptation. The stiffness is set to vary between a maximum of $k_{max} = 1000Nm/rad$, which is set based on the trials conducted in the pre-study and a minimum of $k_{min} = 10Nm/rad$. The Adaptive Stiffness k_{var} is calculated on-line as

$$k_{var} = \left(\frac{(k_{max} - k_{min})}{(f_{min} - f_{max})} \right) (f_{resultant} - f_{min}) + k_{max}. \tag{4.3}$$

The forces f_{max} and f_{min} are the maximum and minimum interaction forces at end-effector from a user which was calculated from prior user interaction. As discussed in Section 4.3.1, an initial warm-up phase is used to calibrate the user's limits. In order to calibrate and personalize the control mode for each user respectively, the force limits are calculated for each user separately. The resultant force, $f_{resultant}$ is the instantaneous

resultant force that the user applied at the end-effector. The mapped stiffness value k_{var} is then filtered using a second order low-pass filter and forwarded to the joint impedance controller of the LWR.

$$\begin{aligned} k_{f_i} &= bk_i + bk_{i-1} + ak_{f_{i-1}} \\ a &= \frac{(1-\alpha)}{(1+\alpha)}, b = \frac{(1-\alpha)}{2} \end{aligned} \tag{4.4}$$

Here, k_{f_i} is the filtered stiffness value at a particular instant, α and β are the filter parameters.

4.3 Experimental validation of Personalized Adaptive Stiffness control

In order to validate the performance of Personalized Adaptive Stiffness control and to compare it with other commonly used interaction control modes in pHRI, a user-study was conducted with both expert and naive users. The study with 49 users evaluated the three constant stiffness modes (High, Medium, Gravity Compensation) and the Personalized Adaptive Stiffness control mode both quantitatively and qualitatively, i.e. with regard to task performance and user satisfaction, respectively. The compared interaction control modes are described in Section 4.3. Based on the characteristics of four compared modes following assumptions were made about the outcomes: The Gravity Compensation mode will be faster but less accurate, High Stiffness mode will be slower but more accurate and Medium Stiffness mode will be in between Gravity Compensation and High Stiffness mode in terms of time and accuracy.

The following experiment answers certain basic questions regarding control mode design for pHRI, such as:

- Can adaptive controllers excel over widely used control modes (Gravity Compensation and Constant Stiffness modes) in terms of performance and interaction quality, when used by non-expert users?
- How much influence does inclusion of human factors bring into interaction quality of pHRI?

Each participant encountered two identical tasks of varying difficulty and all four control modes activated in random order. A key result which emerged from the results of the experiments is that in the more complex task environment adaptive controller assists the users well. The performance of the user increases significantly with the help of personalized adaptive stiffness control in this case. On contrary, the advantage is marginal in case of the low complexity task. Hence, the task dependency is highly significant and needs to be accounted for.

Interaction Control Modes

The control modes compared in this user study are: (Assisted) Gravity compensation, High stiffness, Medium stiffness, and Personalized Adaptive Stiffness. The implementation of these modes are based on the described control scheme described in 4.2, with a

suitable redundancy resolution in-order to facilitate smooth user interaction. The stiffness of the latter is set to different values accordingly or adapted on-line, while the damping is kept constant during the interaction at a value of 0.7 $Nm * s/rad$ for all modes.

In the *assisted Gravity Compensation mode*, the stiffness of the joints is set to 10 Nm/rad such that the forces applied by the users are hardly counteracted by the robot. In this mode the robot is compliant and the user can move the robot through physical interaction. As implemented in [77], the native Gravity Compensation of the LWR is reimplemented using the above specified control scheme.

In the *High Stiffness mode*, the stiffness of the robot is set to 800 Nm/rad. The high value of joint stiffness increases the resistance the robot offers to the user. The users are expected to move the robot slowly which eventually will result in higher task accuracy.

In *Medium Stiffness mode*, the joint stiffness is set to an intermediate value of 400 Nm/rad. In this mode, the robot moderately resists the displacement caused by the user interaction. The stiffness values of High and Medium Stiffness modes were selected based on the pre-studies.

4.3.1 Study Setup

The robotic system for the user-study was designed to emulate common industrial applications (e.g. welding or gluing) where the robotic arm is used as a tool and the user moves the arm kinesthetically by physically touching the robot and its end effector while fulfilling the given task. Fig. 4.4 shows the experiment setup.

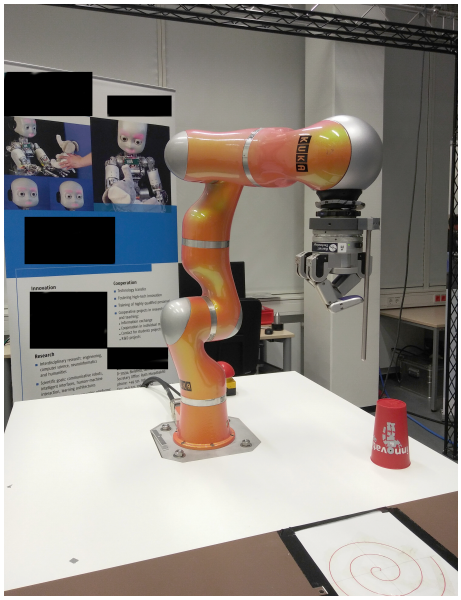

Figure 4.4: The experiment setup, 7 DOF KUKA LWR IV equipped with BarrettHand and unmountable tool

To compare the four control modes, a within-subjects study design was chosen, where each participant experiences all four control modes. This design has been chosen, because it is economic and eliminates possible influences from individual-related confounding variables [78]. The interaction control modes were activated in random order to prevent the

occurrence of sequencing effects (like learning or tiring effects). Quantitative performance measures were computed from the data recorded and a subjective evaluation of the interaction quality for each participant is done utilizing a questionnaire.

As introduced in [62], the user-study was divided into two phases. The first phase is an initial warm-up phase. Here, the user interacts with the robot and the individual force profile is subsequently recorded for calibration of the adaptive stiffness mode. The second phase is the task phase where two tasks are executed by the users. The tasks are executed in the same order for all participants but using a random controller activation order. At the beginning of each task, an instruction video demonstrating how to accomplish that particular task was shown to the users. Fig. 4.5 illustrates the experiment flow.

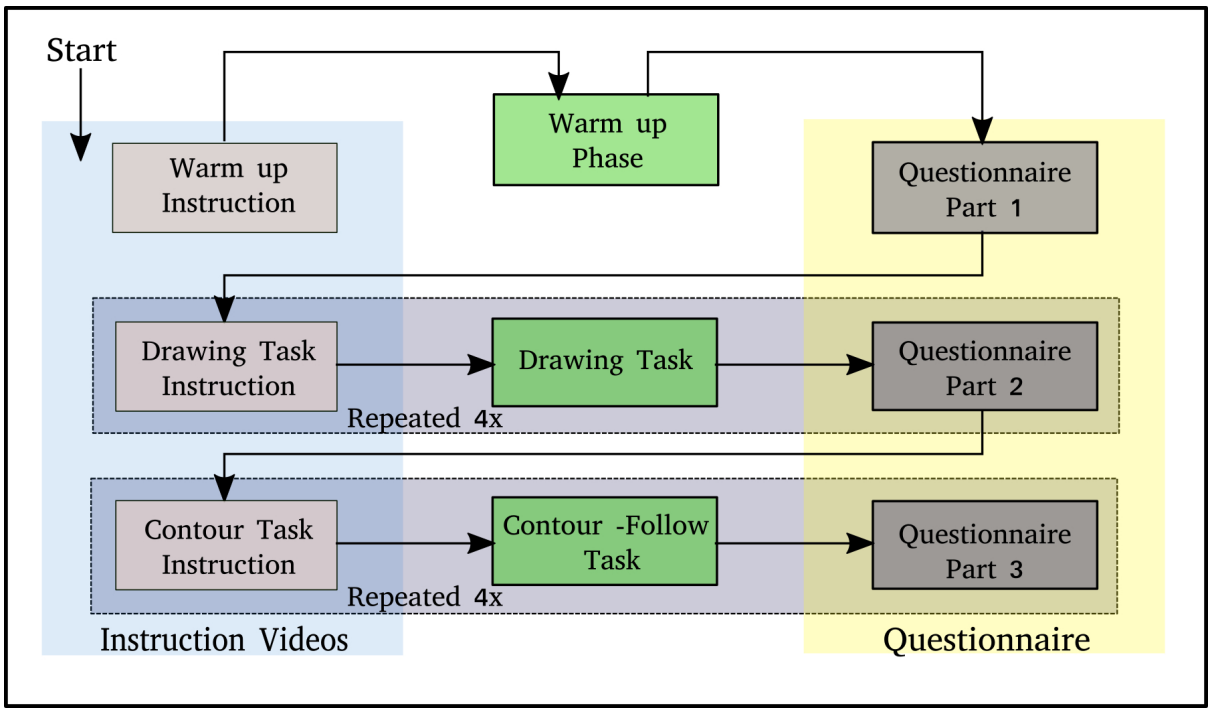

Figure 4.5: The experiment flow is shown in this figure, the users have to finish both phases in order to successfully complete the study.

Warm-up Phase

In this phase, the users get themselves familiarized with the robot, and they were required to play a pick and place game. The users physically interacted with the robot to move its end-effector and to pick up five randomly placed objects in the work-space. The objects are grasped with the help of the palm sensor in the Barret Hand, which is programmed to open and close when pressure is sensed. As the users press the hand on to the object, the grasping is done. Fig. 4.6a shows one of the participants accomplishing the warm-up phase.

The warm-up phase had an important secondary purpose. While the user interacts with the end-effector, a force observer program continuously monitors the forces applied by the user on the end-effector and calculates the minimum (f_{min}) and maximum (f_{max})

interaction forces applied by each user. In this phase, the robot's stiffness is set to a medium value. The underlying assumption, which is supported by the pre-studies and previous experiments, is that each user has different physical capabilities and hence the force applied by each user will vary significantly. Calibrating an adaptive stiffness controller to work within these force limits accounts for these varying physical capabilities [68].

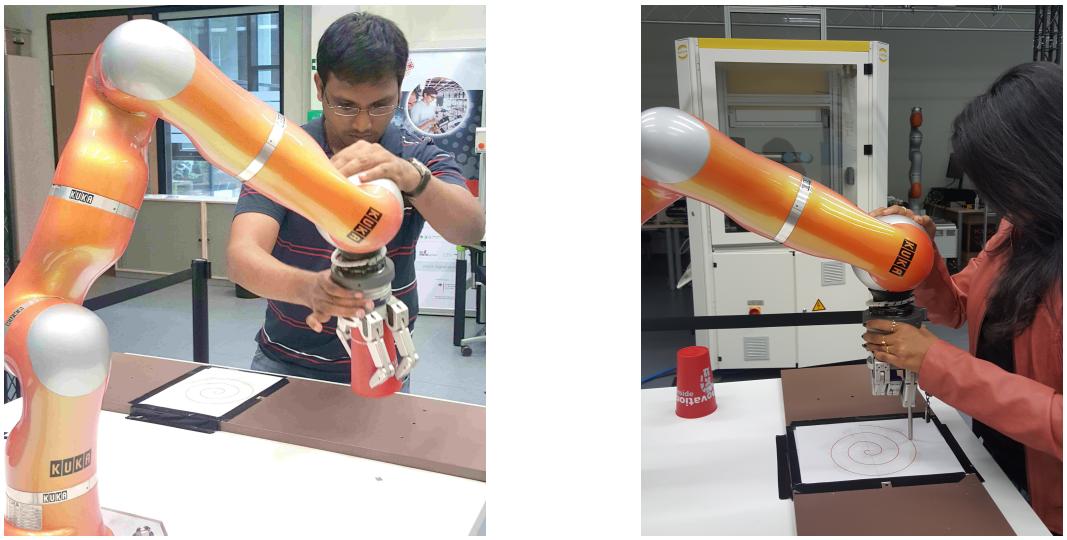

(a) (b)

Figure 4.6: Figure illustrating the different phases in the user-study. (a) Warm-up Phase (b) Task Phase: Drawing Task

Task Phase

In this phase, the users were asked to perform two meaningful tasks with all four different control modes. The tasks were designed in such a way that it resembles common industrial tasks like welding or gluing. The idea was to have an interaction scenario where the robot assists the user by holding the heavy workpiece, and the user moves the heavy tool in a predetermined trajectory for completing the task. It was determined from the preliminary studies that the defined task should neither be too easy nor too complicated for naive users.

Drawing task The first task was a drawing task where the users were asked to follow a predefined inward spiral on a flat surface, re-drawing it with a pen attached to the end-effector on a sheet of paper. The inward spiral was sketched on a paper in the same position in the workspace for each user for standardization. The users followed this spiral trajectory starting from the outside of the curve and ending at the center point. The users were asked to be as accurate as possible in this task while maintaining contact with the flat surface. As experienced in the pre-study, it is not easy to keep contact on the surface while moving the robotic arm along the curved path. Hence, this task was classified as a complicated task for the users. Fig. 4.6b shows a study participant executing this task.

Figure 4.7: Figure illustrating an user performing the Contour-following task

Contour-following task An easy but not trivial task was chosen as the second task, which was in contrast to the first task. This task was inspired by the wire-loop game mentioned in [62]. Here the participant moves the tool along the edge of a wooden 3D structure in the workspace of the robot. Unlike the first task where the user had to maintain contact to the surface, there were no constraints on the user in this task. Fig. 4.7 shows a study participant performing the Contour-following task.

4.3.2 Evaluation Measures

Questionnaire

The participants were asked to fill in a questionnaire during the experiment. This questionnaire was divided into three sections: In the first section the participants were briefed about the experiment and were asked to answer several questions on control variables (e.g., previous experience with robots). In the second the participants rated how they perceived the interaction with the robotic arm concerning controllability and reliability of the robot, user satisfaction and how enjoyable the task was during each trial. This section was filled after each interaction with the robot, i.e., four times during each task. The criteria used for this evaluation are elaborated in Section 2.3.1. The third section had to be filled in after completion of both the tasks, here the participants answered additional questions on demographic variables. The participants rating were done based on a 5-point answer scale (I agree/I do not agree). Table A.1 shows one example item for each qualitative criterion.

4.4 Experimental Results

4.4.1 Participants

A total of N= 49 users participated in the experiment, where 74.5 % were male, M_{age} = 31.67, SD_{age} = 10.46, and 78.7 % right-handed. Two participants were removed because of inconsistencies in the data. The participants were mainly full-time working

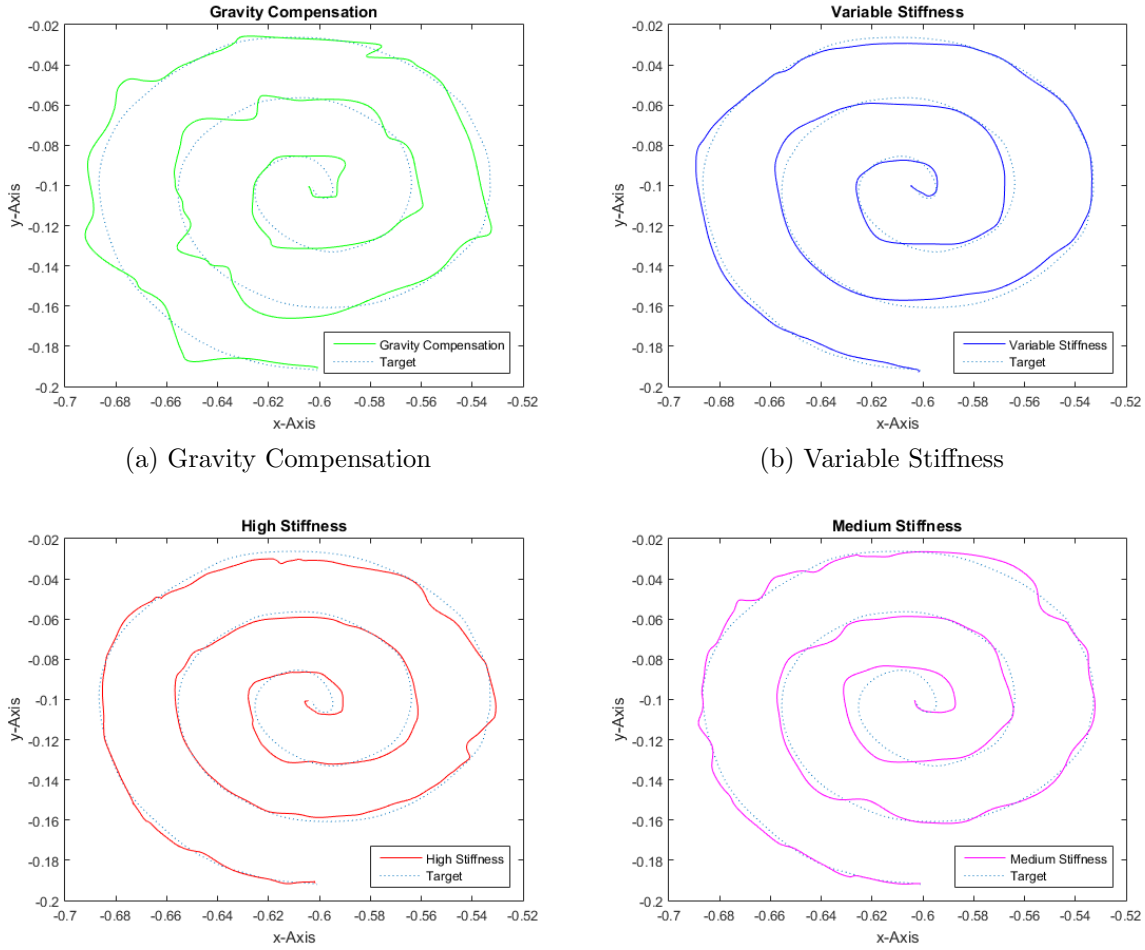

(a) Gravity Compensation

(b) Variable Stiffness

(c) High Stiffness

(d) Medium Stiffness

Figure 4.8: Performance of one user in Drawing task with 4 different control modes.

44.7 %, 31.9 % were students, 10.6 % part-time working and 4.3 % not working. The educational level was high, with 53.2 % having a university degree, 25.5 % having a higher vocational education. The participants in the study where acquired through snowball sampling system [79], following an initial advertisement. The user study titled *Human-Robot Interaction User Study* has been approved by Ethics-Commission of University of Bielefeld [80].

4.4.2 Hypotheses

Based on the characteristics of the four control modes described earlier, the following hypotheses were made on the outcomes of this comparison:

- H1: The gravity compensation mode will be faster but less accurate than medium stiffness or high stiffness.
- H2: The high stiffness mode will be slower but more accurate than medium stiffness or gravity compensation.

	Grav		Adaptiv.		Med.		High	
	M	SD	M	SD	M	SD	M	SD
Peaks	71.95	20.18	61.5	17.17	65.82	17.19	67.93	20.48
Proc.	0.53	0.20	0.63	0.17	0.54	0.20	0.64	0.20
Time	29.53	8.00	30.26	8.81	30.40	8.19	34.19	9.44
Jerk	1.46	0.16	1.36	0.15	1.46	0.13	1.39	0.18
Arc	0.87	0.03	0.84	0.02	0.85	0.02	0.84	0.02
Ease.	3.91	0.67	4.31	0.57	4.31	0.56	4.11	0.72
Enjoy	3.75	0.94	4.00	0.91	4.20	0.89	3.79	0.95
Reliab.	3.58	1.03	4.23	0.95	4.21	0.91	4.09	0.84
Cntrl	3.98	1.02	4.63	0.46	4.41	0.79	4.38	0.68
Satis.	3.84	1.04	4.44	0.85	4.30	0.83	4.09	0.95

Table 4.1: Mean and Standard Deviation of the Drawing task.

- H3: The medium stiffness mode will be in between gravity compensation and high stiffness mode in terms of time and accuracy.

- H4: The adaptive stiffness mode excels the other modes in terms of time and accuracy.

4.4.3 Results from the Drawing Task

Quantitative Performance Measures

On conducting Repeated measures ANOVA on the dataset of *time* a significant difference between different controllers ($F(2.57) = 13.95, p < 0.001, \eta^2 = 0.233$) were noticed. Comparison of Adaptive Stiffness and High Stiffness, ($p < 0.001$) shows a significant difference. Analysis of *procrustes* shows a significant difference between the performance of the controllers ($F(3) = 7.19, p < 0.001, \eta^2 = 0.14$). Adaptive Stiffness and Medium Stiffness ($p = 0.040$), and Adaptive Stiffness and Gravity Compensation ($p = 0.009$) also differ significantly. The dataset *number of peaks* shows a significant difference between the performance of the controllers ($F(2.54) = 12.38, p < 0.001, \eta^2 = 0.216$). Adaptive Stiffness and High Stiffness ($p = 0.007$), Adaptive Stiffness and Medium Stiffness ($p = 0.008$) and Adaptive Stiffness and Gravity Compensation ($p < 0.001$) differ significantly.

The means and standard deviations of the performance analysis criteria are tabulated in Table 4.1 and ranking based on significance is tabulated in Table 4.3, the modes have the same ranking if the difference is not significant. Fig.4.8, shows the performance of one user while performing this task.

User satisfaction and perceived quality of interaction

The dataset of *ease of use* shows a significant difference between the controllers ($F(3) = 9.05, p < 0.001$). Adaptive Stiffness differs significantly from Gravity Compensation ($p < 0.001$). The *perceived enjoyment*, ($F(3) = 3.40, p = 0.020$) and *reliability* ($F(3) =$

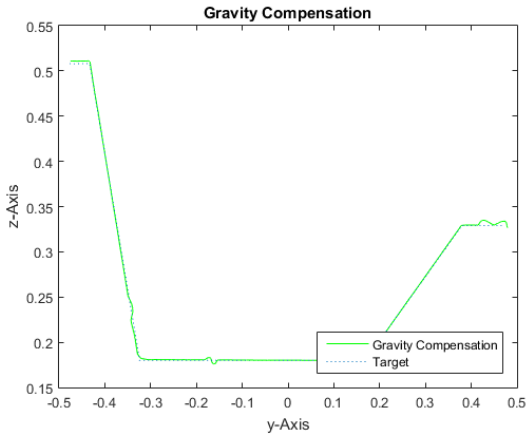

(a) Gravity Compensation

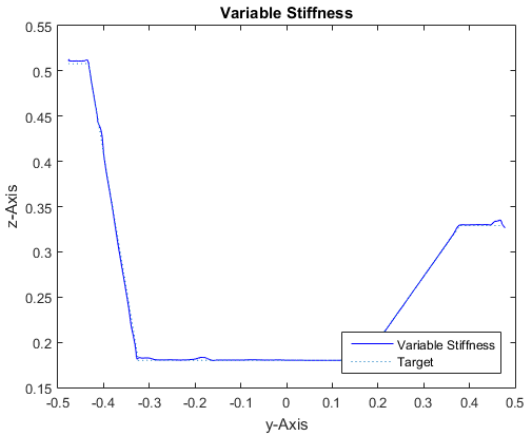

(b) Variable Stiffness

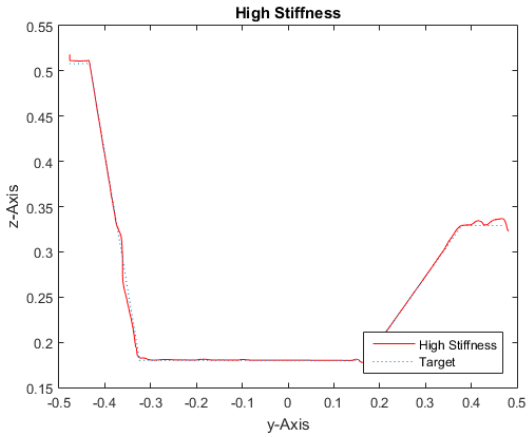

(c) High Stiffness

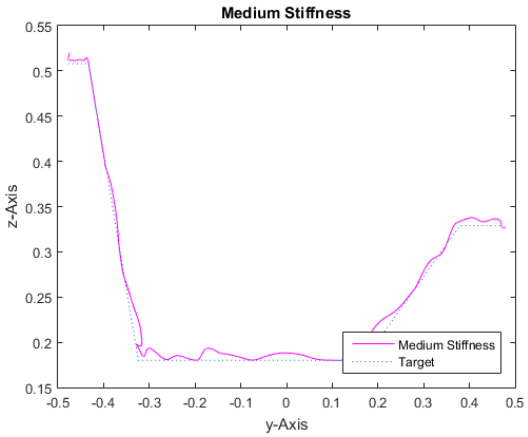

(d) Medium Stiffness

Figure 4.9: Performance of one user in Contour following task with 4 different control modes.

	Grav		Adaptiv.		Med.		High	
	M	SD	M	SD	M	SD	M	SD
Peaks	70.0	27.3	56.65	18.66	62.93	30.37	62.38	23.62
Proc.	0.94	0.13	0.94	0.13	0.94	0.12	0.95	0.02
Time	31.07	11.7	29.61	8.82	31.20	13.52	34.02	11.68
Jerk	1.35	0.19	1.37	0.17	1.31	0.19	1.36	0.18
Arc	1.25	0.16	1.19	0.11	1.21	0.14	1.20	0.75
Ease.	4.20	0.66	4.34	0.60	4.60	0.40	4.35	0.55
Enjoy	4.02	0.78	4.15	0.89	4.28	0.77	4.10	0.85
Reliab.	4.36	0.92	4.66	0.48	4.61	0.53	4.54	0.67
Cntrl	3.97	1.03	4.35	0.75	4.56	0.79	4.28	0.85
Satis.	4.18	0.90	4.35	1.02	4.53	0.73	4.46	0.70

Table 4.2: Mean and Standard Deviation of the Contour Following task.

$7.21, p < 0.001$) also shows a significant difference between the controllers. Adaptive Stiffness and Gravity Compensation ($p = 0.005$), Gravity Compensation and High Stiffness ($p = 0.014$), Gravity Compensation and Medium Stiffness ($p = 0.009$) differ significantly in case of *reliability*. Analysis of *external control* shows a significant difference between the controllers ($F(2.53) = 9.79, p < 0.001$). In this case, Adaptive Stiffness and Gravity Compensation ($p = 0.001$), Gravity Compensation and High Stiffness ($p = 0.011$) and Medium Stiffness ($p = 0.012$) differ significantly. Analysis of the dataset *user satisfaction* shows a significant difference between the controllers ($F(3) = 7.86, p < 0.001$). Adaptive Stiffness and Gravity Compensation ($p = 0.001$), Adaptive Stiffness and High Stiffness ($p = 0.017$), Gravity Compensation and Medium Stiffness ($p = 0.021$) differ significantly. Fig. 4.10 illustrates the performance of control mode for each comparison criterion. The the data is normalized to 1 here so that a direct comparison between multiple metrics is possible. Table 4.1, shows the detailed comparison of each controller.

4.4.4 Contour-following Task

Quantitative Performance measures

On conducting Repeated measures ANOVA on *Procrustes* no significant difference between the performance of the controllers were visible, while Mean procrustes are similar for all modes. The dataset *time* shows a significant difference between the time needed using the different controllers ($F(3) = 4.173, p = 0.007$). The mean time for Adaptive stiffness is lower than all other modes. Analysis of the dataset *number of peaks* shows a significant difference between the performance of the controllers ($F(2.53) = 6.529, p = 0.001$). In this case, there is a significant difference between the performance of Adaptive Stiffness and other control modes, Gravity Compensation ($p < 0.001$), High Stiffness ($p = 0.07$), Medium Stiffness ($p = 0.087$). The Mean number of peaks for Adaptive Stiffness is lower than other three control modes. The means and standard deviations of the performance analysis criteria are tabulated in Table 4.2. Fig.4.9, shows the performance of one user while performing this task.

		Peaks	Proc.	Time	Ease.	Enjoy.	Reliab.	Control	Satis.	Net
D.T	Grav.	3	2	1	3	3	3	3	3	1/8
	Adaptiv.	1	1	1	1	2	1	1	1	7/8
	Med	2	2	2	1	1	1	2	1	4/8
	High	2	1	3	2	3	2	2	2	1/8
C.F.T	Grav.	3	1	2	3	3	3	3	3	1/8
	Adaptiv.	1	1	1	2	2	1	2	2	4/8
	Med	2	1	2	1	1	1	1	1	6/8
	High	2	1	3	2	3	2	2	2	1/8

Table 4.3: Ranking of the modes in each criterion for both tasks.

User Satisfaction and Perceived Interaction Quality

There is a significant difference between the controllers ($F(3) = 7.7172, p < 0.001$) in terms of *ease of use*. The controller Variable Stiffness differs slightly from Gravity Compensation ($p = 0.89$) and similar to High Stiffness. Medium Stiffness differs significantly from High Stiffness ($p = 0.004$), Adaptive Stiffness ($p = 0.025$) and Gravity Compensation ($p = 0.001$). Analysis of *external control* shows a significant difference between the controllers ($F(3) = 6.025, p = 0.05$). The controller Medium Stiffness differs significantly from Gravity Compensation ($p = 0.006$). The performance is marginally significant from High Stiffness ($p = 0.228$) and slightly better than Adaptive Stiffness ($p = 0.012$). Analysis of the dataset *user satisfaction* shows a significant difference between the controllers ($F(3) = 7.86, p < 0.001$). Gravity Compensation ($p = 0.001$) and High Stiffness ($p = 0.017$), Gravity Compensation and Medium Stiffness ($p = 0.021$) differ significantly.

4.5 Discussion

It is clear from the results discussed in the previous Sections 4.4.3 and by comparing the means values from Table 4.1, that drawing task is achieved faster with the Assisted Gravity Compensation mode. At the same time, the High Stiffness mode is accurate but slower, and the interaction quality is lower compared to the other methods. These results verify the hypotheses H1 and H2 mentioned in Section 4.4.2. Considering the time of completion, the Personalized Adaptive Stiffness and Gravity Compensation mode have no significant difference. Also, the smoothness of Adaptive Stiffness mode is even superior to High Stiffness, having a lower number of peaks. The Procrustes in the task completion shows no significant difference between Adaptive Stiffness and High Stiffness. These both results together verify the hypothesis H4.

The results regarding the criteria for interaction quality were discussed in Section 4.4.3. It is clear from the results that the Adaptive Stiffness control is preferred over the Gravity Compensation mode concerning the ease of use, reliability, control and overall user satisfaction. When compared to the High Stiffness mode, the Adaptive Stiffness mode has better ratings concerning ease of use, external control, and overall user satisfaction. It is clear from the Table 4.3, that the Adaptive Stiffness mode ranks high in every comparison criterion used in the analysis. It has a net rating of 7/8, where it got

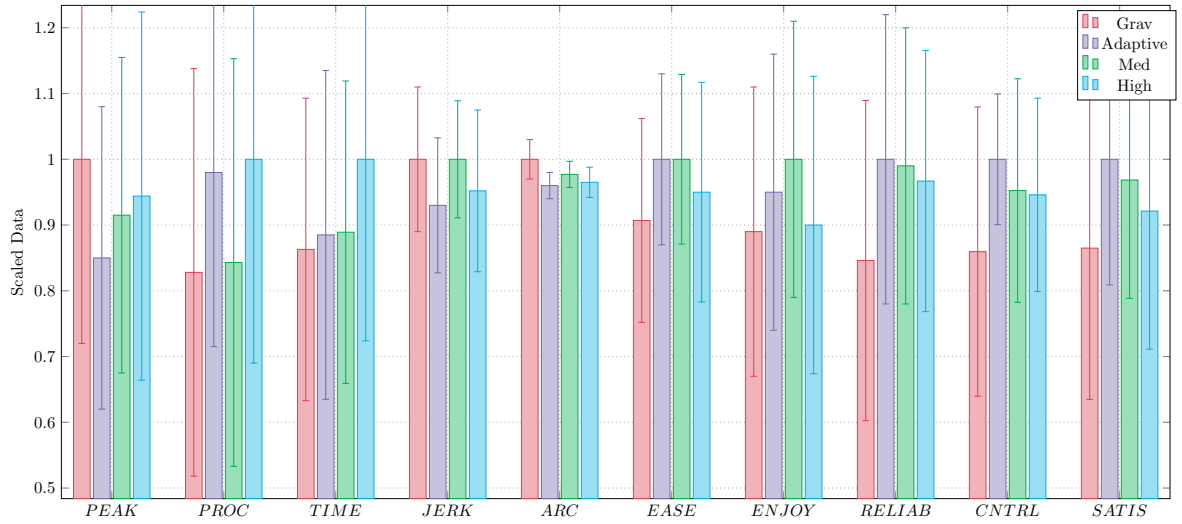

Figure 4.10: Scaled data comparison of Drawing Task.

7 top ranks in 8 compared criteria. Medium Stiffness with 4/8 is the second best mode, and Gravity Compensation comes last with a rating of 1/8, although commonly used in practice. We could infer that, the on-line adaptation of stiffness personalized for each user receives the best outcome regarding interaction quality and performance, although the adaptation scheme is rather simple and directly proportional to the measured force. The accuracy of Adaptive Stiffness mode is comparable to High Stiffness mode, we can hence hypothesize that a more advanced adaption scheme may not achieve much better performance. However, it is possible to improve the interaction quality and ergonomics by reducing the user effort.

The analysis of the contour-following task in Section 4.4.4 and Section 4.4.4 highlights an interesting aspect. The users preferred the Medium Stiffness mode better for work on the contour-following task. It has high user ratings in all the interaction quality criteria. Concerning accuracy, all the modes performed similarly and regarding time of completion Medium Stiffness, and Gravity Compensation is not significantly different. From Table 4.3, it can be observed that the Medium Stiffness mode has the best ranks in criteria of subjective interaction quality, it has an overall rank of 6/8. While the Gravity Compensation is the least preferred mode having the lowest rank of 1/8. From these results, it could be inferred that if the task is simple, no adaptation of stiffness or robot parameters is necessary. It seems that rather a medium stiffness mode is sufficient and will result in good performance. This strong difference in the results between the two tasks indicates that task specificity is highly relevant when designing interaction strategies for pHRI. Fig. 4.10 and Fig. 4.12, shows the comparison on control modes under different criteria, the data is scaled for easier comparison.

4.6 Conclusion

In the scope of the discussed user study, data from 49 users was collected, and the results of the analysis support the hypothesis that Personalized Adaptive control takes pHRI to

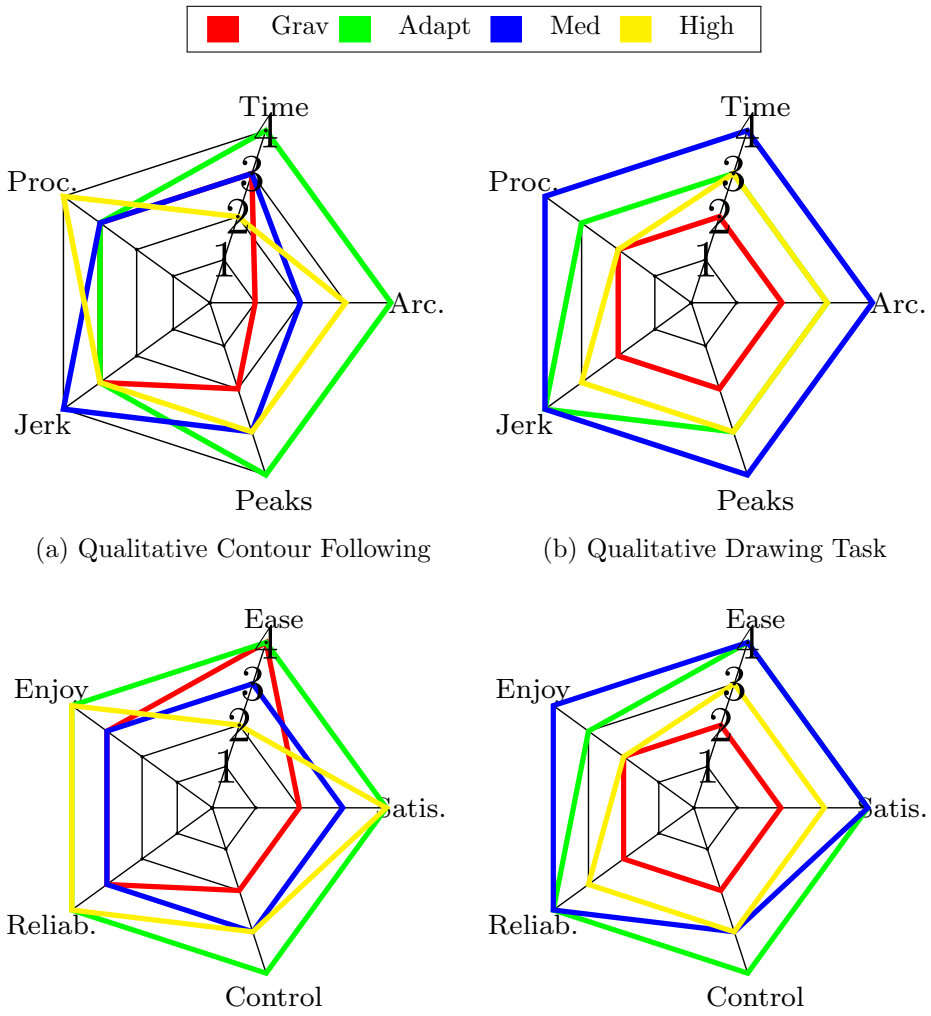

(a) Qualitative Contour Following

(b) Qualitative Drawing Task

(c) Quantitative Contour Following

(d) Quantitative Drawing Task

Figure 4.11: Radar chart showing the ranking of the control modes for each performance criterion depending on their statistical significance, 4 ranks the best while rank 1 is the worst.

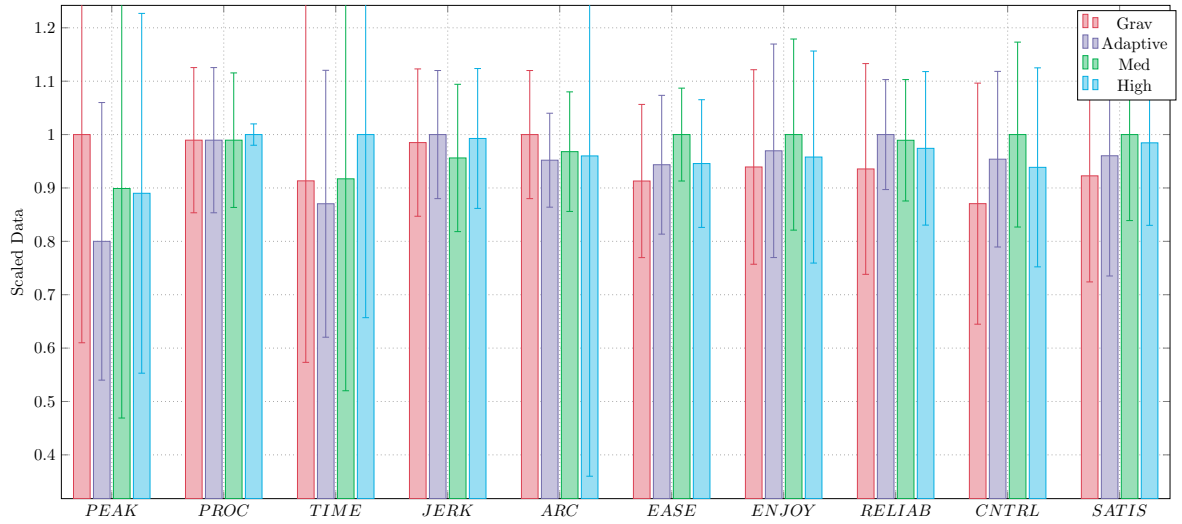

Figure 4.12: Scaled data comparison of Contour Following Task

the next level, if the task is sufficiently complex. Although the personalization scheme tested in this user study is relatively simple and calibrated only for the force limits of the users, the first experiment clearly showed that the Personalized Adaptive control was suited for collaborative task execution and will result in good performance. It can be inferred that consideration of more human factors could not only improve the system as a whole, but also enhance the user's experience and satisfaction, especially when the task difficulty increases. The results also strongly suggest that considering task parameters while designing control strategies can further improve the control. However, if the task is simple, a medium stiffness appears to be sufficient and thus there may be a lot of cases in daily practice, where complex adaptations do not lead to better results. In combination, the results point to a high relevance of task specificity in addition to adaptation of the system for the respective users. In the next chapter, the task specificity will be explored in detail.

Chapter 5

Task Specificity in pHRI

In chapter 4, personalized adaptation scheme was discussed in detail. The proposed force based personalized adaptation scheme was compared against standard control modes used in industry for pHRI. The results from the user-study discussed showed the significant improvement the personalized control modes can bring to pHRI. The results from the two cases considered in the user-study hinted at control modes performing differently for different tasks.

This chapter discusses the importance of task specificity while designing control modes for pHRI. The results of both tasks in the user study is compared in detail and various factor and human parameters which might affect the interaction quality is discussed. The concept of manipulability is introduced here and a detailed analysis of results are shown in this chapter. This chapter is based on the results published in [80] and [81].

5.1 Task Specificity: Influence of task parameters in overall interaction

The task specificity and the influence of the task and task related factors in pHRI are discussed in detail in the following sections. It was clear from the results of the previous user study that the performance and interaction quality both change while the task is varied. Even when the control modes are the same, the performance of a user is strongly influenced by slight variation in the task.

5.1.1 Statistical Comparison of Results

In order to find differences between the task, a detailed statistical analysis was done on the data from the user study mentioned in Chapter 4. Table.A.2, tabulates the means, interaction effect and the main effect between the tasks and controllers.

Repeated measures ANOVAs were conducted to find differences between the tasks, the controllers and their interaction. Factors such as, task (contour-following / drawing) and controller (Gravity Compensation / Adaptive Stiffness / Medium Stiffness / High Stiffness) and their interaction term are included as independent variables for this analysis. A statistical interaction occurs when the effect of one independent variable on the dependent variable changes depending on the level of another independent variable. A

main effect is the effect of one of the independent variables on the dependent variable, ignoring the effects of all other independent variables.

The results of the analysis show if the criteria of performance and interaction quality differ significantly in these cases, a) between the tasks, when the controllers are not considered, b) between the controllers, when the tasks are not considered and c) between the controllers, dependent on the task that is fulfilled. Here, a) displays the difference in difficulty between the tasks, b) confirms the results from section 4.4.3 and 4.4.4 and c) shows whether the controllers might be able to compensate for effects of task difficulty. The full ANOVA test statistics and the differences of the means ($M_{Diff} = M_{contour} M_{drawing}$) are displayed in Table A.2. This analysis was not run for the criterion time of completion, because the time of completion is highly task specific and its analysis will not give any information about differences in performance caused by task difficulty.

Analysis of Quantitative performance

The results for data of procrustes analysis show significant main effects for tasks ($M_{contour} = 0.94; M_{drawing} = 0.58$) and for controllers. In addition, there is a significant interaction effect. Here, the difference between the tasks is smaller when the Adaptive Stiffness or High Stiffness controllers are used, compared to Gravity Compensation and Medium Stiffness. For number of peaks, there is only a significant main effect for controllers, but neither a main effect for task nor an interaction effect. For jerk cost, there is a main effect for task ($M_{contour} = 1.35; M_{drawing} = 1.23$), but no main effect for controllers. There is a marginally significant interaction effect. The difference between the tasks is the smallest with Medium Stiffness and the largest with Adaptive Stiffness.

Analysis of Qualitative performance

For ease of use, there is a significant main effect for task ($M_{contour} = 4.38; M_{drawing} = 4.16$) and for controllers. The interaction effect is significant as well. The difference between the tasks is smaller when the Adaptive Stiffness controller is used, compared to the other controllers. For enjoyment and reliability, there is a main effect for task ($enjoyment : M_{contour} = 4.14; M_{drawing} = 3.89; reliability : M_{contour} = 4.29; M_{drawing} = 4.03$) and for controllers, but there is no significant interaction effect. For control, there is a main effect for task ($M_{contour} = 4.55; M_{drawing} = 4.35$) and for controllers. There is a marginally significant interaction effect. The difference between the tasks is the smallest when the Adaptive Stiffness controller is used, compared to the other controllers. For user satisfaction, there is a main effect ($M_{contour} = 4.38; M_{drawing} = 4.17$) for task and for controllers as well as a significant interaction effect. The difference between the tasks is smaller and opposed when the Adaptive Stiffness is used, compared to the other controllers.

5.2 Task Specificity

To learn about the effects of task parameters on the task execution and the individual interaction, the forces that users exerted on the end-effector are analyzed in this section. In addition to the forces, the manipulability and human specific parameters like arm

lengths are analyzed for the drawing task. For the latter part four distinct users are selected with different body proportions and their data is analyzed for observing the effects of user specific parameters on task execution. For this particular task human arm is modeled as a 3 DOF articulate arm with two links. The human interaction model can be defined as shown in Fig. 5.1, here h is the height of the user's shoulder, d is the distance to the task l_1 and l_2 are the arm parameters. This simplified human arm model is used for further analysis.

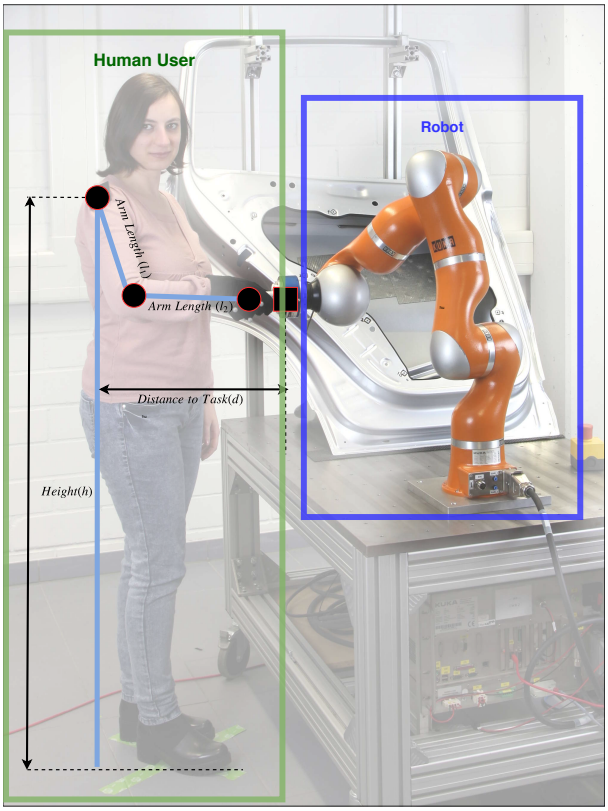

Figure 5.1: The interaction model of the user while interacting with the robot for task execution, the parameters height of the user, distance to the task and arm lengths are used for later analysis

The distance to the task is known from the experiment set-up and the other human parameters where measured manually. Table 5.2 shows the arm parameters of the selected users. The users were classified based on their height and the arm link lengths, the selection of users whose data are evaluated is made in such a way that $user1$ has the minimum height and arm lengths and $user4$ has the maximum body proportions among the participants. The $user2$ and $user3$ were chosen to have intermediate proportions. The human user is modeled as shown in the Fig. 5.1. The Table 5.2 also tabulates the difference in arm parameters and the maximum and minimum manipulability of the four selected users. The above mentioned difference in body proportions are clearly visible form the data. There is a clear difference in task accuracy by each user, the reasons for this variance is discussed in the following sections.

Table 5.1: Variation of the arm parameters of four selected users, the predicted manipulability and task accuracy

	Forearm (l_2) (cm)	Upperarm (l_1) (cm)	Height (h) (cm)	MaxManip (m^3)	MinManip (m^3)	Avg. Proc
User1	25	26	131	0.0242	0.0160	0.72
User2	27	33	144	0.0332	0.0198	0.82
User3	28	34	148	0.0373	0.0224	0.84
User4	29	38	156	0.0239	0.0002	0.40

5.2.1 Force Analysis

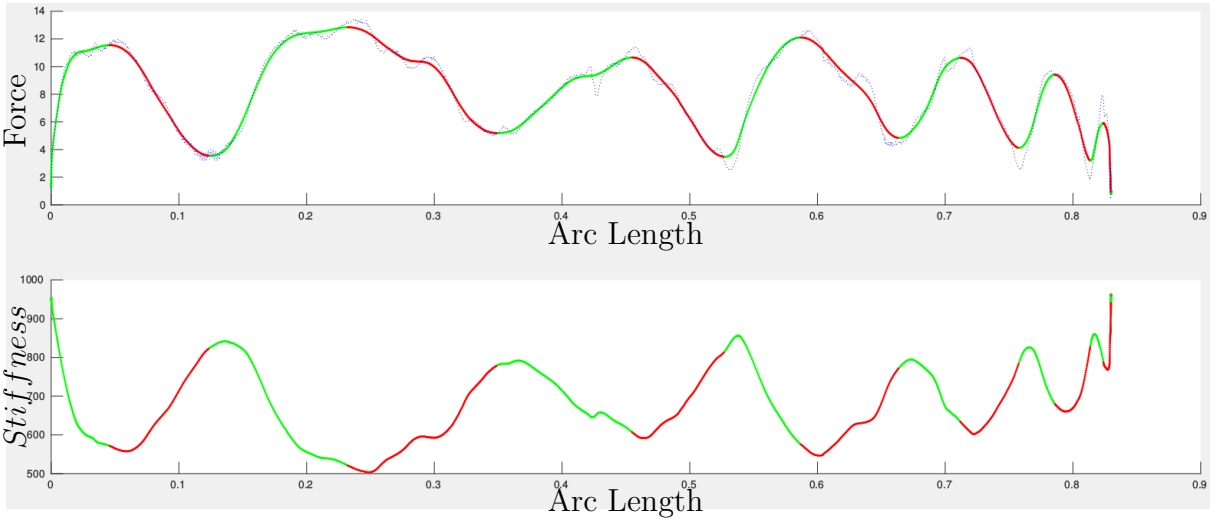

Figure 5.2: The plot shows one of the participants performing the Drawing task. The force profile of the user and corresponding stiffness adaptation is shown here.

To study more about the interaction features of individual user, the force profile generated by the user while interaction was checked into in detail. The forces of one of the study participants while performing the drawing task are shown in Fig. 5.2. The green sections in the plot corresponds to the region of increasing force and the red sections of the plots corresponds to the decreasing interaction force.

A clear pattern is visible: Each peak in the force plot corresponds to a particular section in the task. This strongly points at the correlation between task characteristics and variation of the user interaction forces. Further inspection of the data showed that the observed pattern is apparent for each user who performed the drawing task. By analyzing the plots we can see that this occurrence is not random. Each peak in the force plot corresponds to a particular section in the task. Fig. 5.3 also shows data of 10 users plotted in 3D, by visual inspection it is clear that the pattern observed extends to each

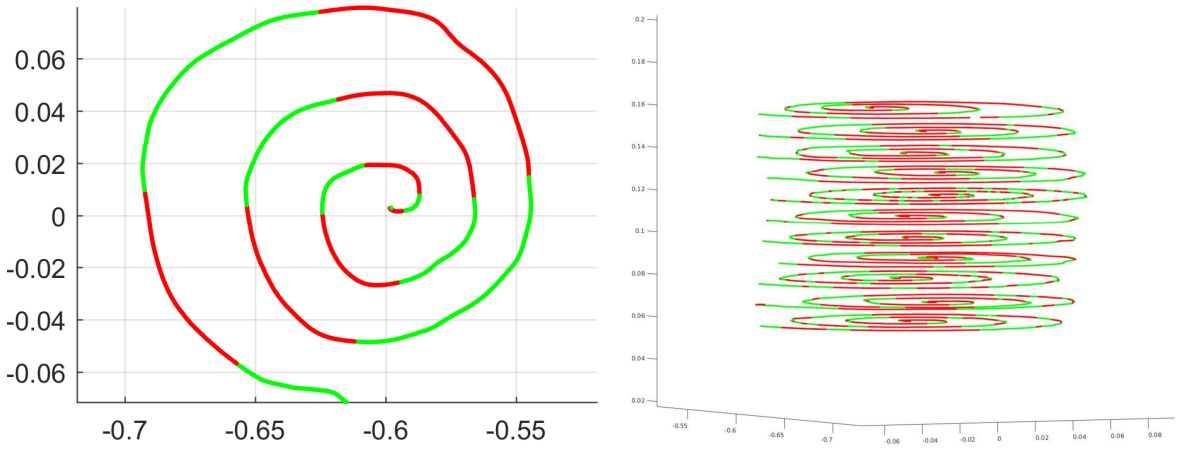

(a) Pattern in Force Profile

(b) Repeating patter for 10 users

Figure 5.3: Performance of one user in Task2: (a) Force profile along the task trajectory. (b) Force profile pattern of 10 users, z axis shows the pattern of each users.

user who performed the drawing task. This task dependency could be used to further improve the user interaction based on local properties of the task.

5.2.2 Manipulability

The concept of manipulability was proposed by [82] as a quantitative measure of the ability in positioning and orienting of robotic arms. It is useful for conducting a task space analysis of robotic manipulators in terms of their ability to generate the velocity, acceleration and the exerted forces [83]. This information can be used to determine the best configuration for task execution and also for designing experimental set-ups which are suited for certain tasks [84]. [85] studied the manipulability related to human arm and proposed a method that allows the user to perform tasks in arm configurations which are otherwise unsuitable due to lack of manipulability.

The manipulability is given by:

$$w = \sqrt{det\left(\mathbf{J}_t \mathbf{J}_t^T\right)} \tag{5.1}$$

where $\mathbf{J}_t$ is the translational Jacobian.

Based on the discussed human model the variation of manipulability for the drawing task for each human parameter is calculated. Fig. 5.4 shows the variation of manipulability when each parameter changes. The maximum and minimum manipulability for the task is calculated for each parameter variation and plotted. It is noticeable that the manipulability increases initially as the parameters vary and suddenly drops after a particular threshold. This points out to a possible singularity and hints at the fact that there exists a single configuration of human model which gives optimal performance for a particular task. In other words, for each user there exists a particular task configuration where the manipulability is maximized.

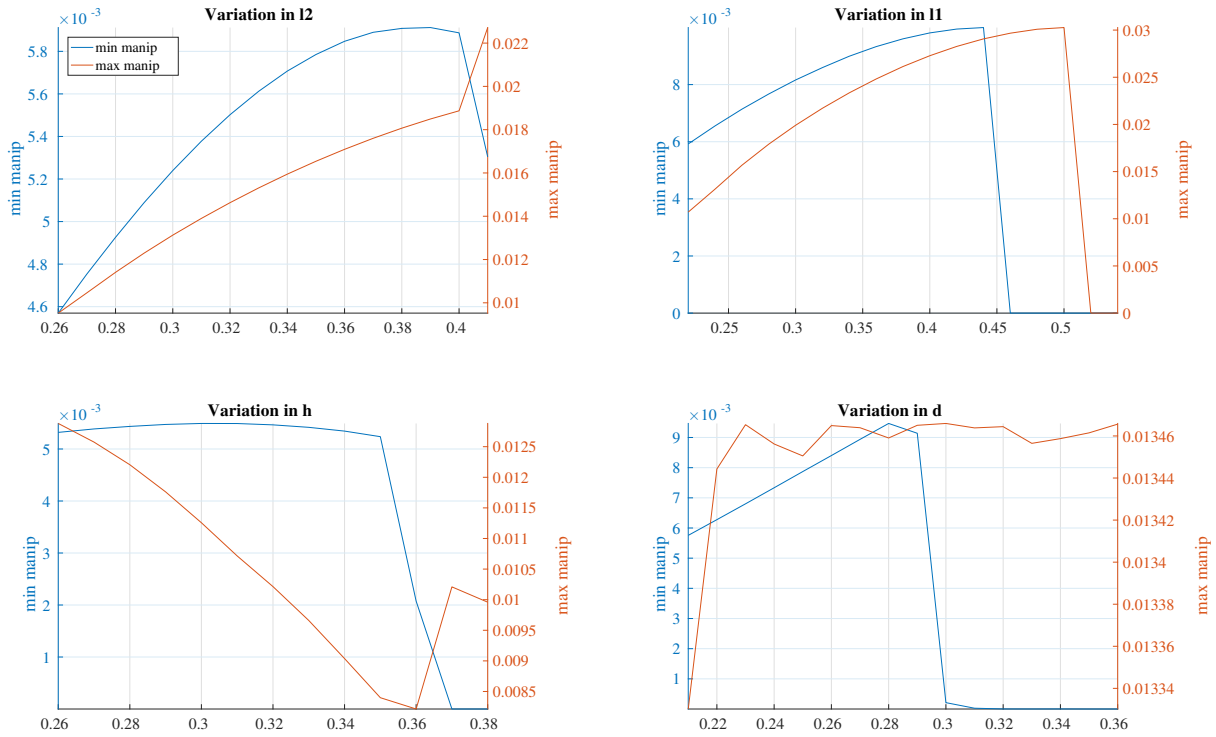

Figure 5.4: Variation of the manipulability for the considered task when the human parameters are varied, the parameters are varied one at a time keeping others constant. The maximum and minimum manipulability are shown in right and left vertical axis. The x-axis represents the length in (m).

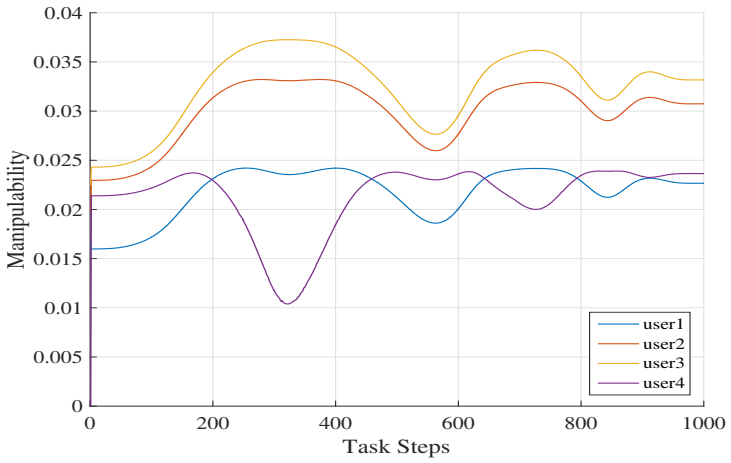

Figure 5.5: Plot showing the variation of the manipulability for four considered users while doing the same task.

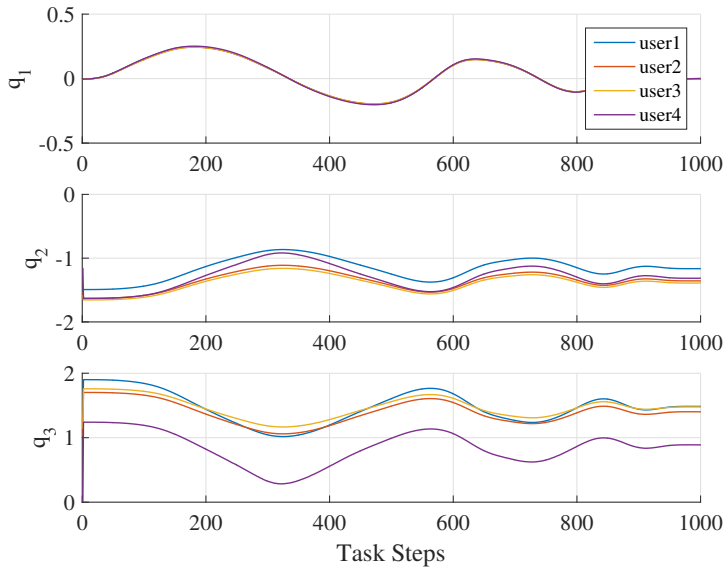

Figure 5.6: The plot showing the variation of joint angles in human model for the 4 user during the task completion. The angles q_1, q_2 are the shoulder joint and q_3 is at elbow joint of the human model, the angle variations are smooth and no sudden change in direction occurred.

To validate the above mentioned hypothesis, the manipulability variation of four considered users while completing the discussed task is calculated and the manipulability variation along the task is plotted, see Fig. 5.5. For *user*1, *user*2 and *user*3 the pattern of manipulability variation along the task is similar, while for *user*4 the manipulability variation differs from other users. This variation in pattern could be because of the kinematic constraint imposed on the *user*4 by the task configuration. The variation of the joint angles of the arm can been seen from the Fig. 5.6.Procrustes analysis is conducted on the user generated trajectory to find how accurately the user was able to finish the task. The tasks are repeated four times and the average similarity over four trials are used for further analysis.

The magnitude of the manipulability suggests that the task might have been easier for *user*2 and *user*3. This can be verified from the results of Procrustes from the Table 5.2, here the results of Procrustes analysis for four task repetition shows that the accuracy of these two users is much higher than *user*1 and *user*4. Thus the human parameters, distance to task and height to the task are important factors to be considered while designing tasks involving HRI.

5.2.3 Transmission Ratio

The concept of velocity and force transmission ratio is mentioned in [86], where the maximization of manipulability in a certain direction was discussed.

For an n-DOF manipulator and m-dimensional task space, Cartesian velocity is given by:

$$\dot{x} = J\dot{q} \tag{5.2}$$

where $\dot{x} \in \mathcal{R}^m$ is the task velocity, $\dot{q} \in \mathcal{R}^n$ is the joint velocity vector and J is mxn Jacobian matrix. The Force Transmission Ratio α and Velocity Transmission Ratio β can be represented as:

$$\alpha = \left\| J^{\dagger} \frac{\dot{x}}{\|x\|} \right\|, \quad \beta = \frac{1}{\alpha} \tag{5.3}$$

These quantities can be used to maximize the manipulability of a robot along a desired direction [86]. Thus by analyzing these ratios we can observe the change in direction of the task and its effect in interaction forces. A higher Force Transmission ratio results in larger forces applied and lower error transmission rate. The same effect will result from low Velocity Transmission ratio due to Kineto-static duality. Knowing this information beforehand will facilitate designing of Kinesthetic teaching and other interaction modes keeping in mind the workspace of human and configurations which permits maximum precision. This will also sets benchmarks for training users in industry to accomplish interaction tasks efficiently.

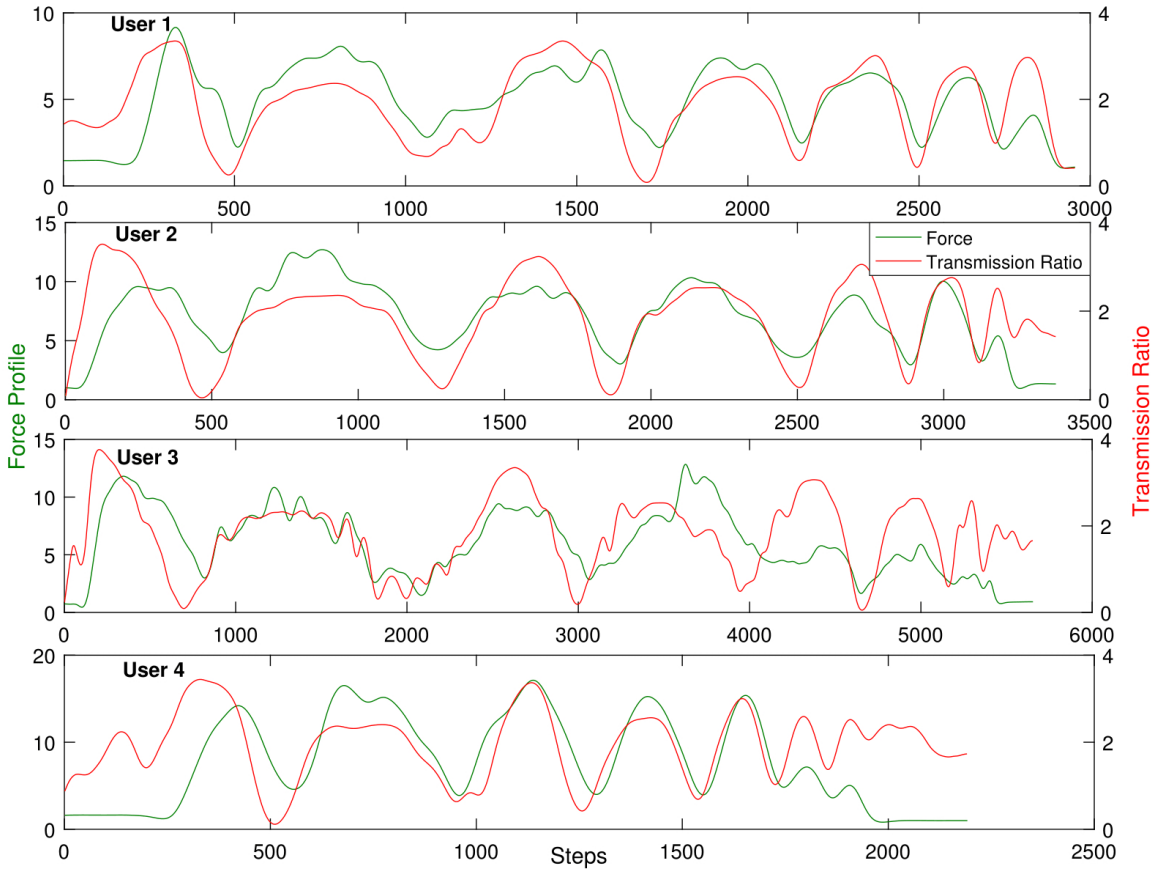

Figure 5.7: Graph showing predicted transmission ratio along the trajectory and its correlation with user' interaction forces.

Using the simplified human arm model discussed earlier, the transmission ratio for the human arm while executing the task is calculated. Fig. 5.7 shows the correlation between

the force transmission ratio and the interaction forces for the four users while performing the same task using the same control modes under same condition. It is clearly noticeable that the transmission factor and the interaction forces are strongly correlated.

5.3 Discussion

The possibility of taking into account humans' arm manipulability in pHRI scenarios was discussed in this chapter. The human manipulability that was discussed, combines both the task characteristics and human kinematics in a meaningful way and gives us a relative performance measure which can be used for improving the HRI.

The preliminary results shows relevant contribution of humans' physical attributes to overall task execution quality. Taking into account these physical properties of the human counterparts, not only contributes to better task execution, but more importantly it facilitates the task completion with less effort for the user. Furthermore, the idea of incorporating these results in industrial HRI scenarios where humans' ease and comfort is used to reconfigure the task and robot configuration needs investigation.

The variation of interaction forces of one participant while performing the drawing task is shown in Fig. 5.2, by visual inspection it is clear that the pattern observed extends to each user who performed the drawing task and this pattern is task dependent. This variation of force is a clear task specific parameter and this information could be used constructively to improve the user interaction by incorporating this information while designing the task. By observing the results discussed in Section 5.2.3 it can be inferred that this correlation is not only a result of the task specificity but also the user kinematics. The manipulability measure discussed in Section 5.2.2 and the transmission ratio results discussed in 5.2.3 clearly point out the effects of task dependency and in addition to this strongly points out the fact that estimation and inclusion of human specific parameters are also important for better task design. By including these parameters the systems can be designed in such a way that the users never run into singularities of their arm configurations and at the same time the task could be pre-optimized from an ergonomic perspective.

In addition, from the presented results it is possible to hypothesize that by using the kinematics of the human-arm and in turn calculating its manipulability over a given task it is possible to quantify and predict the performance of a user for a given task and task configuration. Hence, considering the human manipulability will help improving the pHRI further, since it is possible to adapt the task configuration or the robot parameters to compensate for the changes in human-manipulability. Hence, if human-manipulability is taken into consideration, then the resulting adaptation scheme which will maximize the user performance and user comfort. Such an adaptation can be used in parallel with a personalized adaptation mode which adapts not only to the varying user forces. This combination can be used quite conveniently by the users to overcome difficulties arising from task configuration and physical constraint, since it adapts to both task and physical characteristics.

5.4 Conclusion

The analysis conducted in this chapter supports the hypothesis that task parameters plays an important role in pHRI and their inclusion into the control mode design takes pHRI to the next level. The results show that deploying a human model coupled with task parameters may result in efficient physical Human-Robot Interaction. The human manipulability which was discussed combines both the task characteristics and human kinematics in a meaningful way and gives us a relative performance measure which can be used for improving the pHRI. In the following chapters various control modes based on the manipulability measures discussed will be proposed and will be evaluated using extensive user-studies.

Chapter 6

Manipulability based Personalized Adaptation modes

In chapter 5, task specificity in pHRI is discussed in detail. The results presented showed how the manipulability of the human arm can be exploited for facilitating pHRI. Manipulability and Force Transmission Ratio were discussed as a method for quantifying task and human parameters.

In this chapter, a novel approach of adapting the robot's stiffness based upon the human's arm manipulability is discussed. Three manipulability based control modes are introduced and their performance is compared. This chapter deals with two facets: At first, three manipulability based stiffness adaptation methods for compliant robot platforms are introduced. The proposed control modes are implemented by taking into consideration the task and human parameters. Second, the proposed control modes are validated with users of varying expertise on two tasks with distinct interaction characteristics. The user study is conducted with 40 users comparing the three proposed control modes against the popular Constant Stiffness mode.

6.1 Manipulability in pHRI

Moving further towards human comfort, in [87] several aspects of pHRI such as ergonomics and human effort are discussed. Here safety of human is achieved through monitoring a shared workspace. The minimization of the effort from human counterpart through positioning a heavy object by robot assistance is achieved. On-line modeling and estimation of complete human arm stiffness was discussed in [36]. This approach could be used in teleoperation as well for identifying stiffness regulation in the human arm. Here the robot uses a whole-body dynamic model of the human to optimize for the position of the co-manipulation task in the workspace. Force manipulability is investigated in [88] to find the relationship between human arm movements and operational feeling. Manipulability serves as a quantitative measure of the manipulating ability in positioning and orientation of the robotic arm at a particular configuration, as was proposed in [82]. This measures point at the capability of a manipulator for executing a specific task in a given configuration [89].

The effect of human manipulability and its effects on task completion was discussed in [80]. The results from this user study suggest a strong correlation between task specific

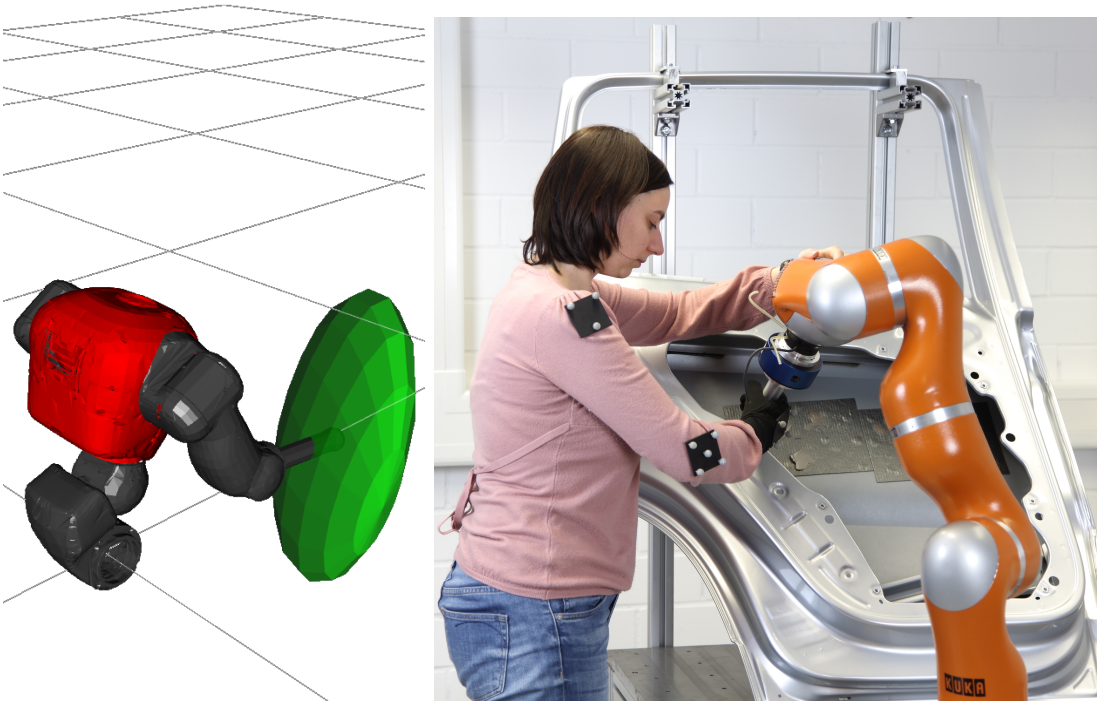

Figure 6.1: Left: Classical shoulder-elbow-wrist kinematic structure that is common in robotics and its manipulability ellipsoid. Right: Human arm model is treated same as the humanoid robot depicted.

parameters and human factors. It was also demonstrated that these two paradigms, task specificity and personalization of human factors, could be combined and quantified by considering the manipulability of human arm. These are significant factors which are often ignored, although they can be pivotal in increasing the efficiency and improving the interaction. Take for instance the case of a welding task on a factory floor, where the human's torso and hip motions are limited. It is reasonable to assume that very tall operators will have different performance compared to operators with average height. Same can be applied for demanding tasks in constrained workspaces, where workers with different body parameters might perform differently regarding the same task configuration. It is hypothesized that, by using the kinematics of the human arm and in turn calculating its manipulability over a given task profile, it is possible to quantify the performance of a user. This information could be used for on-line stiffness adaptation of a compliant robot and thereby increasing the performance of the human user.

In [80] a simplified model is used in order to analyze the human factor in pHRI. It is rational to adapt a simplified model since one of the goals of this thesis is to demonstrate how effective even a simplified model could be. Furthermore, such a system may work as an initial step towards more sophisticated systems that take into consideration more aspects of human ergonomy.

The user study conducted for comparing various manipulability based adaptation schemes empirically proved that, by combining both task and human factors pHRI is

improved. The human physiognomy and dexterity were taken into account and the results show that physical characteristics can be a determining factor in pHRI. Inclusion of human factors in pHRI not only improves the overall quality of the task execution, but also the work satisfaction. A pattern emerged from analysis of the user study which shows that the human behavior within the same task is distinct in different difficult regions in the task. The preferred control mode in each such region also varies but this cannot be coincidental since a pattern has emerged.

The implemented control methods exploit the manipulability of human arm for improved pHRI by adapting the impedance parameter of the robot, namely stiffness, to suit the human's physical characteristics. It is demonstrated that for a given task, human dexterity contributes to the overall quality of task execution and improves the interaction. This is a contributing factor in designing control modes for pHRI.

6.2 Manipulability Measures

In this section different manipulability measures and corresponding stiffness adaptation schemes that are compared in the user-study are introduced. The concept of manipulability is not limited to robotic manipulators. It can also be applied to the human counterpart. To adapt the robot's stiffness based on the manipulability measures of the human arm, three approaches are discussed: Scalar Manipulability, Manipulability ellipsoid and Force Transmission Ratio.

Scalar Manipulability

Considering the human arm as a four DOF kinematic chain similar to [90], the translational Jacobian matrix ($\mathbf{J}_t$) can be computed, knowing the end-effector and the shoulder positions. The scalar manipulability is calculated using Eqn. 5.1.

Manipulability Ellipsoid

Manipulability could be considered as an ellipsoid in the n-dimensional Euclidean space. The major axis of the ellipsoid represents the direction in which the end-effector has the better capacity of motion and like-wise the minor axis represents the direction with the worst capability of motion. It is possible to calculate the major and minor axes of the manipulability ellipsoid by applying singular value decomposition (SVD) to the translational Jacobian matrix of the human arm.

$$[\mathbf{U}\mathbf{\Sigma}\mathbf{V}^T] = SVD(\mathbf{J_t}) \tag{6.1}$$

$$\mathbf{U} = [\mathbf{u}_1, \mathbf{u}_2, \ldots, \mathbf{u}_m] \tag{6.2}$$

$$\mathbf{V} = [\mathbf{v}_1, \mathbf{v}_2, \ldots, \mathbf{v}_n] \tag{6.3}$$

$$\mathbf{\Sigma} = \left[\begin{array}{cccc|c} \sigma_1 & & & & \\ & \sigma_2 & & & \\ & & \ddots & & 0 \\ & & & \sigma_m & \end{array}\right] \tag{6.4}$$

In (6.1-6.4) $\mathbf{U}$ and $\mathbf{V}^T$ are formed by the left and right singular vectors of Jacobian. Columns of $\mathbf{U}$ and $\mathbf{V}^T$ are orthonormal vectors which can be regarded as basis vectors. $\mathbf{\Sigma}$ is a diagonal matrix consisting of singular values (for a redundant robot with n degrees of freedom performing an m dimensional task ($n > m$), some zero columns should be padded to the matrix).

Considering the translational part of the Jacobian, the manipulability ellipsoid of the arm can be generated using the left singular vectors, scaled by respective singular values. In other words, the left singular vector associated with the smallest singular value (for this 3D task $\mathbf{u}_3$ and $\boldsymbol{\sigma}_3$) represent the direction in which the arm is least capable of generating velocities. The magnitude of such incapability is expressed by $\boldsymbol{\sigma}_3$. Fig. 6.1 illustrates the manipulability of the arm of a kinematic structure.

Force Transmission Ratio

Force or Velocity transmission ratio can be used to maximize the manipulability of a robot along a desired direction [86]. By analyzing these ratios, the change in direction of the task and its effect in interaction forces [80] can be observed. A higher force transmission ratio results in larger forces applied and a lower error transmission rate. As shown in [86], given a unit vector $\boldsymbol{\nu}$ representing the Cartesian direction, force transmission ratios can be calculated as:

$$ft = \left(\boldsymbol{\nu}^T \left(\mathbf{J}_t \mathbf{J}_t^T\right) \boldsymbol{\nu}\right)^{-1/2} \tag{6.5}$$

6.2.1 Hypotheses

The manipulability measures of the human arm are calculated during the execution of the task and this information is used to adapt the robot stiffness. The main hypotheses considered here are:

H1. When the manipulability of the human arm is below a certain threshold (e.g., fully extended arm), the task accuracy will decrease and hence the user needs more assistance (i.e., the robot needs more stiffness).

H2. When the manipulability is high the human has more control over the task and the robot can be less stiff.

The three respective schemes based on the aforementioned hypotheses are tested. The first scheme is based on the simple scalar value of manipulability as in (Eqn. 5.1), the second one is based on the SVD of the task Jacobian (Eqn. 6.1-6.4), and the third scheme is based on force transmission ratio (Eqn. 6.5).

6.2.2 Adaptation Schemes

Scalar Adaptation

In this scheme, the manipulability measure calculated from Eq. (5.1) is mapped linearly to the robot's stiffness. A similar heuristic as used in [68,80] is applied for this mapping. The

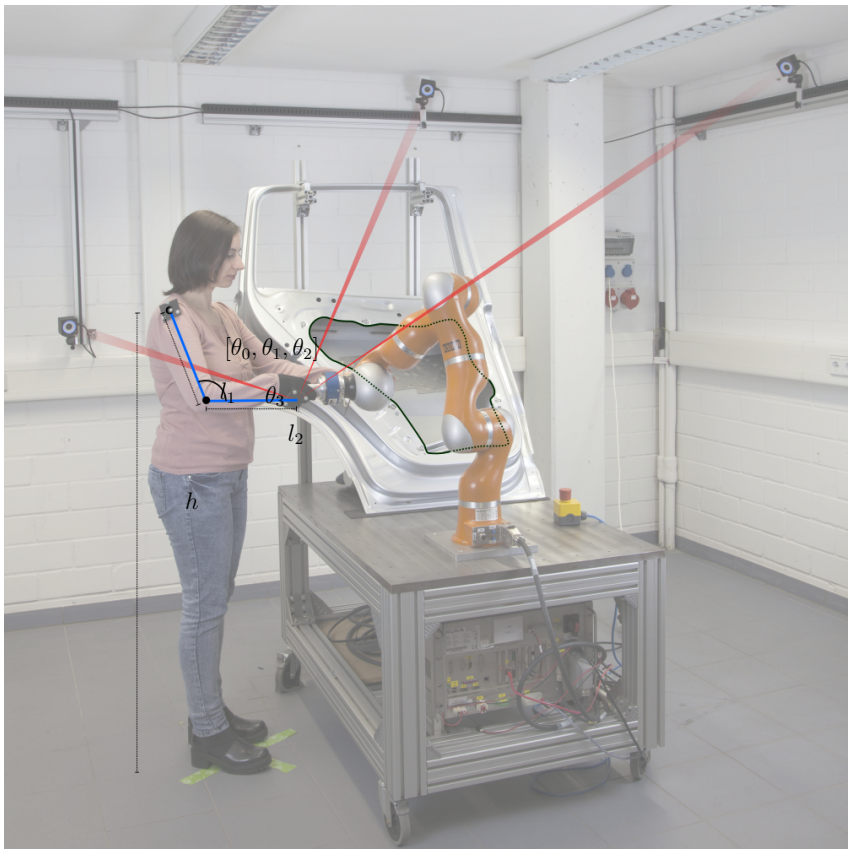

Figure 6.2: The figure illustrates the study setup, here the user's arm configuration is tracked on-line.here $\theta_0, \theta_1, \theta_2, \theta_3$ are the joint angles, l_1, l_2, h are the arm lengths and height.

stiffness range in translational space (k_{max}, k_{min}) is $(5000N/m, 10N/m)$ and in rotational space is $(300N/m, 0.7N/m)$. The stiffness k_t at any time (t) is given by:

$$k_t = \left(\frac{(k_{min} - k_{max})}{(m_{max} - m_{min})} \right) (m_t - m_{min}) + k_{max} \tag{6.6}$$

where, m_t is the scalar manipulability measure at current instance.

The values of m_{max} and m_{min} are calculated using the data obtained from an initial warm-up phase. Based on the user interaction in the calibration phase a relative frequency histogram for the manipulability and the corresponding normal distribution is plotted. The manipulability at inverse normal probability distribution of 98% is chosen as the manipulability limits m_{max} and m_{min}, see Fig. 6.3. The parameterization of force transmission ratio limits ft_{max} and ft_{min} is also done in a similar manner.

Directional Adaptation

This scheme is a Directional Adaptation based on principle axes of manipulability ellipsoid calculated from Eq. (6.1). The length of the manipulability ellipsoid axis is normalized and the stiffness of the robot in cartesian space is varied in each axis independently based on the normalized lengths. The multiplying factor derived from the normalization of $\boldsymbol{\sigma}$ is

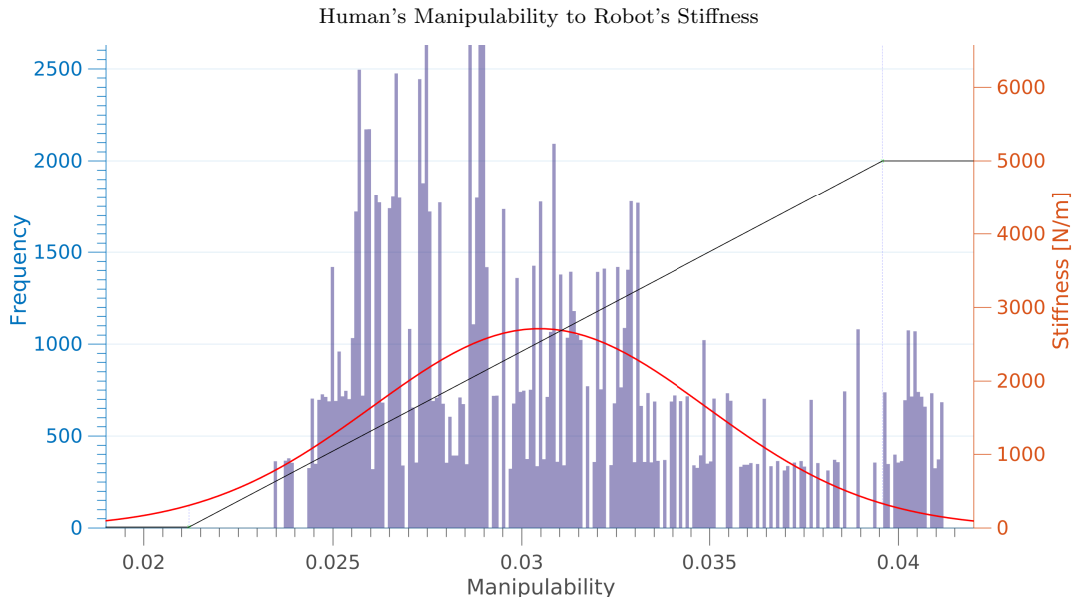

Figure 6.3: The stiffness adaptation scheme based on manipulability measure is shown here, the frequency data is collected from the initial warm-up phase.

used to manipulate the stiffness values on the Cartesian space in the direction specified by $\mathbf{u}_i$. The stiffness in each axis is calculated by

$$\boldsymbol{k} = \frac{\boldsymbol{\sigma}}{\|\boldsymbol{\sigma}\|_\infty} k_{max} \tag{6.7}$$

Force Transmission Ratio based Adaptation

In this scheme, the force transmission ratio calculated from (6.5) is used to adapt the stiffness of the robot. The mapping is done using the same heuristic used in the Scalar Adaptation. Here, the values of ft_{max} and ft_{min} are parameterized from the warm-up phase data as mentioned earlier. The stiffness k_t at any time (t) is given by:

$$k_t = \left(\frac{(ft_{min} - ft_{max})}{(m_{max} - m_{min})} \right) (ft_t - f_{min}) + k_{max} \tag{6.8}$$

where, ft_t is the force transmission ratio at time t.

6.3 Experimental evaluation of Manipulability based adaptation schemes

For evaluating and comparing the control methods, a robotic system consisting of a 7-DOF KUKA Light Weight Robot (LWR IV) [70] equipped with a 6 axis Force-Torque sensor is setup. Fig. 6.2 shows the experimental setup. The robot is an active compliant robot and has an impedance based control scheme [72]. For on-line estimation of user's arm configuration, a rigid body tracking system based on reflective markers is used. The tracking is done using OptiTrack [91], though any camera system capable of on-line

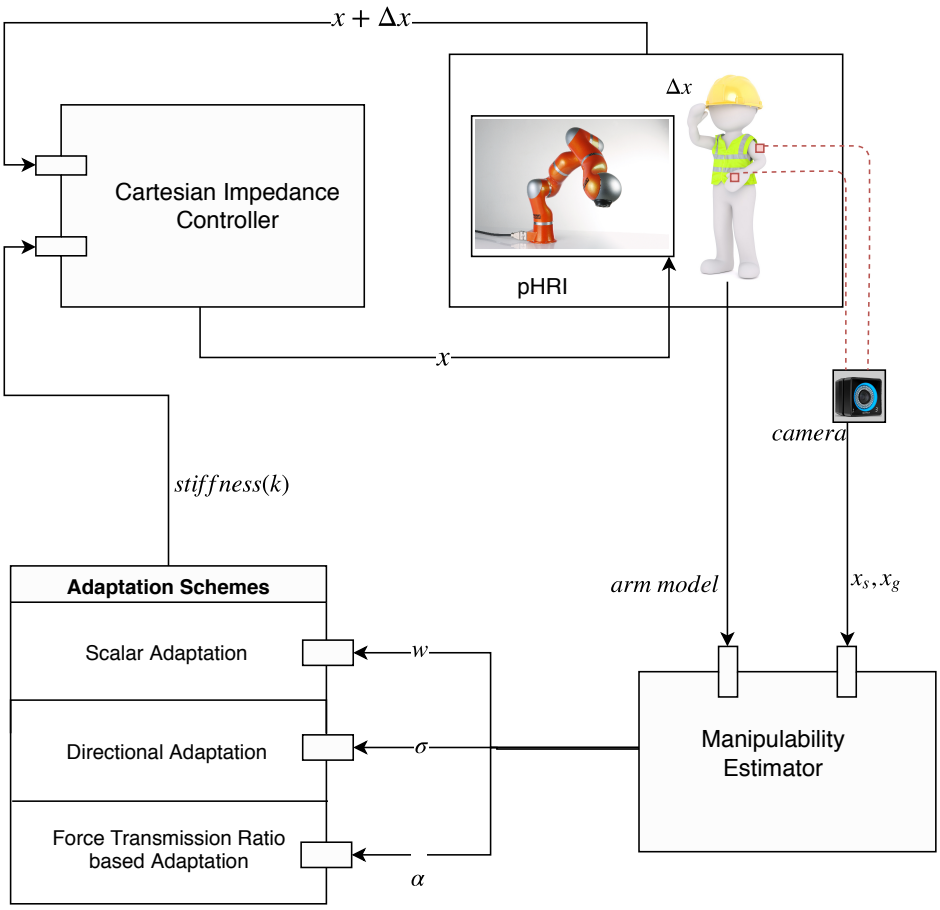

Figure 6.4: Illustration of the control scheme used in this experiment. The shoulder position(x_s) and the grip position(x_g) are tracked on-line to calculate the different manipulability measures.

tracking of markers or rigid bodies could be used. The shoulder position ($\boldsymbol{x_s}$) and the grip position ($\boldsymbol{x_g}$) are tracked on-line.

For estimating the manipulability measures, modeling of the human arm is required. A four DOF human arm model similar to [90] is created, with the height of the user's shoulder (h), the distance to the task (d) and the arm length (l_1, l_2) as the basic parameters. The additional DOF at the shoulder was considered in this experiment to increase the efficiency of the model. Reflective markers were placed on the human arm and the tracking system continuously monitors the shoulder frame and the wrist frame of the human arm, see Fig. 6.2. The manipulability measures mentioned in Section 6.2 are calculated each time the human frames are updated. The controller for interaction and the control architecture is implemented as described in [68]. The Cartesian impedance mode of the KUKA LWR is used for facilitating the pHRI. The required stiffness is calculated from corresponding manipulability measure of each mode as described in Section 6.2.2. The resultant stiffness from each mode is then given to the Cartesian impedance controller of the robot. Fig. 6.4 illustrates the control architecture used in the experiment.

6.3.1 Study Design

In the user study, three different control modes based on the adaptation scheme mentioned in Section 6.2.2 are compared, along with a Constant Stiffness mode which is normally used for Kinesthetic Guidance. A within-subject design is used for comparing the four control modes, where each participant interacts with the robot using all the four control modes. In order to prevent sequencing effects like tiring and learning effect, the activation order of control modes is randomized for each user independently. The qualitative performance of the users was analyzed by means of a questionnaire and the quantitative performance is analyzed from the recorded data. The participants in the study where acquired through snowball sampling system [79], following an initial advertisement. The different evaluation measures used in this study are elaborated in Section 2.3.

Before starting the user study, Bielefeld University's ethics committee was consulted, which approved of the study as being ethically innocuous. In addition, the study setup was inspected and approved by the official safety officer. Each of the participants was given a short briefing prior to the experiment containing information about the study process and data that would be assessed. The subjects had also the possibility to ask questions before the experiment and were insured that it was possible to quit participating at every point in time and that in this case the incomplete data would be deleted and not enter the analysis. All participants gave their written informed consent in accordance with Declaration of Helsinki. This was in agreement with usual practice in such studies and in accordance with Bielefeld Universitys ethic committee guidelines. After finishing the experiment, the participants were debriefed and given additional information regarding the study.

6.3.2 Study Setup

Each participant was required to finish three objectives in the experiment consisting of two phases. The initial phase was a warm-up phase which is followed by a task phase where the users completed two tasks. The users were given instructions about each task through an instruction video which demonstrates the task execution. Additional written description about the task was also provided. After each trial, the users filled in a questionnaire about the particular trial.

Warm-up Phase

In this phase, the participants are asked to interact with the robot by holding its end-effector and move it along the inner contour of the car body. This phase aims at familiarizing the participants with kinesthetic guidance and help them to gain some knowledge about how to interact with the robot. Additionally this phase serves as a calibration phase, here the interaction data from each user is recorded and the limits of their manipulability (m_{max}, m_{min}) and their force transmission ratio (ft_{max}, ft_{min}) are calculated.

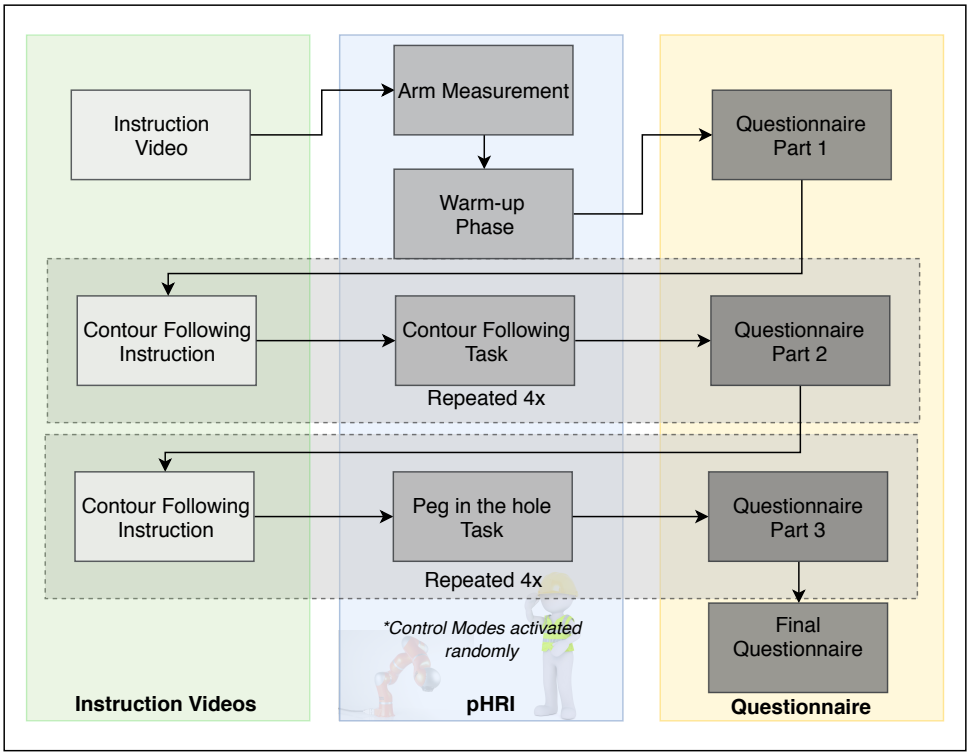

Figure 6.5: Illustration of the user-study flow.

Task Phase

In this phase, the users have to perform two tasks with the robot in the same workspace. The tasks require the users to interact differently while working with the same constraints. The task one is a contour following task where the user needs to maintain the contact with the workpiece through out the task and have to care for the accuracy. This task requires from the user high amount of concentration and patience and is physically imposing. The second task in designed to be similar to a peg in a hole task, here the user only needs to concentrate towards the end of each goal.

Contour Following Task: The first task is a typical task similar to applying gluing rubber sealant on an automobile part. An instruction video is shown to the users demonstrating how the task can be completed. The users are asked to stand on an assigned position on the floor to perform this task. They are free to move their shoulder and to lean slightly on to the workspace. Fig. 6.6 shows the task used for this experiment. In this task the users have to move the robot end-effector accurately along the black rubber seal in the interior of the car door. This task is designed to have areas of varying manipulability and hence varying difficulty, as shown in Fig. 6.9. In the areas of low manipulability the participants will have to either stretch their arms or the angle at the elbow will be too low and vice-versa.

Peg in the hole Task: In this task the users are asked to perform and task which is similar to a peg in the hole task or a non continuous riveting task on the car body. The user constraints are similar to the task one. There are 10 drill holes in the door profile

Figure 6.6: The figure illustrates the contour following task, the user have to move the robot end effector along the black rubber sealant.

numbered from 0 to 9, at the start of each trial the end effector is placed at 0. The users have to move the end effector out of the initial hole and move it to the next hole and repeat it sequentially until they reach back to the initial position. Similar to the first task, the execution difficulty at each hole varies. Based on the user feedback the difficulty is classified into four types. Fig. 6.7, shows a user performing the Peg in the hole Task and Fig. 6.10, illustrates the task.

The users are asked to repeat each task four times using different control modes and the results are compared qualitatively and quantitatively. The considered control modes are Scalar Adaptation mode (`Manip`), Directional Adaption mode (`XYZ`), Force transmission ratio based Adaptation (`FT`) and a Constant Stiffness mode (`Const`) which is normally used for Kinesthetic teaching and pHRI.

6.4 Evaluation

6.4.1 Participants

The users for the user study were acquired through snowball sampling system, 40 users participated in the user study. The user study consisted of three phases and each user completed these three phase succesfully. A total of 74.36% of the participants were male, 84.6% right-handed, 30.7% were full-time working , 58.9% were students, 10.2% part-time working and 2.5% not working. The educational level was high, with 84.6% having

Figure 6.7: The figure illustrates the peg in the hole task, the user have to move the robot end effector into each marked drill holes in the car body.

a university degree. The mean age of users were, $M_{\text{age}} = 27.07$, $SD_{\text{age}} = 6.28$. The body parameters of the users are (in cm): $M_{\text{upper arm}} = 27.29$, $SD_{\text{upper arm}} = 2.28$, $M_{\text{lower arm}} = 31.27$, $SD_{\text{lower arm}} = 2.28$ and $M_{\text{height}} = 174.75$, $SD_{\text{height}} = 7.34$. Three participants were removed because of inconsistencies in the data.

6.4.2 Contour Following

Overall Performance

The evaluation measures mentioned in Section 2.3 are calculated and the repeated measures ANOVA is conducted on the results. The results of the ANOVA is tabulated in Table A.3 and the means and standard deviations are tabulated in Table 6.2 and Table Table 6.1.

On analyzing the time of completion, the Directional Adaptation is far superior to Constant Stiffness. The other two methods have similar performance and both are superior to Constant Stiffness. ANOVA shows a slightly significant difference in the data. In the data set for smoothness in trajectory, ANOVA shows a significant difference ($p < 0.001$). Directional Adaptation have the minimum number of peaks and the Constant Stiffness have the most number of peaks, the other two modes are superior to Constant Stiffness with both having similar performance. The results of Procrustes are similar for all the three manipulability based modes, while the Constant Stiffness is

Table 6.1: Table showing mean and standard deviation of all comparison criteria.

	Time [s]		Smooth *		Proc.		FSM *		Arc. [m]	
	M	SD	M	SD	M	SD	M	SD	M	SD
Const	45.74	18.35	164.09	68.71	0.95	0.04	248.56	99.96	2.10	0.17
Manip	44.75	16.70	113.94	59.19	0.97	0.01	244.25	101.80	2.00	0.06
XYZ	40.57	13.79	103.63	47.17	0.97	0.02	223.92	91.71	2.00	0.07
FT	43.05	18.35	118.80	63.87	0.96	0.02	232.44	99.85	2.02	0.10

*Smoothness and Force Smoothness are measure by the number of peaks.

Table 6.2: Table showing mean and standard deviation of all qualitative comparison criteria.

	Enjoy.		Contrl		Satis.		Ease		Reliab.	
	M	SD	M	SD	M	SD	M	SD	M	SD
Const	3.71	0.74	3.55	0.79	3.70	0.44	3.63	0.70	3.74	0.67
Manip	3.95	0.68	3.88	0.60	3.78	0.50	4.00	0.56	3.97	0.55
XYZ	4.01	0.69	4.00	0.66	3.80	0.43	4.10	0.53	4.04	0.59
FT	3.90	0.68	3.75	0.79	3.65	0.48	3.94	0.60	3.92	0.67

slightly inferior in this measure. Similarly the ANOVA of Force Smoothness measure shows no significant difference between three manipulability based modes but is better then Constant Stiffness. The Directional Adaptation has the best performance in this case. The result of Arc Length shows a significant difference ($p < 0.001$) between the control modes. The Directional Adaptation and the Scalar Adaptation performed identical, while the Constant Stiffness performance was the worst.

Evaluation of the qualitative measures also shows similar results as above where the manipulability based approaches are far superior. The ANOVA shows a significant difference ($p = 0.003$) in the data set for Enjoyment. The Directional Adaptation have best performance while Constant Stiffness have the worst performance. The dataset for External Control shows a significant difference between the performance of Directional Adaptation and the Constant Stiffness, while Scalar Adaptation is better than Force Transmission Ratio based Adaptation. The results of User Satisfaction shows no significant difference between the four control modes, the Directional Adaptation is slightly better with higher mean value for this measure. Analysis of Ease of Use shows a significant difference ($p < 0.001$) between the control modes. The Directional Adaptation is the best while, the Constant Stiffness have the worst performance. When it comes to reliability, the manipulability based methods are far better compared to the Constant Stiffness. The Directional Adaptation is the best control mode in this measure.

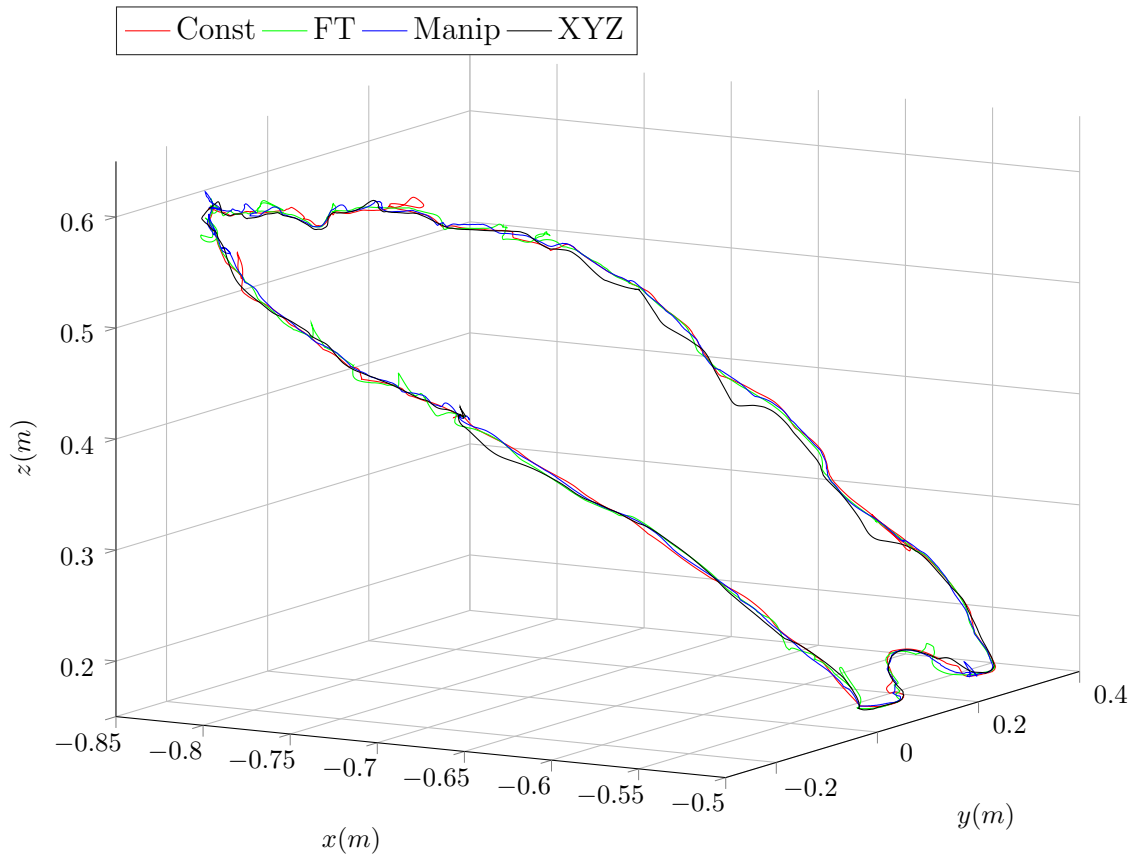

Figure 6.8: TCP trajectories of user 35 under 4 control modes.

Performance in each region

For evaluating the performance of control modes under different difficulty constraints, the task is divided into four areas of difficulty as shown in the Fig. 6.9. Region A1 represents a region with difficulty level easy, here the user hand configuration is near to the highest manipulability. In the hard difficulty region the users have to extend their arm thereby limiting the optimal movements and the manipulating capabilities, A2 and A4 represent this difficulty region. A3 is a region of hardest difficulty here the users arm is mostly extended and it was noticeable from the pre-studies that the users struggled in this region.

The performance analysis of the users in above mentioned 4 regions is represented in the Table 6.3. It is noticeable that the user performance in each area is different for each control mode. In A1 manipulability based adaptation schemes have similar performance when it comes to Time of Completion, while the Constant Stiffness method has the worst performance. Smoothness of the force profile is better for the Force transmission ratio method, while the Scalar and Directional Adaptation have similar performance. Constant Stiffness is worst in this case. While considering trajectory smoothness and Arc Length, Scalar Adaptation is slightly better than other control modes with Constant Stiffness performing the worst. While considering the Procrustes the Directional and Scalar Adaptation are performing similar while the Constant Stiffness is performing worse.

Analysis of the region A2 shows that the Directional Adaptation has better perfor-

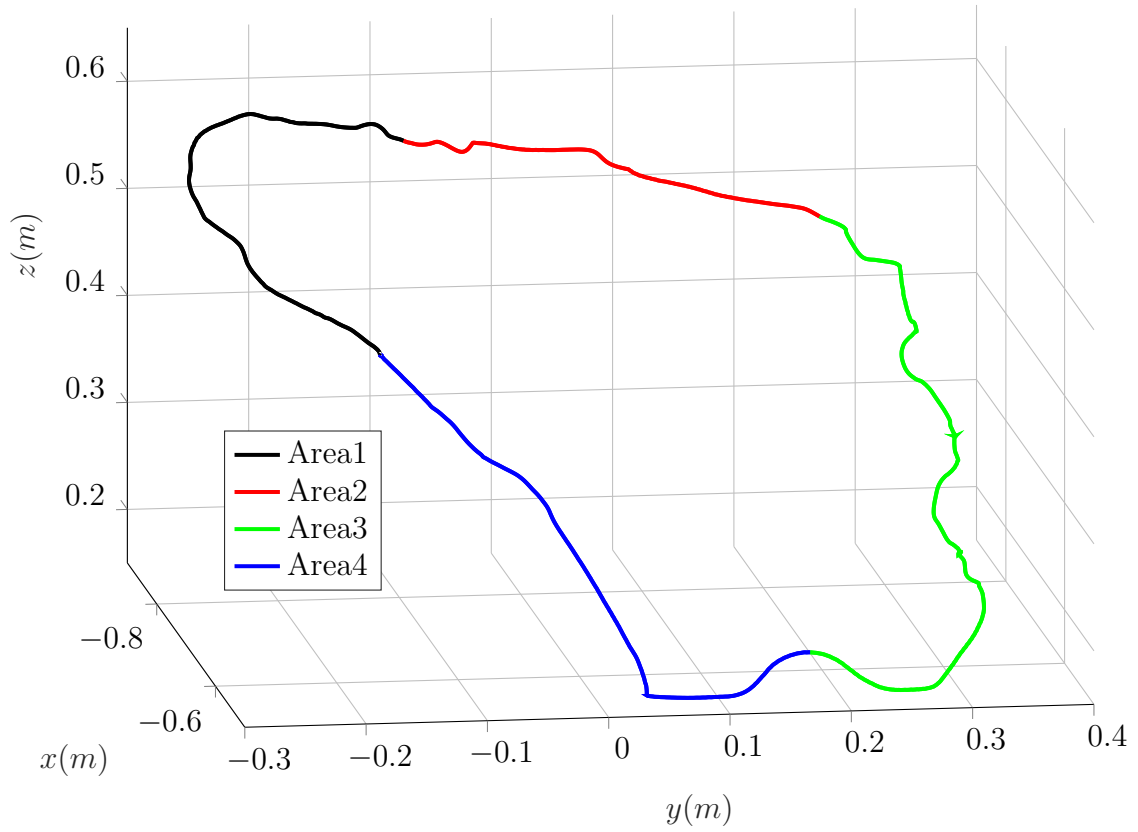

Figure 6.9: Task divided into 4 regions of difficulty.

mance in the criteria of time of completion, trajectory smoothness and arc length. The results of Procrustes shows that all the adaptive controllers perform similar. In terms of force smoothness the Force transmission ratio based Adaptation is better. In this region the Directional Adaptation is working better while the Constant Stiffness is the worst. In the region A3, Force transmission ratio based Adaptation performs better for time of completion, force smoothness, trajectory smoothness and arc length. Scalar Adaptation has a better performance in Procrustes analysis, while the other two adaptation schemes performed similar. In this region the Force transmission ratio scheme performed better and Constant Stiffness was the worst.

It is noticeable from the performance analysis of the region A4 that the Directional Adaptation is much better compared to the other control modes for each criterion. While the Constant Stiffness is the worst control mode for this region. The performance of Scalar and Force transmission ratio based Adaptation is similar in this region.

6.4.3 Peg in the hole

In task two, the analysis is done for each hole separately, the performance for the criteria such as arc length, force smoothness, trajectory smoothness and time of completion for each control mode are compared here. The user interaction on each hole while approaching and receding are analyzed. The results are shown in Table A.4 and Table A.5. The performance of each control mode in each hole is illustrated in Fig. 6.10, it is noticeable

Table 6.3: User performance in four areas of difficulty

Areas	Creiteria	Const		Manip		FT		XYZ	
		M	SD	M	SD	M	SD	M	SD
A1	Time of Comp.	12.21	4.41	10.96	3.41	10.48	3.84	10.62	3.56
	ForceSmooth	68.31	28.36	59.66	23.61	56.14	23.63	57.57	23.32
	Traj Smooth	58.94	32.73	30.20	16.82	33.20	19.91	32.54	23.15
	Arc Length	0.391	0.023	0.383	0.015	0.385	0.026	0.384	0.018
	Procrustes	0.943	0.040	0.976	0.018	0.966	0.027	0.973	0.029
A2	Time of Comp.	6.63	3.18	6.83	2.65	6.62	2.87	6.52	2.55
	ForceSmooth	35.97	18.72	36.20	16.70	35.83	18.48	37.34	17.14
	Traj Smooth	19.17	17.32	15.89	9.47	16.49	11.26	14.80	11.73
	Arc Length	0.353	0.025	0.343	0.011	0.347	0.021	0.343	0.015
	Procrustes	0.985	0.012	0.989	0.011	0.986	0.018	0.987	0.009
A3	Time of Comp.	14.05	5.57	14.34	6.04	13.37	5.69	13.69	5.53
	ForceSmooth	73.44	36.69	73.41	42.48	69.24	32.72	73.18	37.00
	Traj Smooth	47.14	29.98	32.20	20.39	31.77	17.99	32.63	15.26
	Arc Length	0.502	0.071	0.460	0.027	0.458	0.026	0.461	0.026
	Procrustes	0.980	0.015	0.987	0.010	0.983	0.009	0.982	0.016
A4	Time of Comp.	11.00	4.03	10.31	3.58	9.48	3.47	9.33	3.55
	ForceSmooth	62.69	24.44	59.20	27.62	56.14	24.08	54.34	26.70
	Traj Smooth	43.46	28.00	26.77	16.63	26.71	15.60	23.00	12.32
	Arc Length	0.437	0.038	0.424	0.034	0.420	0.017	0.410	0.013
	Procrustes	0.942	0.069	0.977	0.028	0.964	0.040	0.981	0.020

that the Directional Adaptation has an overall good performance.

The holes are divided into 3 categories depending upon their difficulty based on the user feedback. The holes which are easily accessible for the user and which is easier to work on is classified as 'easy'. The holes which are further from where the user stands requires the users to exert more effort. The human arm manipulability at this points are low and hence more physical strain on the users. These are categorized as 'hard' and 'very hard' holes.

While approaching the hole 1, Directional Adaptation has a higher performance in terms on smoothness of force profile, trajectory and time of completion. In this case all control modes have similar performance for arc length. While receding, Force transmission ratio based Adaptation has a better overall performance. Considering the receding in hole 2 and 3, Scalar Adaptation works better in all criteria. While approaching the arc length for hole 2 is similar for both scalar and Directional Adaptation, in other criteria Directional Adaptation have a better performance. Directional Adaptation works well in hole 3 for approach except in terms of force smoothness. In hole 4 while receding, the arc length is same for all the control modes, while Directional Adaptation is performing better for force smoothness and time of completion. While approaching force transmission ratio based mode is preferred. In hole 5, arc length is similar for all modes and Directional Adaptation is preferable for other criteria during receding. In approach Directional

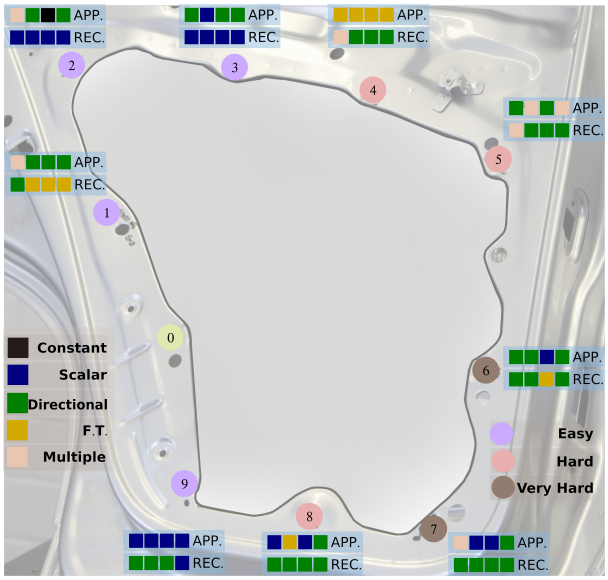

Figure 6.10: The figure illustrates the task two and the performance results, the user have to move the robot end effector to each holes starting at 0. Each square box represents the considered criteria (Time of Completion, Force Smoothness, Trajectory Smoothness and Arc Length)

Adaptation is better for arc length and trajectory smoothness. The performance in similar for all adaptation schemes other criteria. In hole 6 while approaching, Scalar and Directional Adaptation have similar performance in arc length. Directional Adaptation is better in terms of force smoothness and time of completion. During receding Directional Adaptation is better except in terms of trajectory smoothness where Force transmission based Adaptation is better. In hole 7, during approaching Scalar Adaptation is better for arc length, force/trajectory smoothness, while Directional Adaptation is better for time of completion. While receding Directional Adaptation is preferred over all criteria. Considering approaching in hole 8, the adaptation schemes perform better in terms of arc length and force smoothness. Directional Adaptation works better in terms of time of completion. During receding, directional adaption works best for arc length time of completion and trajectory smoothness. In hole 9, Scalar Adaptation works best for approach in all criteria and during receding Directional Adaptation is better.

6.5 Discussion

By analyzing the results in Section 6.4, it is clear that manipulability based control modes have a superior performance compared to the considered Constant Stiffness mode. Among the manipulability based approaches, Directional Adaptation has the best performance. Fig. 6.13 shows the ranking of each control modes based on their statistical significance. The Directional Adaptation have the best ranks in both criteria with overall rank of 10/10. Scalar Adaptation is the second best with overall rank of 7/10, this mode shares similar performance when it comes to qualitative measures. Force Transmission based adaptation has an overall rank of 5/10 and Constant Stiffness has the worst ranking of

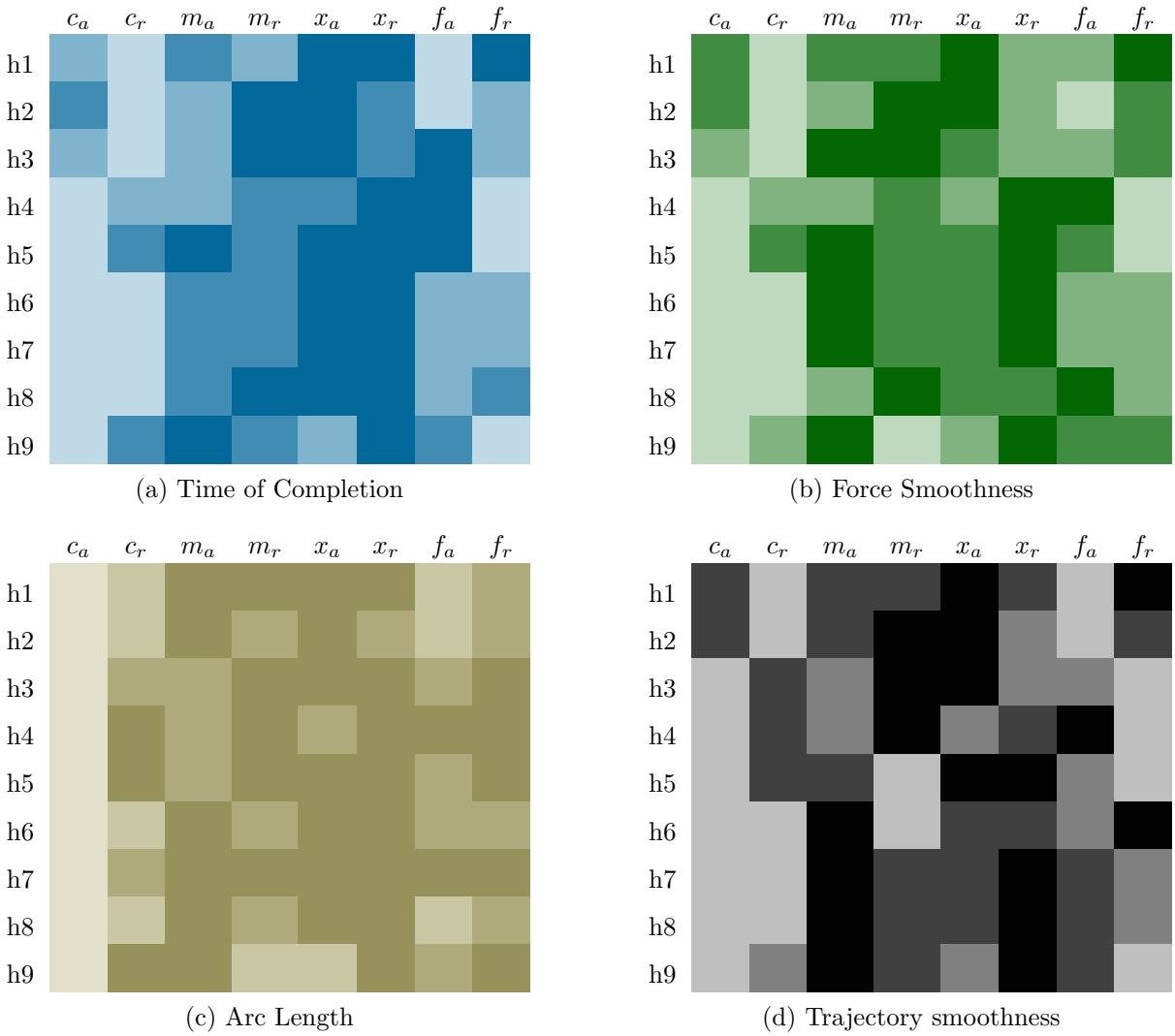

(a) Time of Completion

(b) Force Smoothness

(c) Arc Length

(d) Trajectory smoothness

Figure 6.11: Heat maps showing performance of the control modes in approach and recede for different comparison criteria

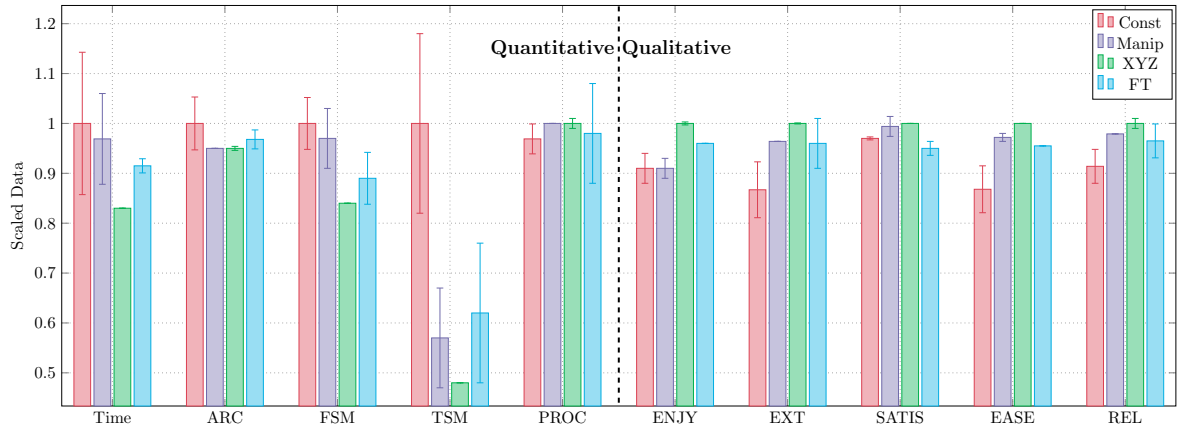

Figure 6.12: The figure illustrating the performance of each control mode in each criterion for Contour following task.

1/10.

It can be observed from Fig. 6.8 that the users have a better performance with Directional Adaptation, where the trajectory is smoother than other modes and the users have more control over the robot. This better performance could be down to the fact that the stiffness is performed on the three axis separately. This differential adaptation is more stable as it constraints unwanted user motion in each direction, hence the users make less error in each direction which leads to a smoother interaction. The feedback from the users revealed that they were having more control while using this mode. Furthermore the results support the hypotheses **H1** and **H2** stated in the Section 6.2.1. The errors in the three manipulability based approaches are low compared to Constant Stiffness mode which is generally used in Kinesthetic Teaching. The smoothness of the trajectory and force profile is better for manipulability based approaches, this means the users did not have to change their interaction forces often. This is an important result as the strain for the user is less and will reduce the chance of user fatigue. The similar performance in the qualitative analysis also supports the initial hypothesis of considering the kinematics of human arm for increasing the human's performance. Fig.6.12, clearly demonstrates the superiority of the Directional based adaptation in both qualitative and quantitative analysis.

The analysis of the user data based on the difficulty regions points is an important result. Performance of the Constant Stiffness based adaption compared to manipulability based approaches are inferior in all the considered criteria. In the region A1 where the task difficulty is lowest Scalar Adaptation has a better performance. At A2 and A4 where is difficulty is hard the Directional Adaptation has a better performance. In Region A3 where the difficulty is hardest, Force Transmission ratio is performing better, though the performance of other manipulability based modes are comparable. These results shows a clear preference for different control modes in regions of varying difficulty. It can be also noticed that for a contour following task when the difficulty is low normal adaptation works better and the user gets more help from complex adaptation once the task difficulty increases.

For the Peg in the hole task, the results are more diverse than for the first task. Based

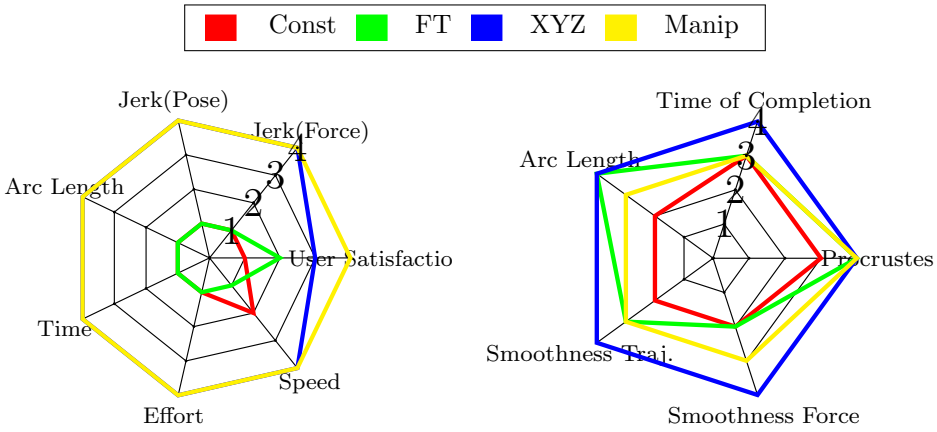

(a) Qualitative (b) Quantitative

Figure 6.13: Radar chart showings the ranking of the control modes for each performance criterion depending on their statistical significance, 4 is best rank and 1 is the worst.

on the user feedback the holes were categorized based on the difficulty they felt. Both approach and recede cases were analyzed separately for this task to check the suitability of control modes for each task. It is clear from the results that Directional Adaptation has a better overall performance. Fig. 6.11 clearly shows this result, here the performance of each controller in approach and recede in each hole for four different performance criteria is shown. Holes are represented as h with the hole number as subscript. Control modes are represented as c,m,x,f for Constant Stiffness, Scalar, Directional and Force Transmission ratio based Adaptation respectively. The subscript a stands for approach and r stands for recede. Fig. 6.4.3 shows the heat map for the Time of completion. High intensity for the colors in the heat-map stand for better performance and vice-versa. In all the four cases considered the intensity is high near the middle of the plot which is represented by Directional and Scalar Adaptation. Among these two Directional Adaptation is performing better in most regions.

Fig. 6.10 and Tables A.4, A.5 comprehensively illustrate the noticeable results of the Peg in the hole task. The figure illustrates the best performing controller with respect to the compared criteria in each hole for approach and recede. While receding, when it is easier the Scalar Adaptation is preferred, eg. holes 2,3 and 9 and when it is hard, directional adaption is preferred, eg. holes 4,5,6,7,8 and 9. Force Transmission ratio is preferred for receding in hole 1 but the difference with other methods is not significant. For approaching Directional Adaptation is preferred except at hole 9 and 4. It can be observed that while approaching Directional Adaptation provides more assistance even in easier cases. The possible explanation for this results based on the user observation are that during approaching the users are careful and need more time for the completing the task (Mean time required: $[M_{const} = 1.28, M_{man} = 1.08, M_{xyz} = 1.07, M_{ft} = 1.17$ seconds). While receding they do it faster (Mean time required ($[M_{const} = 0.67, M_{man} = 0.57, M_{xyz} = 0.56, M_{ft} = 0.62]$ seconds). Therefore the assistance is more needed in approach case where the users aim for more accuracy and control.

These results are significant as they solidify the claims made about inclusion of human factors in designing of control modes for pHRI. At the same time these results shows that with prior knowledge about the task the task could be split and categorized into regions

based on the difficulty it might pose to the users and eventually appropriate control modes suitable for each regions could be automatically assigned for the user interaction.

6.6 Conclusion

In this chapter, the focus was on combining both the task characteristics and human kinematics in a meaningful way by considering humans' manipulability. The control modes discussed here and the results of the subsequent user study proves that the manipulability measure used as a relative performance measure can be used for improving pHRI. The manipulability based adaptation schemes performed better than the Constant Stiffness counterpart while performing the same task.

The Directional Adaptation has better performance and offers more assistance when the task difficulty is higher. It also has better overall performance, therefore this scheme is the best among the considered proposed manipulability based control modes. The better overall performance of Directional Adaptation is down to the fact that it takes into consideration the directionality. It assists the user in a direction specific way and improves the quality of interaction. These results shows relevant contribution of the humans' physical attributes to overall task execution quality.

The significant performance of Directional Adaptation accomplish the major goals of this thesis mentioned in Section 1.3. A control mode which takes into consideration various human factor and at the same time consider task parameters, with human as the center is proposed here. Both the human and task specific parameters are combined in a meaningful manner in Directional Adaptation. As envisioned, the proposed control mode is validated through a user-study involving both naive and expert users. These methods are simple and could be integrated into industrial scenarios easily. There are no complex training routines necessary and at the same time it is intuitive for the users.

The results also pointed out the strong influence the task can have while choosing the control methods. Even though Directional Adaptation was having good overall performance, the segregation of tasks into regions based on their difficulty could facilitate switching between the control modes for improved performance. Having prior task knowledge could pave way for hybrid control methods which can optimize the human interaction. The insights gained from this experiment could be used in future to optimize the performance of such control methods. Furthermore, this approach could be extended to Co-Manipulation scenarios by explicit consideration of the task geometry.

Chapter 7

Experimental Evaluation of pHRI control modes

In chapter 6, different control modes which take into account human arm kinematics were compared. The best solution for pHRI from the proposed control modes was determined experimentally. The results of the conducted user study showed that by using manipulability ellipsoid based adaptation (Directional Adaptation) it is possible to combine both the task specificity and the human parameters effectively.

In this chapter, the Directional Adaptation is studied and compared against other established methods to validate the claims of its helpfulness and to study in detail if this adaptation scheme helps the users while performing tasks. The results of a user-study conducted with 50 users is reported in this chapter, this user-study was part of a Master thesis supervised by the author in context of pHRI. The author of this thesis contributed to the study design, establishment of the research questions and the experimental setup. The programming of machine learning based approaches was accomplished by the Master thesis student under the supervision of the author. The author further contributed to the data analysis and the programming of the other control approaches.

7.1 Evaluation of control methods

As seen in the current literature, various complex algorithms are proposed for improving the pHRI, most of them are never tested or validated under real task situations. Fuzzy logic based adpatation schemes were proposed in [20, 25, 26]. A scheme based on machine learning which predicts the intent of the human worker was proposed in [28]. Another approach where policy optimization was used in [16]. All these methods seems promising as they involve advanced machine learning techniques, but like discussed earlier their usefulness were never been tested under real use case scenarios. Ideally most of these methods require extensive training and a large chunk of time should be dedicated for training the algorithms.

In such cases it is safe to hypothesize that even after proper training they might not work as efficient as manipulability based approaches, as the human factors are not considered most of the times. Major parameters that are optimized in most of the cases are interaction forces and task velocity. Except for the interaction forces most other human related parameters such as the human body proportion and the distance to the task are

ignored. While simple adaptation schemes mentioned in Chapter 4 and Chapter 6 makes the adaptation faster and can be used for on-line stiffness adaptation without extensive prior training, most of the other methods consider change in direction of Cartesian velocity/force or try to predict the human intent based on trained interaction model etc. This is explained in depth in Section 2.2. There exist very few schemes that takes into consideration the fact that the inter-personal differences can affect the interaction and therefore a personalized scheme which is individualized for each person might be more effective.

It is imperative that the control modes proposed in this thesis should be compared with other approaches to find its real effectiveness and to prove the improved intuitiveness and reduced complexity. For this purpose, in this chapter the proposed interaction modes are compared with standard machine learning based control schemes. The control schemes are explained in the following sections. An extensive user-study is later being conducted with two set of users to validate the control modes and measure their performances. This chapter intends at finding answers to the following questions:

- Among Simple/Complex adaptation schemes, which is better?
- Does the inclusion of Human factors improves pHRI?

For answering these questions a user-study was conducted where five different control methods for pHRI are compared in an industrial scenario where naive users are asked to interact and rate the control methods. A Constant Stiffness mode, Linear Forced based adaptation, Manipulability based adaptation, Neural network based adaptation and a Polynomial Regression based method is compared.

7.2 Compared Control modes

This section discusses the five different control modes which are being used in the user-study for evaluation of control modes suited for pHRI. Fig. 7.1 shows the control architecture used in the experiment.

7.2.1 Directional Adaptation

The adaptation scheme based on manipulability ellipsoid which was discussed in Chapter 6 is used in the user-study. In this Chapter this adaptation schemes is denoted as MK, for Manipulability based Stiffness(k) adaptation.

7.2.2 Constant Stiffness

In [80] a user-study was conducted and the results clearly indicates that a medium stiffness based control scheme works much better than high or low stiffness schemes. It was found that medium stiffness mode offers comparable or even better qualitative performance while the task is not complex and intuitive. For this reason the task chosen for this task is not complex and involves very few directional changes. This is done in order to have a standard basis of performance for all the control methods.

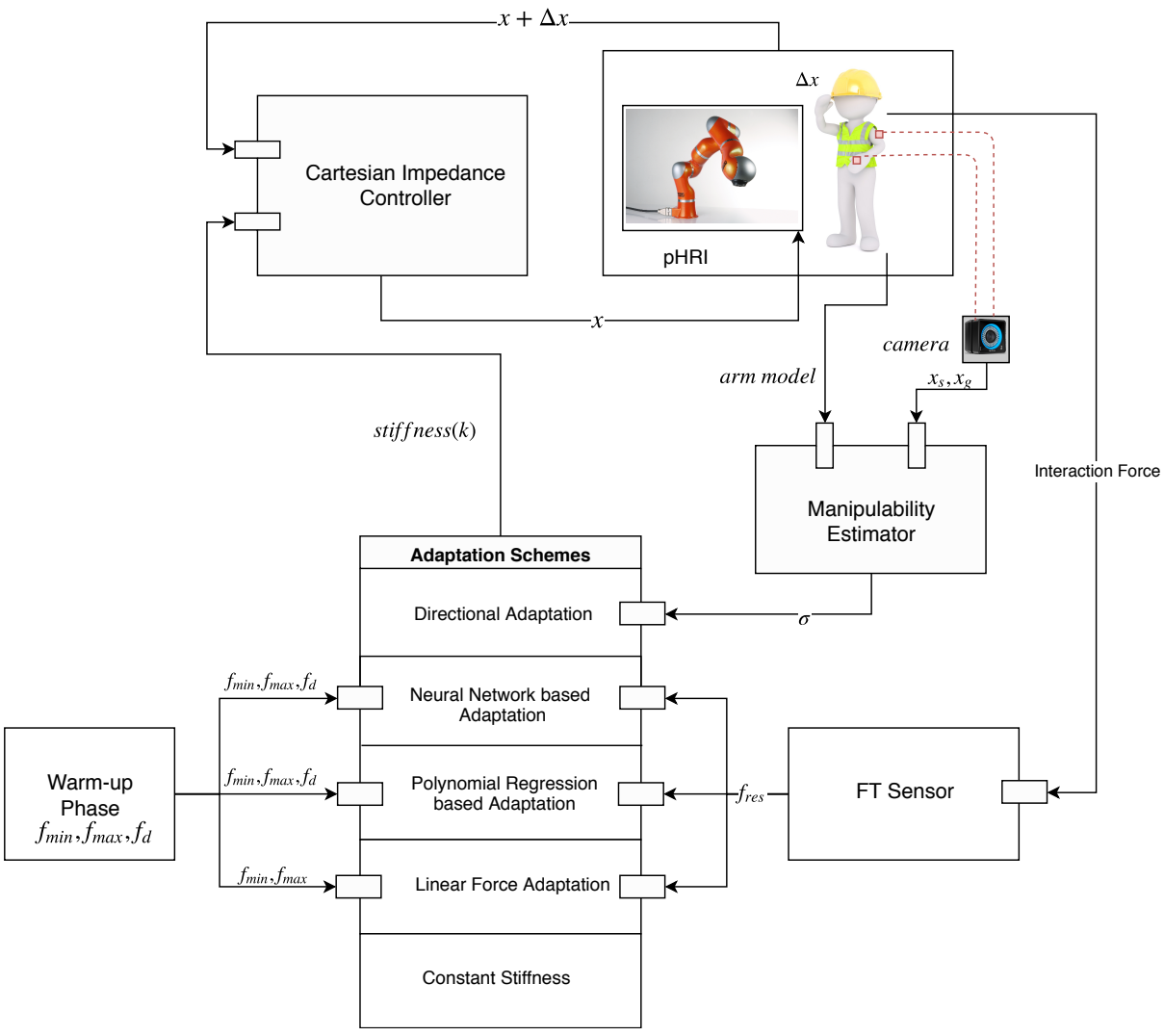

Figure 7.1: Control Architecture used for the user study

The stiffness value for this control mode is calculated from the results of a training phase conducted. The optimal stiffness value for the interaction was calculated as 2150 Nm/rad. In this Chapter this adaptation schemes is denoted as CK, for Constant Stiffness(k) adaptation.

7.2.3 Personalized force based Adaptation

The Personalized Force based Adaptation proposed in [68] is used in this method. The earlier force based adaptation was done in joint space and Joint Impedance controller of KUKA LWR was being used. The stiffness of each individual joints were changed with respect to the interaction forces. The range of stiffness was from 10 Nm/rad to 2000 Nm/rad. In this experiment, Cartesian Impedance scheme is employed the Cartesian stiffness values in the task space is changed linearly with respect to the interaction forces. Here, the stiffness range is chosen from 10 Nm to 5000Nm/rad for translation and 0 to 300 Nm/rad for rotation. In this Chapter this adaptation schemes is denoted as LK, for Linear force based Stiffness(k) Adaptation.

7.2.4 Force-Difference based Adaptation Methods

The methods discussed in this section adapts the stiffness of impedance control to the force difference between the desired force and the instantaneous interaction force. Inspired from [92], the idea is to minimize the difference between the actual interaction force and the desired optimal force required for a good pHRI.

By varying the stiffness of the robot, the error between the interaction force and desire force can be optimized. According to [92], if a human wants to push an object with high force, then the high force is achieved by increasing the stiffness of the human arm and vice-versa hold true for less force. The same approach can be used for a robot, by adjusting its stiffness depending on the contact situation. Based on this idea, the desired force is personalized for each user and the stiffness in this method is regulated based on the force difference. The intention of this method is to try to minimize the force difference by adapting stiffness of the robot.

For comparing and to validate the effectiveness of methods based on machine learning and other complex methods, a training phase is conducted with 20 users interacting with the robot achieving a certain task and their data is being recorded. With the selected data, two models are trained, to find the relationship between the force difference and the stiffness difference. The proposed methods are:

- Polynomial Regression based Adaptation - finding a polynomial relation between input and output;
- Neural Network based Adaptation- using multilayer perceptron to describe the relationship between input and output.

Most of the related work based on the force adaptation does not take into account the users force limitations. If the user's desired interaction force f_{des} is known then if we reduce the error between the interaction force and the desired force, $d_f = f - f_{des}$ the user will always work in their preferred comfort zone. Therefore, in this approach the

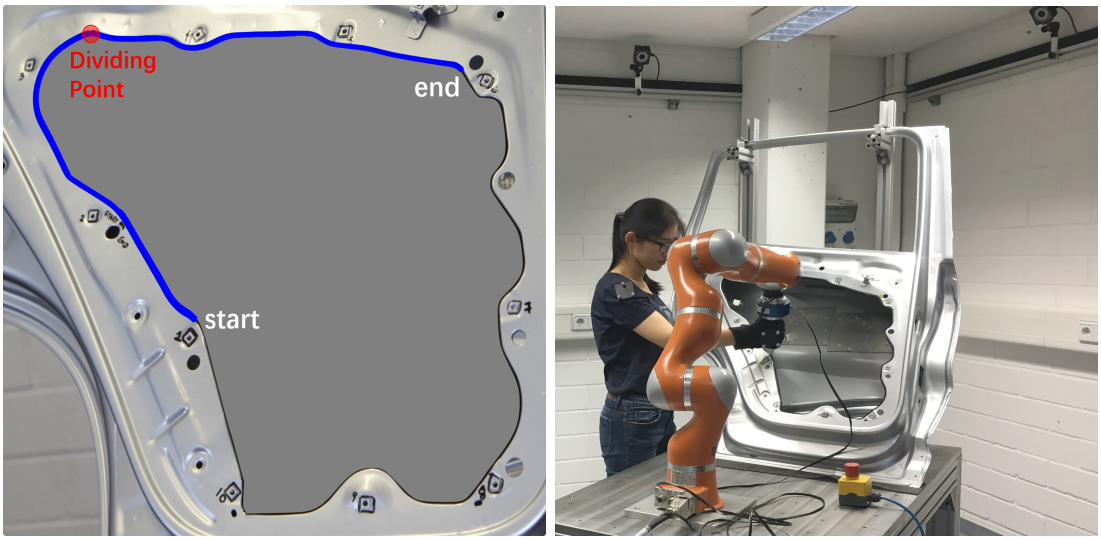

(a) Task (b) Participant executing the task

Figure 7.2: Figures illustrating (a): Task considered in the user-study (b) User interacting with the robot for performing the task

desired interaction force of each user is found out and the algorithm is modeled to reduce the error between the desired force and the instantaneous interaction.

The input and output of the model to be trained could be defined as

$$\begin{aligned} Input: \ d_f &= f - f_{des}, \\ Output: \ d_k &= k - k_{des}, \end{aligned} \tag{7.1}$$

In this Chapter these adaptation schemes are denoted as NK, for Neural network based Stiffness(k) adaptation and PK, for Polynomial Regression based adaptation (PK) respectively.

7.2.5 Training phase

A two stage training phase was implemented, the objectives of this phase was to parameterize the best stiffness range, find the optimal stiffness where most users work effectively and to train the model for the Polynomial Regression based Adaptation and the Neural network based Adaptation.

Calibration

From the previous experiments it is known that the human worker does not work effectively in all the stiffness range. They are less accurate in low range, needs more time and finds it tedious to work on higher stiffness range. Therefore, to get a good working adaptation it is important to select the best working range. For this purpose 15 stiffness values are selected uniformly in the range 0 to 5000. The selected values are : $[100, 450, 800, ..., 4300, 4650, 5000]$. Each user in the first stage were asked to complete a given task 15 times with each of this stiffness value and each time the users were asked

to fill in a questionnaire regarding, how they felt in each trial. The similarity based on Procrustes analysis, time of completion and the results from the questionnaire is used to calculate a combined criterion which is used to quantitatively define the best performance range as in Eqn. 7.2. The weighing factors a, b and c are determined by trial and error. Results of the analysis are depicted in Figure A.1, here each curve shows the average criterion result of the users with the various weighting factors. The range is selected between 450 and 4300 as the performance drops drastically below 450 and above 4300.

$$C = a \cdot similarity + b \cdot (-time) + c \cdot questionnaire, \tag{7.2}$$

Training

Both the methods mentioned in this section need training data to train their respective models. At the same time this phase is also used to find the best value of stiffness for the Constant Stiffness method.

The users were required to interact with the robot and accomplish the given task in-order to collect the data. For this purpose, 15 stiffness sub ranges are defined based on the results from the calibration phase: $[450-750, 750-1000, ...3750-4000, 4000-4300]$. Each user was required to accomplish the task 15 times with each of these sub range, the order of the sub range is activated randomly. Fig. 7.2a, shows the task, it was noticed from the calibration phases that the users felt the first half of the task was easy and the second half slightly difficult. Therefore, while modeling the trajectory was divided into two separate parts and these two parts are modeled separately to ensure better adaptation. Force data, stiffness, time of completion and the trajectory is being recorded for each trial. To find the stiffness zone where every user performs good, the same approach used for finding the best stiffness range using the combined criterion was employed. Fig. A.2, shows the performance of users in each stiffness zone. The best performance occurs in the stiffness zone 7, i.e. $[2000 - 2500]$ and the best stiffness value, k_{des} is calculated as mid point of this zone to be 2150 Nm/rad by considering the mean of the zone 7.

The force data is normalized at first in order to train the models. For the Polynomial Regression method the order of the equation and all coefficients, which reflects the property of the regression model is determined. Different possibilities were tested to find the most suitable polynomial order, the orders of both contour parts are set at the same value of nine to ensure the consistency of both models. In this control mode, when the current position is located in the first contour part, the first model is used to adjust the current stiffness value and when the current position is in the second part the stiffness adapts itself based on the second model.

For the Neural Network approach, a feed-forward network with one hidden layer was trained, where a sigmoid function is used as an activation function in each neuron. The parameters related to weights and bias were determined by a training process with the Levenberg-Marquardt back-propagation algorithm, the number of neurons in both models is set at the same value of 15. The implementation of the trained model is shown in Algorithm 1.

When the participant guides the robot to move, the interaction force is determined and before the actual interaction a warm-up phase is being done to determine the force characteristics of the participant. Hence, the f_{min}, f_{max} and f_{des} are personalized. For

both methods, the d_f is calculated and the d_k is obtained. From this, the required stiffness values is calculated and fed to the Cartesian Impedance controller. As the maximal rotational stiffness is 0.06 times the stiffness in translational axis, the instantaneous rotational stiffness is calculated accordingly.

7.3 Experimental evaluation of pHRI control methods

A user study was conducted to compare the five different control modes mentioned in this chapter. The robotic system and the experiment set up used in this study is similar to the experiment set up in Section. 6.3. Fig. 7.2 shows the task and the experiment setup used in this study. A total of 50 users participated in the user study, of which 20 users participated in the training phase and 30 users participated on the main study. Among the participants, 72 % were male and 28% female.

Before starting the user study, ethics committee of TU Braunschweig was consulted, the user study titled *Comparison of adaptive control modes for pHRI*, was officially approved by the ethics commission with the official number **MA-2018-02**. The study setup was inspected and approved by the official safety officer and each of the participants was given a short briefing prior to the experiment containing information about the study process and data that would be assessed. The subjects had also the opportunity to ask questions before the experiment and were insured that it was possible to quit participating at every point in time and that in this case the incomplete data would be deleted and not enter the analysis. All participants gave their written informed consent in accordance with Declaration of Helsinki. This was in agreement with usual practice in such studies and in accordance with Bielefeld Universitys ethic committee guidelines. After finishing the experiment, the participants were debriefed and given additional information regarding the study.

7.3.1 Study Setup

The overall study was divided into two phases, a first training phase followed by the main study phase. The main phase like the previous experiments, was divided into a warm-up phase and task phase. Fig. 7.3 shows the flow of the user study.

Training Phase

In the training phase, 20 users participated and the users were asked to accomplish a contour following task 15 times as explained in Section 7.2.5. In this phase, which is subdivided into two stages, the best stiffness range for the control methods to work is calculated in the initial stage. In the second stage the best stiffness range for the users to work on, k_{des} is estimated and at the same time the models for Polynomial Regression and Neural Network based Adaptation is trained.

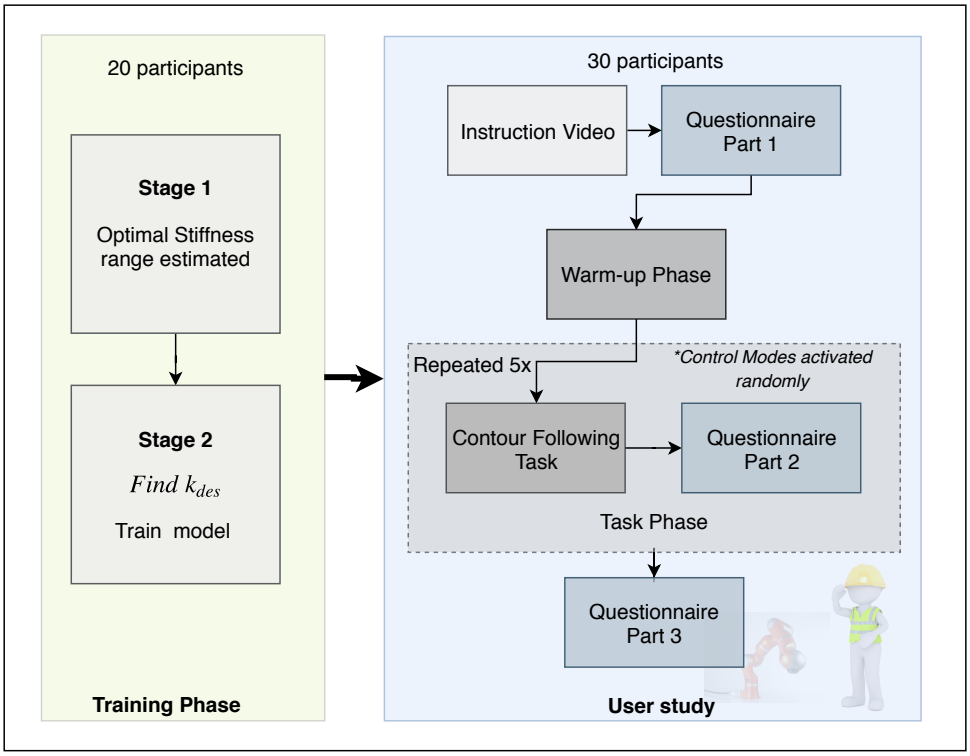

Figure 7.3: Control Architecture used for the user study

User-study

The second part of the experiment was the main user study where the 30 users participate. This stage had two phases initial warm-up and a task phase. Before the experiment, the users were shown and instruction video and was given a questionnaire to be filled which had the information about the study as well as the general information about the user.

Warm-up Phase

This phase had two objectives, the first one was to make the users familiar with the robot and pHRI. Most of the user did not have any experience handling robot or working together with them, therefore it is imperative that they be given a chance to interact with robot so as not to bias the experiment data with learning effects.

The second objective of this phase is to learn about the physical force limitations of the users. As already mentioned in the previous section, the Force based Adaptation needs to be personalized for each user, therefore the f_{min}, f_{max} and f_{des} for each user is determined in this phase. These parameters are then used in Neural Network based, Polynomial Regression based and Personalized Force based Adaptation.

Task Phase

In this phase the users were instructed to complete the task five times, each time a different control mode is activated randomly and the users are unaware of which control mode they are using. The task used in this phase is same as the one that is used in the

Criteria	CK		LK		MK		PK		NK	
	M	SD	M	SD	M	SD	M	SD	M	SD
PROC	0.963	0.019	0.966	0.019	0.97	0.011	0.967	0.019	0.964	0.02
TIME	23.82	13.5	23.2	14.3	22.1	9.8	23.5	12.4	24.9	15
TSM	51.42	32.3	53.76	47.7	49.96	25.45	51.00	31.18	53.96	34.23
FSM	73.34	49.46	67.11	50.47	65.57	40.18	70.4	44	73.84	48.92
ARC	0.0375	0.022	0.032	0.017	0.023	0.014	0.034	0.012	0.033	0.015
EFFORT	224.6	144.9	217.0	143.2	197.4	120.9	223.0	138.3	226.7	151.1
FORCE	8.32	1.07	8.17	0.98	7.61	0.79	8.28	1.20	8.13	0.96

Table 7.1: Table showing the results of quantitative analysis for five control modes

training phase. After each trial the users were asked to fill in the questionnaire which had questions relating to the qualitative analysis of the control methods. After five trials are over the users filled in the final questionnaire.

7.4 Evaluation

The data recorded for the user interaction from all five control modes are evaluated both qualitatively and quantitatively. The results of quantitative and qualitative analysis is listed in Table 7.1 and Table 7.2 respectively. The results are statistically compared using repeated measures ANOVA. Three groups are considered, the first group consists of all the five discussed control modes, the second group considered Constant Stiffness, Personalized force based and Directional adaptation, the third group considered Directional, Neural Network based and Polynomial Regression based adaptation. The results of ANOVA is shown in Table A.6 and Table A.7 respectively. The significance values of the ANOVA: p, ph and pm are tabulated in tables.

7.4.1 Quantitative analysis

Analyzing the similarity in task profile, the Procrustes analysis shows the performance of every controllers are similar with Directional Adaptation being slightly better. As for Time of completion, Directional Adaptation ($M_{MK} = 22.1$) has the best performance and the Neural Network based Adaptation ($M_{NK} = 24.9$) is the worse. The mean value for other control modes are similar. Considering Trajectory Smoothness, the control modes performed similar with no significant difference in p values. The Directional Adaptation ($M_{MK} = 49.96$) showed slightly better performance in the analysis of third group. The Neural Network based Adaptation ($M_{NK} = 53.96$) has the worst performance in this criteria. In the analysis of the smoothness of Force profile, the ANOVA shows significance difference between the control modes, with $p = 0.03$. The Directional Adaptation has the best performance ($M_{MK} = 65.57$), while both Constant Stiffness and Neural Network based Adaptation performed worse.

While analyzing the error in the Arc Length, it was found that the Directional Adaptation ($M_{MK} = 0.023$) has better performance in terms of accuracy and the Constant

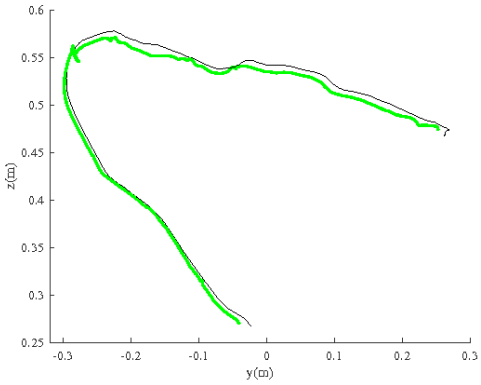

(a) Constant Stiffness

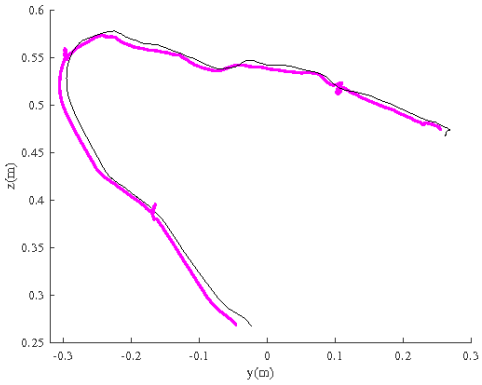

(b) Linear Adaptation

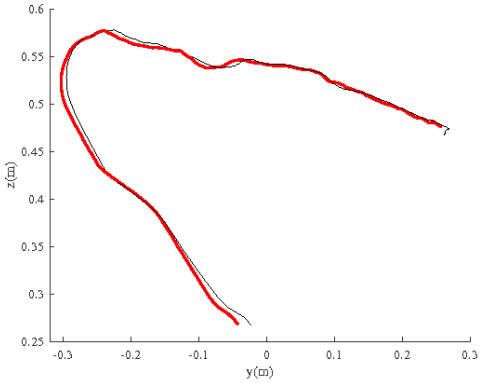

(c) Directional Adaptation

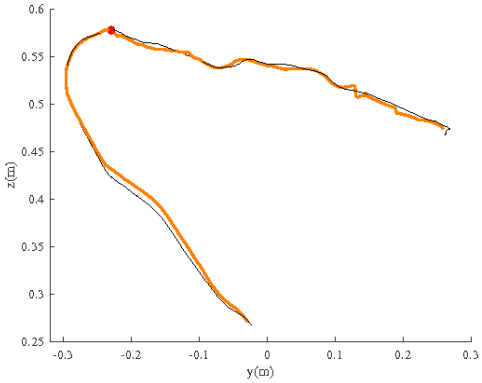

(d) Regression based Adaptation

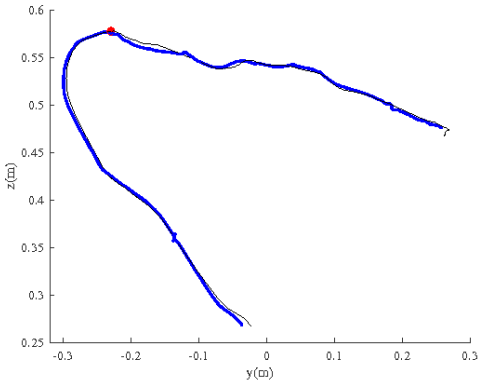

(e) Neural network based Adaptation

Figure 7.4: Trajectories of one user under five modes:$(a) - (e)$ show the generated trajectory under different control modes.

Stiffness mode ($M_{MK} = 0.037$) is the worst. The ANOVA shows a significant difference with $p < 0.05$ in all three groups. The mean force the users spend on the interaction was recorded and analyzed, it was found that Directional Adaptation ($M_{MK} = 7.61$) has the lowest mean interaction force and the Regression based Adaptation ($M_{PK} = 8.28$) and the Constant Stiffness based Adaptation ($M_{CK} = 8.32$) needed most interaction

Criteria	CK		LK		MK		PK		NK	
	M	SD	M	SD	M	SD	M	SD	M	SD
CONTROL	3.84	0.73	3.84	0.70	3.71	0.58	3.84	0.70	3.98	0.45
EASE	3.84	0.61	3.83	0.65	3.82	0.68	3.82	0.64	3.83	0.64
ENJOY	3.76	0.62	3.63	0.81	3.78	0.73	3.67	0.69	3.78	0.60
RELIAB.	3.86	0.57	3.90	0.57	3.92	0.70	4.00	0.52	3.86	0.64
SATIS.	3.96	0.51	4.01	0.56	4.08	0.53	3.92	0.55	4.04	0.48

Table 7.2: Table showing the results of qualitative analysis for five control modes

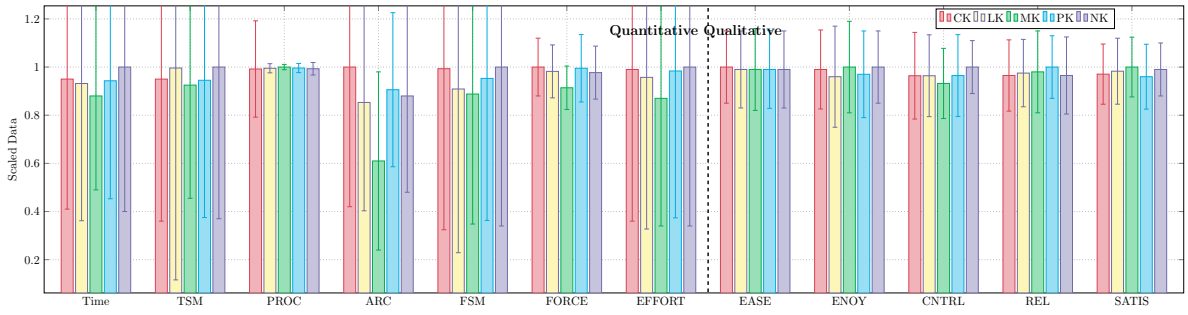

Figure 7.5: The performance of each control mode in each comparison criteria is shown in the figure. The data is scaled for easy comparison.

Force. The user effort is also another important factor for pHRI, it was found that Directional Adaptation ($M_{MK} = 197.4$) has better performance in this criterion and the users need lesser effort. Other methods performed similar in this case. The ANOVA shows a significant difference with $p < 0.05$ in all three groups.

Table A.8 shows the time required for preparation of each control mode. It is clear from the table that Constant Stiffness, Linear and Directional Adaptation can be used without much preparation time.

7.4.2 Qualitative analysis

The analysis of the qualitative criterion yielded similar results for controllers. For Ease of use, users rated all the controllers similar, there was no big difference in mean values and the ANOVA showed no significant difference as well. For Enjoyment, Neural network based ($M_{NK} = 3.78$) and Directional ($M_{MK} = 3.78$) Adaptation are slightly better than other control modes. Force based Adaptation has the worst user rating in this criterion. As for External Control Neural network based Adaptation ($M_{NK} = 3.98$) has the best performance and Directional Adaptation ($M_{NK} = 3.71$) has the worst performance. In terms of Reliability the Control modes are similar with Regression based Adaptation ($M_{PK} = 4.00$) being slightly better. In terms of User Satisfaction, Directional Adaptation ($M_{PK} = 4.08$) is slightly better than the other modes and Regression based Adaptation ($M_{PK} = 3.92$) has the worst user rating.

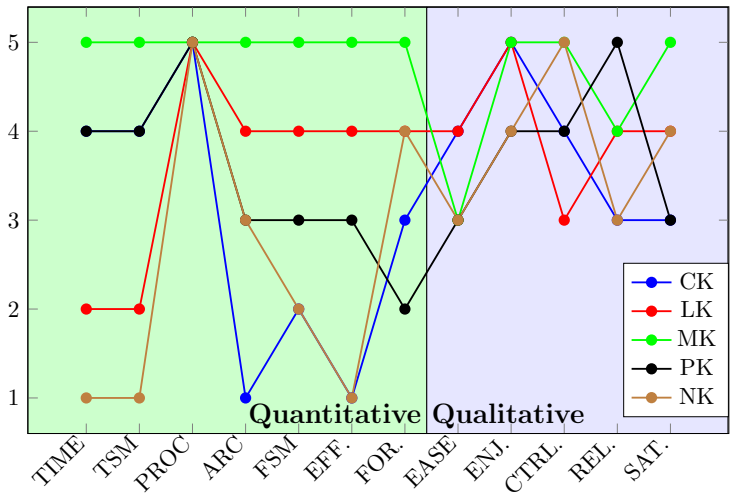

Figure 7.6: Ranking of each control mode for different considered criteria. Rank of 5 means the best and 1 means the worst performance.

7.5 Discussion

The results mentioned in Section 7.4 shows that for quantitative criteria Directional Adaptation has a better performance. The task chosen for this experiment was not so complex as it was already proven in the earlier experiments that the Constant Stiffness mode works best when the task is not complicated. The same can be assumed for other methods, that if the task is made complicated the results will be more biased towards Directional Adaptation since it is already proved to be performing well under difficult tasks.

The most noticeable results from the quantitative analysis are those concerned with the interaction forces. The user required reduced effort and low average force needed for interaction while using the Directional Adaptation scheme as opposed to other control modes. Fig. 7.7 shows the force profile for one user in all five interaction modes. From the Table 7.1, it can be seen that the average for needed interaction is lowest when Directional Adaptation was used. The Regression based Adaptation was worst and the other three methods were similar. Similarly, the effort needed by each user is also less for the Directional Adaptation, the green area in Fig. 7.7 represents the total effort by the user while interacting with the robot. This result is significant since four methods used here were parameterized to minimize the interaction forces and still Directional Adaptation outperformed them in this category. It is visible from the force plot that the force variation in each interaction follows a pattern, which was already stated in [80], hence even for a simple task the task specific parameters have a strong influence. Here, all the five plots shows three major peaks where the user exerts more force for interaction and the results indicate that by taking into consideration the manipulability, the interaction force can be decreased.

For other force based evaluation measures like Effort and Smoothness in force profile, the Directional Adaptation has better performance. A pairwise analysis was done for these criteria. For Effort, there is a significant performance difference between Constant Stiffness and Directional Adaptation ($p = 0.007$), Directional and Neural Network based

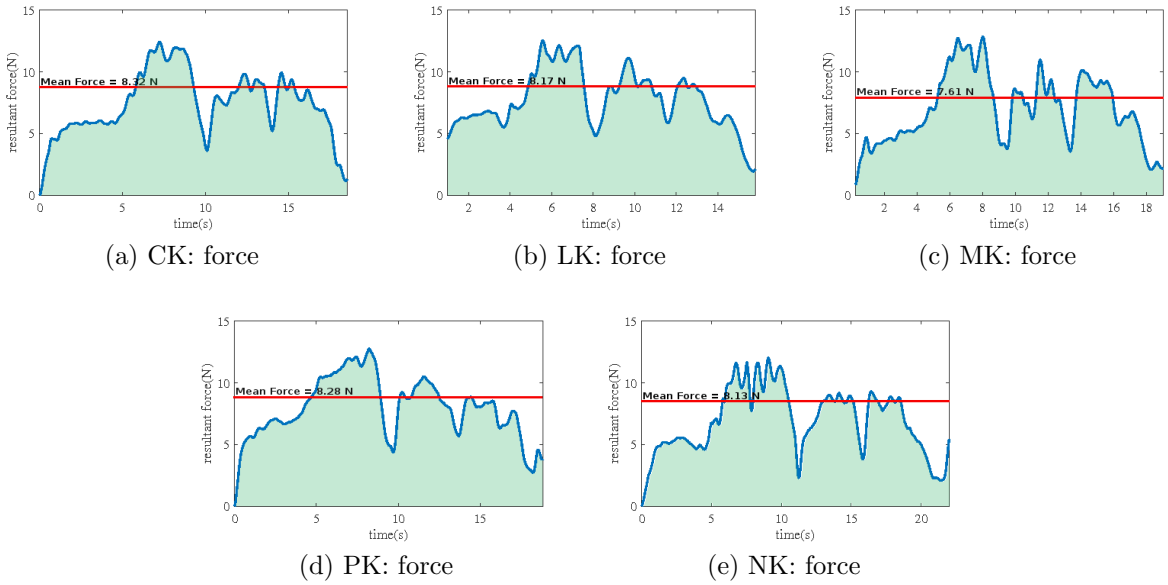

(a) CK: force (b) LK: force (c) MK: force

(d) PK: force (e) NK: force

Figure 7.7: Force profile from one user while performing the task with different control modes, the green area represents the work done by the users.

Adaptation ($p = 0.01$) and Directional and Regression based Adaptation ($p = 0.05$). Pairwise analysis for interaction force showed a significant performance difference between, Directional Adaptation and Constant Stiffness ($p = 0.002$), Directional and Force based Adaptation ($p = 0.006$), Directional and Regression based Adaptation ($p = 0.007$) and Directional and Neural Network based Adaptation ($p = 0.035$). This proves that users gets a good structured assistance from the controller while interacting with robot using the Directional Adaptation scheme. Both Linear Adaptation based on the interaction forces and the Directional Adaptation has better smoothness in the force profile of the users. Fig. 7.4 shows the trajectory generated by one user during the interaction, it is visible that the trajectory from Directional Adaptation is smoother and closely follows the target trajectory compared to the other methods.

For other criteria discussed, Directional Adaptation has the least time of completion, which means the users were able to finish the task faster with this control mode than with other modes. Since the task was designed to be simple in-order to include the Constant Stiffness modes, the Procrustes analysis yielded similar results for each control mode. It is highly noticeable that even for a simple task the error in trajectory execution measures as arc error is low for Directional Adaptation and worst for Constant Stiffness, other three modes performed similar in this aspect. Pairwise analysis was conducted for the criterion Arc error. There is a significant performance difference between, Directional Adaptation and Constant Stiffness ($p = 0.032$), Directional and Regression based Adaptation ($p = 0.010$), Directional and Neural Network based Adaptation ($p = 0.035$) and Directional and Force based Adaptation ($p = 0.032$).

The results of the qualitative interaction shows that all control modes performed similar. The task chosen in this study is simple and the user feedback is similar the results from Section 4.4.4. The Neural network based Adaptation has a slight advantage over other control modes in external control, while Directional Adaptation has the worst

rating. For the criterion ease of use, all control modes has similar performance. The Neural Network based Adaptation and Directional Adaptation has similar results in case of enjoyment. While for reliability, Regression base Adaptation is slightly better. In terms of user-satisfaction the Directional Adaptation is more preferred. Figure 7.6, shows the statistical ranking of the control mode in each criterion, the left green part in the plot indicates the quantitative results and the left part indicate the qualitative results. Its clearly visible that the Directional Adaptation performs better in quantitative fields and the control modes are not that different in qualitative aspect.

Table A.8, shows the time required for preparation of each control mode, this is highly significant. The Constant Stiffness mode can be used instantly by any user but it will have no adaptation. In Linear Adaptation it is required to parameterize the controller to user specific parameter, eg. Force Limits. The time required for this is less than 2 minutes and it is done during the warm-up where the user interacts with the robot. For Directional Adaptation, no warm-up or user parameter identification is necessary as it can be done in run time using the camera system. If not being done by the system, the measurement of user's body parameters will need less than a minute. For the other two adaptation, extensive training is required, for each user around 20 minutes are required and the more the number of users are the better will be the adaptation. Additionally, a warm-up phase was needed to determine individual force characteristics of the user. Hence, it is clear that these methods are not intuitive and is time-consuming. For every change in task the whole process has to be repeated and therefore cannot be easily realized in the industry.

From the results of analysis it is clear that the Directional Adaptation scheme which takes into consideration both task and human parameters is better than the other controller modes while we take into consideration the quantitative performance. Fig. 7.5 shows the comparison of each control mode for each compared criterion. Fig. 7.6 shows the ranks of each control mode for each compared criterion based on their significance.

7.6 Conclusion

The results of the user study conducted with a total of 50 users, proved the effectiveness of Directional Adaptation. The quantitative analysis showed that the Directional Adaptation offers better performance in all the compared criteria. The most important result here is the force and effort requirement. The Directional Adaptation needed the least force and effort from the user and hence would be the most beneficial control mode for the users if used for longer duration.

It is clear that even for a simple task the methods which rely on complicated training schemes and algorithms does not guarantee good performance. Rather, it is important to include the factors and parameters that matters the most, such as human and task parameters. On-line methods based on human parameters are easy to implement, guarantees performance, and it is time efficient. It would be not always feasible to have such time extensive training routine and longer warm-up phases if the task in hand changes regularly, in such cases simple, but effective adaptation schemes are more useful.

Chapter 8

Conclusion

The main focus of this thesis is to establish the importance of human factors in pHRI and to personalize the control schemes for each individual user. In this thesis four control modes which take into consideration various human factors are proposed. Each proposed control mode is evaluated through user-studies involving both naive and expert users. The inferences drawn from each study is used to improve the control modes further. Four user-studies were conducted in the scope of this thesis, where a total of 170 users participated. This thesis followed a meticulous research plan, in each chapter certain hypotheses or control modes were proposed and was evaluated with ample users.

In Chapter 3, the significance of pHRI and kinesthetic guidance in industrial context was established. Various interfaces for Human-Robot Interaction like Keyboard, Spacemouse and Kinesthetic Guidance were compared in this chapter. It was found that the Kinesthetic Guidance which is a form of pHRI is the best method for human intervention in industrial scenarios. The users can readily use their knowledge about task in solving problems and the intuitiveness of pHRI methods are much higher than other standard interfaces compared.

In Chapter 4, the importance of personalization of control modes of pHRI was established. Force based personalized Adaptation scheme for pHRI was proposed in this chapter. The proposed control mode was compared against standard pHRI control modes like, Gravity Compensation, Medium Stiffness and High Stiffness modes. The proposed control mode took into consideration the physical force limits of the user and the results of the evaluation showed that the performance was much better than other compared control modes. The evaluation was done using two distinct tasks of varying difficulty. The performance of control modes for same users varied drastically for both tasks. This was an important result in the thesis as it emphasized the importance of task related parameters in pHRI.

In Chapter 5, the influence of task specific parameters in pHRI was discussed in detail and methods for combining task specificity and human factors were discussed. The effect of human arm's manipulability and its variation for different arm parameters were investigated. Various measures based on human arm manipulability which could include both task and human parameters were proposed in this chapter. The performance of four different users with distinct body proportions performing a task is analyzed in this chapter. The results showed that, ideally for one user there exist a particular task configuration which assure best performance, in other cases the user needs assistance from

the robot. It was also inferred that manipulability measures could be used to quantify the measure of assistance the human user need.

In Chapter 6, three control modes based on manipulability measures were proposed. The proposed control modes were validated through a user-study and compared, while the users performed two distinct tasks of varying difficulty. The results showed that, Directional Adaptation mode which is based on manipulability ellipsoid has the best performance in the areas where interaction was otherwise difficult. The major goal of this thesis was accomplished in this Chapter. A control mode which takes into consideration both task and human factors at the same time was proposed and was validated through user-study involving naive users. The user-study proved that the Directional Adaptation scheme can be used for improving the pHRI by taking into consideration the personal features of the users and its performed well for both difficult and easy tasks.

In Chapter 7, the control modes proposed in Chapter 4 and 6 were compared against other techniques which are similar to commonly proposed methods in literature. The results of the evaluations showed that the Directional Adaptation performs better than other compared modes. The force and effort requirement for the interaction with the robot was reduced through adapting the robot stiffness along each axis by considering the manipulability ellipsoid.

Various problems stated in Section 1.2 have been addressed in this thesis. The results of the conducted evaluations shows that the consideration of human factors while designing control modes of pHRI is an important aspect. Various human factors were identified as important in the context of this thesis including, user's height, arm lengths and the user interaction force limits. Inclusion of these human parameters will improve pHRI as proved in this thesis. The dependency of pHRI on task parameters were also studied in depth in the context of this thesis. It was proven that the task parameters are highly important and mostly follow certain patterns for each task. It was shown experimentally that inclusion of the task parameters can improve the pHRI.

This thesis also analyzed the effectiveness of complex methods for pHRI. It was inferred that complex training methods do not guarantee the performance, rather the overhead created by complicated training routines makes them impractical to be used in real industrial scenarios. In this thesis the proposed control methods were evaluated with extensive user studies and constantly improved based on the drawn inferences. Finally, a control scheme which took into consideration task and human factors is proposed and verified. The results proved that this method (Directional Adaptation) is effective and could be used in industrial scenarios without any complex training and with minimal effort.

Appendix A

Appendix

A.1 Figures and Tables

Table A.1: Questionnaire items.

Criterion	Example Item
Ease of use	'Interacting with the system did not require a lot of my mental effort.'
Control	'I had control over using the system.'
Reliability	'The operation of the robot was dependable.'
Enjoyment	'I found using the system to be enjoyable.'
User Satisfaction	'All things considered, I was very satisfied with the interaction with the robot.'

Table A.2: Differences of means between the tasks for each control mode, Main Effect (M.E) and Interaction Effect (I.E.) between tasks and control modes are also tabulated.

		Proc.	Peaks	Jerk	Ease	Enjoy.	Realib.	Cntrl.	Satis.
M_{Diff}	Grav	0.40	-2.53	0.10	0.30	0.26	0.38	0.40	0.35
	Adapt	0.32	-5.91	0.19	0.04	0.25	0.04	0.17	-0.09
	Med	0.39	-3.42	0.05	0.25	0.26	0.21	0.35	0.23
	High	0.33	-6.21	0.14	0.24	0.31	0.16	0.19	0.32
M.E. tasks	df	1	1	1	1	1	1	1	1
	F	162.64	1.78	43.78	16.32	11.99	10.53	8.78	4.62
	p	**<0.001**	0.189	**<0.001**	**<0.001**	**0.001**	**0.002**	**0.005**	**0.037**
M.E. control modes	df	3	3	3	3	3	3	2.115	2.499
	F	6.19	14.06	0.46	10.93	3.72	6.19	7.32	5.21
	p	**0.001**	**<0.001**	0.713	**<0.001**	**0.003**	**0.001**	**0.001**	**0.004**
I.E.	df	3	2.576	3	3	3	3	3	2.499
	F	3.38	0.58	2.22	2.71	0.50	1.13	2.63	3.72
	p	**0.020**	0.604	**0.089**	**0.048**	0.683	0.342	**0.053**	**0.019**

Table A.3: ANOVA results for different comparison criteria, df, F, and p are the ANOVA parameters.

	Time	Smooth	Proc.	FSM	Arc.	Enjoy	Contrl	Satis.	Ease	Reliab
df	3	3	3	3	3	3	3	3	3	3
F	4.04	19.3	4.15	2.24	12.04	4.99	1.86	3.66	6.64	3.20
p	0.009	**<0.001**	0.008	0.087	**<0.001**	**.003**	0.015	0.14	**<0.001**	0.26

Table A.4: Table illustrating the performance of the control modes while approaching the task

	Arc Length				Force Smoothness				Trajectory Smooth				Time of Completion			
Hole	Const	Man	XYZ	FT	Const	Man	XYZ	FT	Const	Man	XYZ	FT	Const	Man	XYZ	FT
1	0.026	0.018	0.019	0.021	30.30	30.18	27.51	31.33	8.03	7.93	5.45	10.51	1.18	1.11	1.06	1.20
2	0.022	0.018	0.019	0.021	26.00	26.79	24.90	27.00	6.40	7.20	7.05	7.57	0.98	1.00	0.92	1.02
3	0.021	0.019	0.018	0.019	28.57	26.81	27.27	28.06	11.32	9.44	7.67	8.26	1.05	1.052	1.03	1.03
4	0.021	0.019	0.019	0.017	30.23	28.35	28.79	23.32	9.67	8.33	9.54	7.36	1.12	1.01	0.99	0.95
5	0.021	0.019	0.018	0.019	27.51	23.03	23.54	23.75	9.03	7.60	6.57	7.96	1.13	0.95	0.95	0.95
6	0.020	0.016	0.016	0.017	27.74	25.00	22.87	24.90	7.69	4.63	5.42	6.33	1.06	0.89	0.80	1.02
7	0.021	0.017	0.018	0.018	33.51	28.12	28.96	29.57	9.47	7.00	8.35	8.35	1.24	1.09	1.06	1.19
8	0.030	0.022	0.023	0.023	44.97	34.64	34.35	33.45	13.46	10.21	10.71	10.09	1.78	1.36	1.33	1.40
9	0.026	0.020	0.023	0.021	41.63	31.81	40.18	34.88	14.03	9.78	11.96	9.69	1.61	1.23	1.48	1.29

Table A.5: Table illustrating the performance of the control modes while receding from the task

	Arc Length				Force Smoothness				Traj Smoothness				Time of Completion			
Hole:	Const	Man	XYZ	FT	Const	Man	XYZ	FT	Const	Man	XYZ	FT	Const	Man	XYZ	FT
1	0.015	0.013	0.012	0.013	19.00	12.88	13.73	12.33	9.82	6.52	6.88	5.42	0.80	0.57	0.55	0.54
2	0.017	0.013	0.015	0.014	18.24	12.18	14.45	13.48	10.47	4.62	9.24	8.29	0.74	0.53	0.59	0.62
3	0.019	0.017	0.018	0.017	13.24	9.94	11.55	10.73	6.09	5.64	6.21	6.94	0.53	0.43	0.46	0.51
4	0.021	0.021	0.021	0.021	11.73	11.18	10.73	14.18	6.94	6.47	7.19	9.25	0.48	0.46	0.44	0.56
5	0.026	0.027	0.027	0.026	17.73	17.67	17.45	18.73	9.91	10.56	8.38	10.44	0.68	0.68	0.66	0.74
6	0.024	0.023	0.021	0.023	22.55	18.52	16.97	19.33	13.41	11.97	11.72	10.50	0.93	0.79	0.74	0.82
7	0.022	0.021	0.021	0.020	15.39	13.33	12.88	15.06	10.26	9.15	8.59	10.53	0.66	0.62	0.58	0.63
8	0.022	0.019	0.018	0.019	11.44	9.71	10.32	11.18	7.39	5.18	4.52	6.88	0.62	0.50	0.51	0.59
9	0.014	0.015	0.014	0.014	14.12	14.39	11.97	14.03	8.88	8.55	7.39	9.06	0.60	0.60	0.52	0.64

Sig.	PROC	TIME	TSM	FSM	ARC	EFF.	FORCE
p	0.45	0.29	0.86	**0.03**	**0.02**	**0.03**	**0.00**
p_h	0.17	0.27	0.81	**0.01**	**0.00**	**0.01**	**0.00**
p_m	0.31	0.31	0.57	0.25	**0.11**	**0.01**	**0.00**

Table A.6: Table showing the results of repeated measures ANOVA for the three groups for Quantitative criteria.

Sig.	CNTRL	EASE	ENJOY	REL.	SATIS.
p	0.39	0.99	0.57	0.68	0.47
p_h	0.47	0.97	0.42	0.87	0.46
p_m	0.12	0.99	0.54	0.47	0.29

Table A.7: Table showing the results of repeated measures ANOVA for the three groups for Qualitative criteria.

Algorithm 1 Usage of the model PK/NK

Require: f_x, f_y, f_z from force torque sensor; x, y, z (position of end effector);
Ensure: k_x, k_y, k_z, k_A, k_B, k_C of Cartesian impedance control;

repeat
  compute resultant force: $f = f_x^2 + f_y^2 + f_z^2$;
  if x, y, z in contour part 1 **then**
    compute force difference: $d_f = f - fdes_{p1}$;
    normalize and set as input: $Input = norm(d_f)$; ▷ done with $fmin_{p1},\ fmax_{p1}$;
    use trained model: $Output = model_{p1}(-Input)$;
  else
    compute force difference: $d_f = f - fdes_{p2}$;
    normalize and set as input: $Input = norm(d_f)$; ▷ done with $fmin_{p2},\ fmax_{p2}$;
    use trained model: $Output = model_{p2}(-Input)$;
  end if
  compute the stiffness: $k = Output + k_{des}$;
  if $k > 5000$ **then**
    set as maximal value: $k = 5000$;
  else if $k < 10$ **then**
    set as minimal value: $k = 10$;
  end if
  set translational stiffness: $k_x, k_y, k_z = k$;
  set rotational stiffness: $k_A, k_B, k_C = 0.06 \times k$;
until End of the task

Control Mode	Training phase	Warmup phase	Time Required		Remarks
			Training Phase	Warm-up Phase	
Constant Stiffness	No	No	-	-	Stiffness kept constant
Linear Adaptation	No	Yes	-	<2mins	Force limits parameterized during Warm-up phase
Directional Adaptation	No	Optional	-	<1mins	User's arm lengths are measured during Warm-up phase
Regression based adaptation	Yes	Yes	20 mins	<2 mins	Training data is collected in Training Phase. Force characteristics determined in Warm-up
Neural network based Adaptation	Yes	Yes	20 mins	<2 mins	Training data is collected in Training Phase. Force characteristics determined in Warm-up

Table A.8: Table showing the time required for preparation while using each control mode.

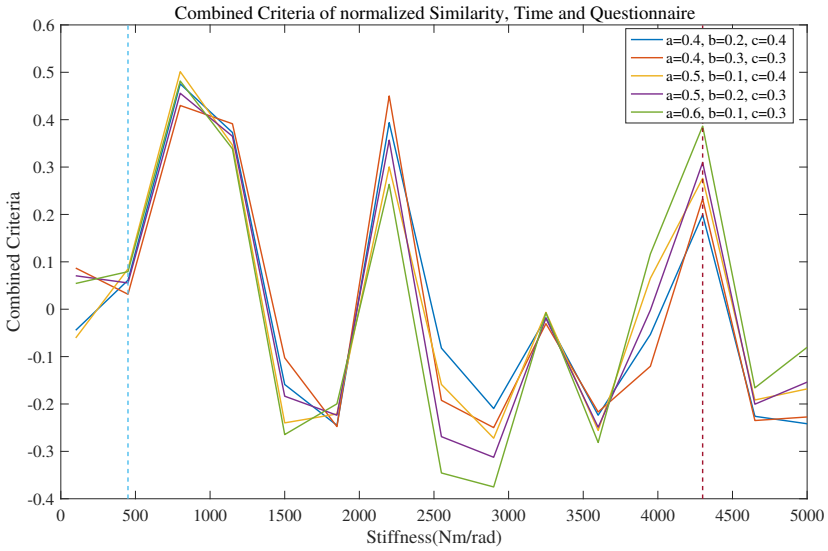

Figure A.1: Combined criterion C results with 5 different combinations of weighting factors.

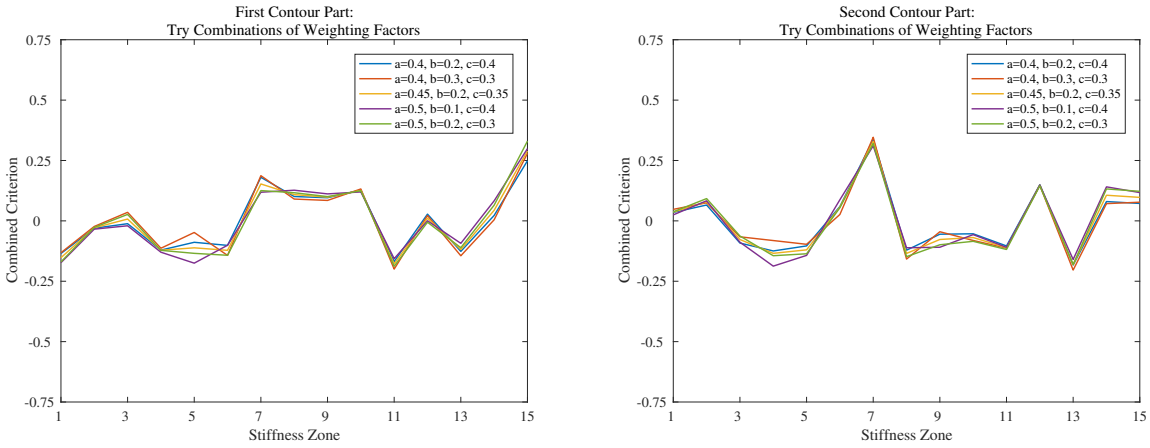

(a) Part 1

(b) Part 2

Figure A.2: Figure showing how Desired stiffness is being calculated from the user data.

A.2 Related references by the author

Contributions to Journals

- Sugeeth Gopinathan, Sonja K. Ötting and Jochen J. Steil. "A user study on personalized stiffness control and task specificity in physical human-robot interaction", In: Frontiers in Robotics and AI, 2017.

  In this work, the importance of task specificity in pHRI is elaborated in detail. All authors contributed to the research design. This work contributes the Chapter 4 and Chapter 5 and the results of this work are elaborated there.

Contributions to conferences

- Arne Muxfeldt, Sugeeth Gopinathan, Thilo Coenders and Jochen J. Steil. "A user study on human-robot-interactive recovery for industrial assembly problems", In: 26th IEEE International Symposium on Robot and Human Interactive Communication (ROMAN), 2017.

  This work establish the importance of pHRI in industrial scenarios where human intervention is necessary. All authors contributed to the research design. This work contributes to the Chapter 3 and the results of this work is elaborated there.

- Sugeeth Gopinathan, Sonja K. Ötting and Jochen J. Steil. "A user study on personalized adaptive stiffness control modes for human-robot interaction", In: 26th IEEE International Symposium on Robot and Human Interactive Communication (ROMAN), 2017.

  In this work, the user interaction force based personalized adaptation for pHRI is proposed. All authors contributed to the research design. This work contributes to the Chapter 4 and the results of this work is elaborated there.

Contributions to Workshops

- Sugeeth Gopinathan, Pouya Mohammedi and Jochen J. Steil. "Improved human-robot interaction: A manipulability based approach", In International Conference on Robotics and Automation, Workshop on Ergonomic Physical Human-Robot Collaboration, 2018.

  In this work the possibility of using human arm manipulability to quantify the effects of human and task factors is discussed. All authors contributed to the research design. This work contributes to the Chapter 5 and the results of this work is elaborated there.

Bibliography

[1] M. A. K. Bahrin, M. F. Othman, N. N. Azli, and M. F. Talib, "Industry 4.0: A review on industrial automation and robotic," *Jurnal Teknologi*, vol. 78, no. 6-13, pp. 137–143, jun 2016.

[2] J. N. Pires, *Industrial Robots Programming*. Springer US, 2007.

[3] M. Brettel, N. Friederichsen, M. Keller, and M. Rosenberg, "How virtualization, decentralization and network building change the manufacturing landscape: An industry 4.0 perspective," *International Journal of Mechanical, Industrial Science and Engineering*, vol. 8, no. 1, pp. 37–44, 2014.

[4] K.-D. Thoben, S. Wiesner, and T. Wuest, ""industrie 4.0" and smart manufacturing – a review of research issues and application examples," *International Journal of Automation Technology*, vol. 11, no. 1, pp. 4–16, jan 2017.

[5] (2018) Smerobotics. [Online]. Available: http://www.smerobotics.org/project.html

[6] R. Baheti and H. Gill, "Cyber-physical systems," *The impact of control technology*, vol. 12, no. 1, pp. 161–166, 2011.

[7] A. Khalid, P. Kirisci, Z. Ghrairi, K.-D. Thoben, and J. Pannek, "A methodology to develop collaborative robotic cyber physical systems for production environments," *Logistics Research*, vol. 9, no. 1, p. 23, nov 2016.

[8] I. S. Sacala, M. A. Moisescu, I. D. C. A. Munteanu, and S. I. Caramihai, "Cyber physical systems oriented robot development platform," *Procedia Computer Science*, vol. 65, pp. 203–209, 2015.

[9] S. Robla-Gmez, V. M. Becerra, J. R. Llata, E. Gonzlez-Sarabia, C. Torre-Ferrero, and J. Prez-Oria, "Working together: A review on safe human-robot collaboration in industrial environments," *IEEE Access*, vol. 5, pp. 26 754–26 773, 2017.

[10] C. Vogel, M. Poggendorf, C. Walter, and N. Elkmann, "Towards safe physical human-robot collaboration: A projection-based safety system," in *2011 IEEE/RSJ International Conference on Intelligent Robots and Systems*, IEEE. IEEE, sep 2011, pp. 3355–3360.

[11] N. Hogan, "Impedance control: An approach to manipulation: Part II—implementation," *Journal of Dynamic Systems, Measurement, and Control*, vol. 107, no. 1, p. 8, 1985.

[12] V. Duchaine and C. Gosselin, "Safe, stable and intuitive control for physical human-robot interaction," in *2009 IEEE International Conference on Robotics and Automation*, IEEE. IEEE, may 2009, pp. 3383–3388.

[13] C. Ott, R. Mukherjee, and Y. Nakamura, "Unified impedance and admittance control," in *2010 IEEE International Conference on Robotics and Automation*. IEEE, May 2010, pp. 554–561.

[14] F. Flacco and A. D. Luca, "Safe physical human-robot collaboration," in *2013 IEEE/RSJ International Conference on Intelligent Robots and Systems*. IEEE, nov 2013, pp. 2072–2072.

[15] T. Fong, C. Thorpe, and C. Baur, *Collaborative control: A robot-centric model for vehicle teleoperation*. Carnegie Mellon University, The Robotics Institute Pittsburgh, 2001, vol. 1.

[16] J. Buchli, E. Theodorou, F. Stulp, and S. Schaal, "Variable impedance control a reinforcement learning approach," *Robotics: Science and Systems VI*, pp. 153–160, 2011.

[17] J. R. Medina, M. Lawitzky, A. Mörtl, D. Lee, and S. Hirche, "An experience-driven robotic assistant acquiring human knowledge to improve haptic cooperation," in *2011 IEEE/RSJ International Conference on Intelligent Robots and Systems*, IEEE. IEEE, sep 2011, pp. 2416–2422.

[18] L. Rozo, D. Bruno, S. Calinon, and D. G. Caldwell, "Learning optimal controllers in human-robot cooperative transportation tasks with position and force constraints," in *Intelligent Robots and Systems (IROS), 2015 IEEE/RSJ International Conference on*. IEEE, 2015, pp. 1024–1030.

[19] W. Kim, J. Lee, L. Peternel, N. Tsagarakis, and A. Ajoudani, "Anticipatory robot assistance for the prevention of human static joint overloading in human–robot collaboration," *IEEE Robotics and Automation Letters*, vol. 3, no. 1, pp. 68–75, jan 2018.

[20] F. Dimeas and N. Aspragathos, "Fuzzy learning variable admittance control for human-robot cooperation," in *2014 IEEE/RSJ International Conference on Intelligent Robots and Systems*, IEEE. IEEE, sep 2014.

[21] N. Hogan, "Adaptive control of mechanical impedance by coactivation of antagonist muscles," *IEEE Transactions on Automatic Control*, vol. 29, no. 8, pp. 681–690, aug 1984.

[22] C. Ott and Y. Nakamura, "Admittance control using a base force/torque sensor," *IFAC Proceedings Volumes*, vol. 42, no. 16, pp. 467–472, 2009.

[23] R. Ikeura and H. Inooka, "Variable impedance control of a robot for cooperation with a human," in *Proceedings of 1995 IEEE International Conference on Robotics and Automation*, vol. 3, IEEE. IEEE, 1995, pp. 3097–3102.

[24] F. Ficuciello, L. Villani, and B. Siciliano, "Variable impedance control of redundant manipulators for intuitive human–robot physical interaction," *IEEE Transactions on Robotics*, vol. 31, no. 4, pp. 850–863, aug 2015.

[25] F. Dimeas and N. Aspragathos, "Learning optimal variable admittance control for rotational motion in human-robot co-manipulation," *IFAC-PapersOnLine*, vol. 48, no. 19, pp. 124–129, 2015.

[26] Z. Du, W. Wang, Z. Yan, W. Dong, and W. Wang, "Variable admittance control based on fuzzy reinforcement learning for minimally invasive surgery manipulator," *Sensors*, vol. 17, no. 4, p. 844, apr 2017.

[27] F. Dimeas and N. Aspragathos, "Reinforcement learning of variable admittance control for human-robot co-manipulation," in *IROS, 2015*. IEEE, sep 2015, pp. 1011–1016.

[28] I. Ranatunga, S. Cremer, D. O. Popa, and F. L. Lewis, "Intent aware adaptive admittance control for physical human-robot interaction," in *2015 IEEE International Conference on Robotics and Automation (ICRA)*. IEEE, may 2015.

[29] I. Ranatunga, F. L. Lewis, D. O. Popa, and S. M. Tousif, "Adaptive admittance control for human–robot interaction using model reference design and adaptive inverse filtering," *IEEE Transactions on Control Systems Technology*, vol. 25, no. 1, pp. 278–285, jan 2017.

[30] S. Grafakos, F. Dimeas, and N. Aspragathos, "Variable admittance control in pHRI using EMG-based arm muscles co-activation," in *2016 IEEE International Conference on Systems, Man, and Cybernetics (SMC)*, IEEE. IEEE, oct 2016, pp. 1900–1905.

[31] C. T. Landi, F. Ferraguti, L. Sabattini, C. Secchi, and C. Fantuzzi, "Admittance control parameter adaptation for physical human-robot interaction," in *2017 IEEE International Conference on Robotics and Automation (ICRA)*, IEEE. IEEE, may 2017, pp. 2911–2916.

[32] A. Lecours, B. M. St-Onge, and C. Gosselin, "Variable admittance control of a four-degree-of-freedom intelligent assist device," in *2012 IEEE International Conference on Robotics and Automation*. IEEE, may 2012, pp. 3903–3908.

[33] V. Duchaine and C. M. Gosselin, "General model of human-robot cooperation using a novel velocity based variable impedance control," in *Second Joint EuroHaptics Conference and Symposium on Haptic Interfaces for Virtual Environment and Teleoperator Systems*, IEEE. IEEE, mar 2007, pp. 446–451.

[34] S. Jlassi, S. Tliba, and Y. Chitour, "An online trajectory generator-based impedance control for co-manipulation tasks," in *2014 IEEE Haptics Symposium (HAPTICS)*, IEEE. IEEE, feb 2014, pp. 391–396.

[35] T. Tsumugiwa, R. Yokogawa, and K. Hara, "Variable impedance control with virtual stiffness for human-robot cooperative peg-in-hole task," in *Intelligent Robots and Systems, 2002. IEEE/RSJ International Conference on*, vol. 2, IEEE. IEEE, 2002, pp. 1075–1081.

[36] C. Fang, A. Ajoudani, A. Bicchi, and N. G. Tsagarakis, "Online model based estimation of complete joint stiffness of human arm," *IEEE Robotics and Automation Letters*, vol. 3, no. 1, pp. 84–91, jan 2018.

[37] C. Yang, P. Liang, A. Ajoudani, Z. Li, and A. Bicchi, "Development of a robotic teaching interface for human to human skill transfer," in *2016 IEEE/RSJ International Conference on Intelligent Robots and Systems (IROS)*, IEEE. IEEE, oct 2016, pp. 710–716.

[38] Y. Li and S. S. Ge, "Human–robot collaboration based on motion intention estimation," *IEEE/ASME Transactions on Mechatronics*, vol. 19, no. 3, pp. 1007–1014, jun 2014.

[39] H. Wang, F. Patota, G. Buondonno, M. Haendl, A. De Luca, and K. Kosuge, "Stability and variable admittance control in the physical interaction with a mobile robot," *International Journal of Advanced Robotic Systems*, vol. 12, 2015.

[40] F. D. Davis, R. P. Bagozzi, and P. R. Warshaw, "User acceptance of computer technology: A comparison of two theoretical models," *Management Science*, vol. 35, no. 8, pp. 982–1003, aug 1989.

[41] B. H. Wixom and P. A. Todd, "A theoretical integration of user satisfaction and technology acceptance," *Information systems research*, vol. 16, no. 1, pp. 85–102, mar 2005.

[42] V. Venkatesh and H. Bala, "Technology acceptance model 3 and a research agenda on interventions," *Decision Sciences*, vol. 39, no. 2, pp. 273–315, may 2008.

[43] V. Venkatesh and F. D. Davis, "A theoretical extension of the technology acceptance model: Four longitudinal field studies," *Management Science*, vol. 46, no. 2, pp. 186–204, feb 2000.

[44] A. Ross, "Procrustes analysis," *Course report, Department of Computer Science and Engineering, University of South Carolina*, 2004.

[45] S. Balasubramanian, A. Melendez-Calderon, A. Roby-Brami, and E. Burdet, "On the analysis of movement smoothness," *Journal of NeuroEngineering and Rehabilitation*, vol. 12, no. 1, p. 1, dec 2015.

[46] E. Burdet, D. W. Franklin, and T. E. Milner, *Human Robotics*. MIT University Press Group Ltd, 2013.

[47] D. R. Olsen and M. A. Goodrich, "Metrics for evaluating human-robot interactions," in *Proceedings of PERMIS*, 2003, p. 4.

[48] V. R. Montes, Y. Quijano, J. C. Quero, D. V. Ayala, and J. P. Moreno, "Comparison of 4 different smoothness metrics for the quantitative assessment of movement's quality in the upper limb of subjects with cerebral palsy," in *2014 Pan American Health Care Exchanges (PAHCE)*, IEEE. IEEE, apr 2014, pp. 1–6.

[49] R. Shadmehr, S. P. Wise *et al.*, *The Computational Neurobiology of Reaching and Pointing: A Foundation for Motor Learning*. MIT press, 2004.

[50] A. Muxfeldt, S. Gopinathan, T. Coenders, and J. Steil, "A user study on human-robot-interactive recovery for industrial assembly problems," in *2017 26th IEEE International Symposium on Robot and Human Interactive Communication (RO-MAN)*, IEEE. IEEE, aug 2017, pp. 824–830.

[51] J. T. C. Tan, F. Duan, R. Kato, T. Arai, and E. Hall, *Collaboration planning by task analysis in human-robot collaborative manufacturing system*. INTECH Open Access Publisher, 2010.

[52] A. Muxfeldt, D. Kubus, and F. M. Wahl, "Developing new application fields for industrial robots - four examples for academia-industry collaboration," in *2015 IEEE 20th Conference on Emerging Technologies & Factory Automation (ETFA)*. IEEE, sep 2015.

[53] S. Wrede, O. Beyer, C. Dreyer, M. Wojtynek, and J. Steil, "Vertical integration and service orchestration for modular production systems using business process models," *Procedia Technology*, vol. 26, pp. 259–266, 2016.

[54] R. Andre and U. Thomas, "Anytime assembly sequence planning," in *Proceedings of ISR 2016: 47th International Symposium on Robotics*, June 2016, pp. 1–8.

[55] U. Thomas and F. Wahl, "Assembly planning and task planning — two prerequisites for automated robot programming," pp. 333–354, November 2010.

[56] D. Ewert, D. Schilberg, and S. Jeschke, "Selfoptimized assembly planning for a ROS based robot cell," in *Intelligent Robotics and Applications*, ser. ICIRA'12. Springer Berlin Heidelberg, 2012, pp. 696–705.

[57] J. F. Broenink and M. L. Tiernego, "The 8th european simulation symposium, ess 96," in *Simulation in Industry, 8th European Simulation Symposium, ESS'96, 1996*. Society for Computer Simulation, 1997.

[58] J. S. Laursen, U. P. Schultz, and L. P. Ellekilde, "Automatic error recovery in robot assembly operations using reverse execution," in *2015 IEEE/RSJ International Conference on Intelligent Robots and Systems (IROS)*. IEEE, sep 2015, pp. 1785–1792.

[59] X. W. Chen and S. Y. Nof, *Automating Errors and Conflicts Prognostics and Prevention*. Springer Berlin Heidelberg, 2009, pp. 503–525.

[60] B. Akgun, M. Cakmak, K. Jiang, and A. L. Thomaz, "Keyframe-based learning from demonstration," *International Journal of Social Robotics*, vol. 4, no. 4, pp. 343–355, jun 2012.

[61] A. Muxfeldt, J.-H. Kluth, and D. Kubus, "Kinesthetic teaching in assembly operations - a user study," in *Proceedings of SIMPAR 2014.* Springer International Publishing, 2014, pp. 533–544.

[62] S. Wrede, C. Emmerich, R. Grünberg, A. Nordmann, A. Swadzba, and J. Steil, "A user study on kinesthetic teaching of redundant robots in task and configuration space," *Journal of Human-Robot Interaction*, vol. 2, no. 1, pp. 56–81, mar 2013.

[63] C. Fellmann, D. Kashi, and J. Burgner-Kahrs, "Evaluation of input devices for teleoperation of concentric tube continuum robots for surgical tasks," in *SPIE Medical Imaging.* International Society for Optics and Photonics, 2015.

[64] A. K. Mishra, L. Peña-Castillo, and O. Meruvia-Pastor, "Evaluation of an inverse-kinematics depth-sensing controller for operation of a simulated robotic arm," in *Design, User Experience, and Usability: Technological Contexts.* Springer International Publishing, 2016, pp. 373–381.

[65] P. Rouanet, J. Bechu, and P. Y. Oudeyer, "A comparison of three interfaces using handheld devices to intuitively drive and show objects to a social robot: the impact of underlying metaphors," in *RO-MAN 2009 - The 18th IEEE International Symposium on Robot and Human Interactive Communication.* IEEE, sep 2009.

[66] L. Schmidt, J. Hegenberg, and L. Cramar, "User studies on teleoperation of robots for plant inspection," *Industrial Robot: An International Journal*, vol. 41, no. 1, pp. 6–14, jan 2014.

[67] A. Aryania, B. Daniel, T. Thomessen, and G. Sziebig, "New trends in industrial robot controller user interfaces," in *2012 IEEE 3rd International Conference on Cognitive Infocommunications (CogInfoCom).* IEEE, dec 2012, pp. 365–369.

[68] S. Gopinathan, S. Ötting, and J. Steil, "A user study on personalized adaptive stiffness control modes for human-robot interaction," The 26th IEEE International Symposium on Robot and Human Interactive Communication, aug 2017.

[69] T. Fong, C. Thorpe, and C. Baur, "Collaboration, dialogue, human-robot interaction," pp. 255–266, 2003.

[70] R. Bischoff, J. Kurth, G. Schreiber, R. Koeppe, A. Albu-Schäffer, A. Beyer, O. Eiberger, S. Haddadin, A. Stemmer, G. Grunwald *et al.*, "The KUKA-DLR lightweight robot arm-a new reference platform for robotics research and manufacturing," in *Robotics (ISR), 2010 41st international symposium on and 2010 6th German conference on robotics (ROBOTIK)*, 2010, pp. 1–8.

[71] W. Townsend, "The BarrettHand grasper – programmably flexible part handling and assembly," *Industrial Robot: An International Journal*, vol. 27, no. 3, pp. 181–188, jun 2000.

[72] A. Albu-Schäffer, C. Ott, and G. Hirzinger, "A unified passivity-based control framework for position, torque and impedance control of flexible joint robots," *The International Journal of Robotics Research*, vol. 26, no. 1, pp. 23–39, jan 2007.

[73] C. Emmerich, A. Nordmann, A. Swadzba, J. J. Steil, and S. Wrede, "Assisted gravity compensation to cope with the complexity of kinesthetic teaching on redundant robots," in *2013 IEEE International Conference on Robotics and Automation*. IEEE, may 2013, pp. 4322–4328.

[74] R. A. Grupen and M. Huber, "A framework for the development of robot behavior," DTIC Document, Tech. Rep., 2005.

[75] A. Nordmann, M. Rolf, and S. Wrede, "Software abstractions for simulation and control of a continuum robot," in *SIMPAR, 2012*, 2012, pp. 113–124.

[76] A. Nordmann and S. Wrede, "A domain-specific language for rich motor skill architectures," *arXiv preprint arXiv:1302.6436*, 2013.

[77] J. J. Steil, C. Emmerich, A. Swadzba, R. Grünberg, A. Nordmann, and S. Wrede, "Kinesthetic teaching using assisted gravity compensation for model-free trajectory generation in confined spaces," in *Gearing Up and Accelerating Cross-fertilization between Academic and Industrial Robotics Research in Europe:*. Springer, 2014, pp. 107–127.

[78] A. Field, *Discovering Statistics Using IBM SPSS Statistics*. SAGE Publications Ltd, 2013.

[79] P. Biernacki and D. Waldorf, "Snowball sampling: Problems and techniques of chain referral sampling," *Sociological Methods & Research*, vol. 10, no. 2, pp. 141–163, nov 1981.

[80] S. Gopinathan, S. K. Ötting, and J. J. Steil, "A user study on personalized stiffness control and task specificity in physical human–robot interaction," *Frontiers in Robotics and AI*, vol. 4, p. 58, nov 2017.

[81] S. Gopinathan, P. Mohammadi, and J. Steil, "Improved human-robot interaction: A manipulability based approach," in *ICRA 2018 Workshop on Ergonomic Physical Human-Robot Collaboration*, 2018.

[82] T. Yoshikawa, "Dynamic manipulability of robot manipulators," in *Proceedings. 1985 IEEE International Conference on Robotics and Automation*, vol. 2. Institute of Electrical and Electronics Engineers, 1985, pp. 1033–1038.

[83] P. Chiacchio, "A new dynamic manipulability ellipsoid for redundant manipulators," *Robotica*, vol. 18, no. 4, pp. 381–387, jul 2000.

[84] N. Vahrenkamp, T. Asfour, G. Metta, G. Sandini, and R. Dillmann, "Manipulability analysis," in *2012 12th IEEE-RAS International Conference on Humanoid Robots (Humanoids 2012)*. IEEE, nov 2012, pp. 568–573.

[85] T. Petrič, J. Babič *et al.*, "Augmentation of human arm motor control by isotropic force manipulability," in *2016 IEEE/RSJ International Conference on Intelligent Robots and Systems (IROS)*. IEEE, oct 2016, pp. 696–701.

[86] M. Faroni, M. Beschi, A. Visioli, and L. M. Tosatti, "A global approach to manipulability optimisation for a dual-arm manipulator," in *2016 IEEE 21st International Conference on Emerging Technologies and Factory Automation (ETFA)*, IEEE. IEEE, sep 2016, pp. 1–6.

[87] C. Thomas, F. Busch, B. Kuhlenkoetter, and J. Deuse, *Process and Human Safety in Human-Robot-Interaction - A Hybrid Assistance System for Welding Applications*. Berlin, Heidelberg: Springer Berlin Heidelberg, 2011, pp. 112–121.

[88] Y. Tanaka, N. Yamada, K. Nishikawa, I. Masamori, and T. Tsuji, "Manipulability analysis of human arm movements during the operation of a variable-impedance controlled robot," in *2005 IEEE/RSJ International Conference on Intelligent Robots and Systems*, IEEE. IEEE, 2005, pp. 1893–1898.

[89] K. L. Doty, C. Melchiorri, E. M. Schwartz, and C. Bonivento, "Robot manipulability," *IEEE Transactions on Robotics and Automation*, vol. 11, no. 3, pp. 462–468, jun 1995.

[90] M. Theofanidis, A. Lioulemes, and F. Makedon, "A motion and force analysis system for human upper-limb exercises," in *Proceedings of the 9th ACM International Conference on PErvasive Technologies Related to Assistive Environments*, ACM. ACM Press, 2016, p. 9.

[91] N. Point, "Inc.: Optitrack-optical motion tracking solutions," 2009.

[92] K. Lee and M. Buss, "Force tracking impedance control with variable target stiffness," *IFAC Proceedings Volumes*, vol. 41, no. 2, pp. 6751–6756, 2008.